Investigation of the Kinetic Resolution of Terminal Epoxides by Al(III), Co(III), and Cr(III)salen Complexes

Quek Cai Zhen Sophie

MSc. By Research

University of York

Chemistry

September 2014

Abstract

Although the industrial era has undoubtedly improved standards of living, it has also resulted in a gradual but definite increase in atmospheric carbon dioxide levels. Consequently, undesirable weather events have intensified. Thus, the use of carbon dioxide as a feedstock is attractive, particularly if the reaction takes place under mild conditions. In this work, we utilise carbon dioxide in the conversion of epoxides to enantio-enriched cyclic carbonates, which may be used en route to the production of valuable pharmaceuticals. The application of aluminium(salen), chromium(salen), and cobalt(salen) catalysts enables this 100 % atom-economical process to take place under 1 bar of CO_2.

The kinetic resolution of epoxides *via* the insertion of carbon dioxide has hitherto been reported only for cobalt(salen) complexes. Jacobsen's study of kinetic resolution of epoxides using water as the ring-opening agent in the presence of the same cobalt(salen) catalysts showed that cobalt(salen) complexes form a "stepped" bimetallic transition state, which presents as a second-order rate dependence on catalyst. In this thesis, we show that ring-opening with carbon dioxide may operate *via* a different pathway as a second-order rate dependence on catalyst was not observed. Investigation of existing crystal structures of aluminium(salen), cobalt(salen), and chromium(salen) complexes in the Cambridge structural database were similarly inconclusive in demonstrating the relationship between the "step" of the complex and the enantioselectivity.

Furthermore, we demonstrate the successful kinetic resolution of both phenyl glycidyl ether and *N*-(2,3-epoxypropyl)diphenylamine in the presence of aluminium(salen) and chromium(salen) complexes, which has not previously been reported. The maximum k_{rel} value obtained for *N*-(2,3-epoxypropyl)diphenylamine as substrate was 15.38 with our aluminium(salen) catalysts, and 7.32 with our chromium(salen) catalysts. In contrast, the maximum k_{rel} value obtained using our cobalt(salen) complexes was 2.26.

List of Contents

List of Tables

List of Figures

Acknowledgements

I would like to thank Prof. Michael North for the opportunity to carry out this project in the Green Chemistry Centre of Excellence in the University of York, as well as his advice and guidance, both inside and outside of the lab. I am also grateful to all members of the group, in particular Xiao Wu, José Castro-Osma, and Katie Lamb.

Author's Declaration

The work in this thesis has been carried out by the author in the Department of Chemistry at the University of York from Oct 2013 to Sept 2014. This work contains no material which has been accepted for the award of any other degree in any other institution. This work contains no material previously written by any other person except where due reference has been made in the text.

1. Introduction

1.1. Hypotheses drawn from the hydrolytic kinetic resolution of epoxides

In Jacobsen's hydrolytic kinetic resolution (HKR) of terminal epoxides, chiral cobalt(salen) complexes ring-open epoxides in the presence of water to form the diol enantioselectively. These catalysts are not only highly enantioselective (k_{rel}>50 for almost all substrates studied, where $k_{rel} = \frac{\ln(1-c(1+ee))}{\ln(1-c(1-ee))}$),[1] but are also applicable to a large range of substrates.

In the presence of a co-catalyst such as a tetrabutylammonium halide salt, Jacobsen's chiral catalysts utilise carbon dioxide instead of water as the ring-opening agent to produce cyclic carbonates (Scheme 1). Literature precedent shows that this reaction is similarly enantioselective. However, enantioselectivity in the formation of cyclic carbonates from epoxides and CO_2 has hitherto been observed only with cobalt(salen) catalysts (Section 1.5.2, page 11),[2-5] i.e. similar metal(salen) catalysts have failed to generate enantio-enriched cyclic carbonates.[6-8] Consequently, we desired to establish if the conclusions drawn from Jacobsen's mechanistic studies could be used to elucidate reasons for this unique characteristic of cobalt(salen) complexes.[9]
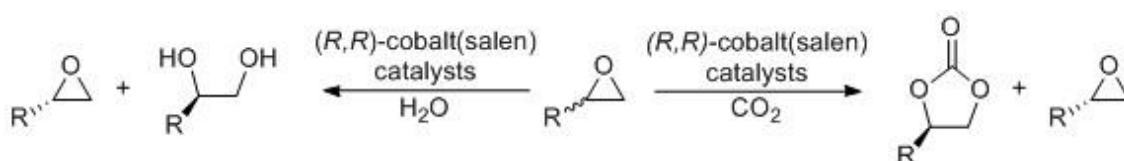
Scheme 1: Conversion of epoxides to 1,2-diols *via* the HKR process (left),[1] and to cyclic carbonates using Jacobsen's catalysts (right).

In the HKR process, stereoselectivity is conferred by the structure of the bimetallic transition state. Although each chiral cobalt(salen) molecule may appear to take on a planar arrangement about the metal centre (Figure 1, left), both crystal structures and computational methods indicate otherwise. Figure 1 (right) clearly displays a significant tilt of both aryl rings with respect to the equatorial plane, which is described as a "step". The comparable activities of cobalt(salen) catalysts with similar steps, but different diamine backbones, is verification of the importance of the step produced as opposed to the identity of the backbone itself.

The putative transition state is formed by the activation of substrate by one catalyst molecule (Figure 1, top right), and the separate activation of water by a second catalyst molecule from the bottom. It follows that the framework significantly hinders the approach of a mismatched epoxide molecule. Approach of the mismatched epoxide is further inhibited by bulky substituents on the aryl rings, as corroborated by enhanced selectivity conferred by catalysts with larger functional groups at the 5,5' position. On the other hand, the R-group of the preferred isomer of substrate projects out into open space (Figure 1, coloured black). As a result, these catalysts are able to kinetically resolve a wide range of epoxides without loss of enantioselectivity. Thus, Jacobsen demonstrates that the stepped conformation of chiral cobalt(salen) catalysts, in combination with a bimetallic transition state, confers stereoselectivity in the HKR process.[9]
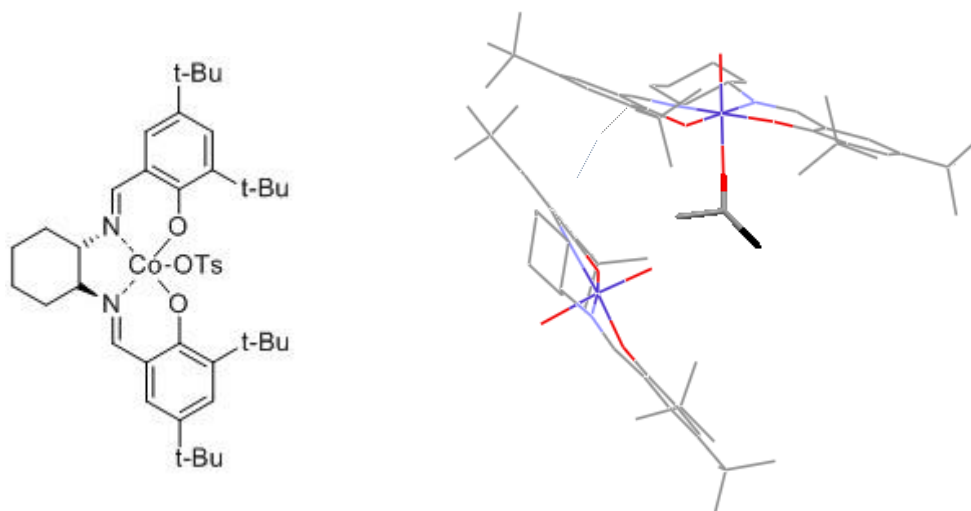
Figure 1: Transition structure formed between two molecules of (*S,S*)-*N,N'*-bis(3,5-di-*tert*-butylsalicylidene)-1,2-cyclohexanediaminocobalt(III) hydroxide and one molecule of *(R)*-propylene oxide. The grey dashed line indicates bond breaking. The blue dashed line indicates bond formation. The R-group of the epoxide (coloured black) projects into unhindered space which explains the broad substrate scope of Jacobsen's catalyst.[9]

There are therefore two hypotheses to be tested for the enantioselectivity of cobalt(salen) catalysts in cyclic carbonate synthesis:

1. The rate is second order w.r.t. cobalt(salen) catalysts, but not w.r.t. aluminium(salen), or chromium(salen) catalysts.
2. Out of the three metal(salen) systems we propose to study, cobalt(salen) complexes exhibit the most pronounced tilt.

1.2. Industrial importance of cyclic carbonates

Cyclic carbonates are industrially important in a wide range of applications such as being used in extraction media and the production of plastics and electrolytes.[10] As cleaning agents, they are also superior to conventional options.[11-13] For example, propylene carbonate, which remains liquid over a wide range (-48 °C to 242 °C) and can therefore be used at elevated temperatures,[10] is soluble in both water and several organic solvents. Additionally, it is easy to recover, low in viscosity, and has good solvating capabilities. Ethylene carbonate (liquid over 36 °C to 246 °C) is similarly versatile, with an added characteristic of being solid at room temperature. Ethylene carbonate may be used as solvent with or without propylene carbonate in the spinning of polyacrylonitrile solutions.[14]

propylene carbonate   ethylene carbonate
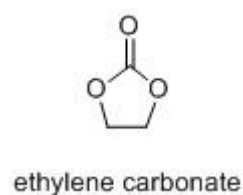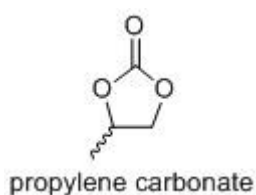
Based on factors such as environmental impact, recycling issues, and both acute and chronic effects on human health, both propylene carbonate and ethylene carbonate are excellent alternatives to traditional hazardous solvents.[15,16] That said, cyclic carbonates are used not only as inert media, but also as reactive intermediates. For instance, they undergo reaction with carboxylic acids, diols, and amines to produce hydroxyalkyl esters, polycarbonates, and hydroxyalkylurethanes.[17,18]

Although cyclic carbonates are frequently used as racemic mixtures, enantiopure cyclic carbonates are equally, if not more, valuable materials. In particular, they may be readily converted into carboxylic esters, amino acids,[19] and ureas, to be used *en route* to the production of pharmaceutically important compounds.[20] In medicines where enantiopurity is pertinent, the consumption of single-isomer drugs would alleviate unintended side-effects arising from the consumption of the undesired isomer.[21,22] An example supporting the cause for enantiopure pharmaceuticals is the drug Citolopam, where only the *(S)-*enantiomer exhibits an antidepressant effect.[23]

However, the cost of enantiopure cyclic carbonates remains prohibitive. According to 2013 chemical catalogue prices on a lab scale, prices exceed GBP 20,000 dm^{-3}. Given the fact that several therapeutic groups are stereoisomeric mixtures, pharmacists have identified chirality in drugs as an "across-the-board" problem.[24] The downstream effects of making enantiopure cyclic carbonates more affordable, would therefore impact many users.

1.3. High-yielding methods for cyclic carbonate production

The traditional route for the large-scale production of dimethyl carbonate involved using phosgene ($COCl_2$) as a C1 building block. When passed through methanol in the presence of concentrated sodium hydroxide, dimethyl carbonate is produced in good yield and purity.[25,26] However, the high toxicity of phosgene will likely see its large-scale use being phased out in favour of safer alternatives.[27]

One such phosgene-free route for the commercial production of dimethyl carbonate involves oxidising cuprous chloride in methanol at 70 °C and 8 atm, followed by the addition of carbon monoxide. The reaction is almost entirely selective in producing dimethyl carbonate from methanol,[28] and is industrially viable on a 12 000 tonne/y scale.[10]

Likewise, phosgene is unneccesary for the production of propylene carbonate. Sakakura *et al.* used homogenous catalyst **1a** for the 100 % atom-economical formation of propylene carbonate from propylene oxide and supercritical CO_2 with excellent yield and selectivity (Scheme 2). Problems typically encountered

4

during catalyst/product separation were neatly sidestepped due to phase separation concurrent with the accumulation of propylene carbonate. Removal of the lower phase containing the desired product, followed by replenishment of epoxide, enabled catalyst recycling without significant loss of activity for three consecutive runs.[29]
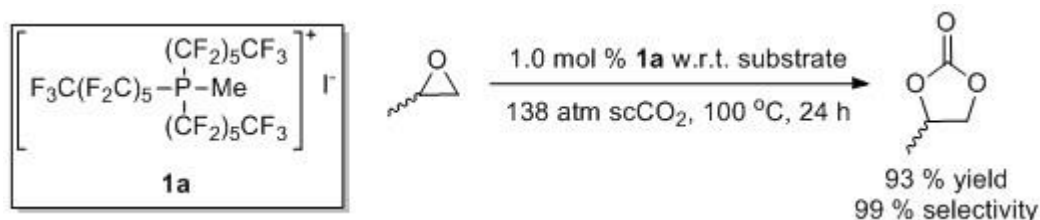
Scheme 2: Synthesis of propylene carbonate from propylene oxide by Sakakura *et al.*[29]

In 2008, Yin and Shimada reported 98 % yield of propylene carbonate using robust bismuth complex **1b** (Scheme 3). Such complexes are postulated to behave as Lewis acids, and are highly active at ambient temperature and pressure (1 atm CO_2, 25 °C),[30] resulting in an net consumption of CO_2 on top of 100 % atom economy. It follows that similar reactions not requiring heating, cooling, or pressurising, represent excellent sequestration options for CO_2.
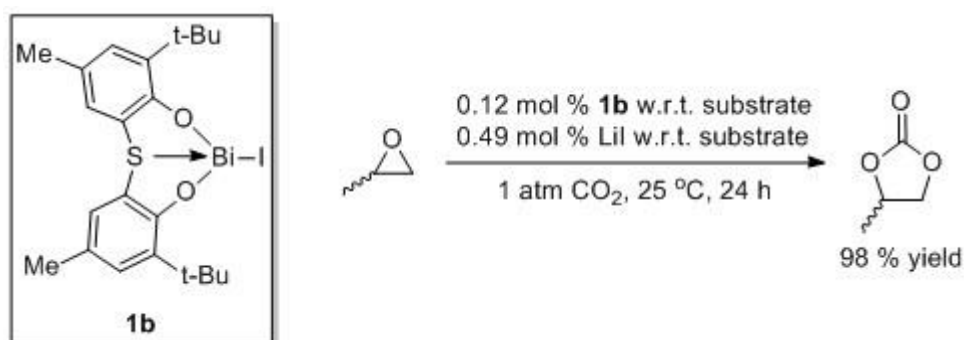
Scheme 3: Synthesis of propylene carbonate by Yin and Shimada.[30]

As a direct result of deforestation and fossil fuel combustion, CO_2 levels have risen by 35 % since the industrial era. Because CO_2 both absorbs and emits infrared radiation, an increase in levels produces a warming effect on the Earth's climate. In turn, heat waves, downpours, and similar extreme weather conditions are intensified,[31,32] hence the urgent need for CO_2 capture and sequestration.[33] Furthermore, being non-toxic, abundant, cheap, and renewable, CO_2 is an environmentally-friendly and affordable feedstock in the large-scale manufacture of carbonates.[25]

While many metal(salen) catalysts have been known to catalyse the synthesis of racemic carbonates from epoxides, the production of enantiopure cyclic carbonates is far more difficult. While stereoselective synthesis from enantiopure epoxides may be achieved with relative ease,[8,34] it remains an extremely costly option. To illustrate, 2013 chemical catalogue prices for enantiopure propylene oxides (99 % purity) exceeds GBP 20,000 dm^{-3}. In contrast, the same catalogue indicates a mere GBP 25 dm^{-3} price tag for the racemate (99 % purity). Therefore, from a commercial perspective, the production of enantiopure carbonates from inexpensive racemic terminal epoxides *via* chiral catalysts would be advantageous.

1.4. Basis for the kinetic resolution of cyclic carbonates using metal(salen) catalysts

Because salen complexes are active for a broad range of reactions, they have been described as "privileged".[35] For instance, besides being used in the HKR process and our desired synthesis of cyclic carbonates from epoxides, metal(salen) complexes are also used in the epoxidation of alkenes[36-38] and in the formation of oxazolidinones from epoxides and isocyanates.[39,40]

Chiral cobalt(salen) catalysts are able to carry out kinetic resolution because they form diastereomeric transition states with enantiomers (Figure 2). As a result one pathway has a lower activation energy than the other, thus favouring the formation of one enantiomer of the desired product. Ideally, the reaction would come to a standstill on depletion of the favoured enantiomer, thus producing a theoretical maximum yield of 50 % from racemic substrate.
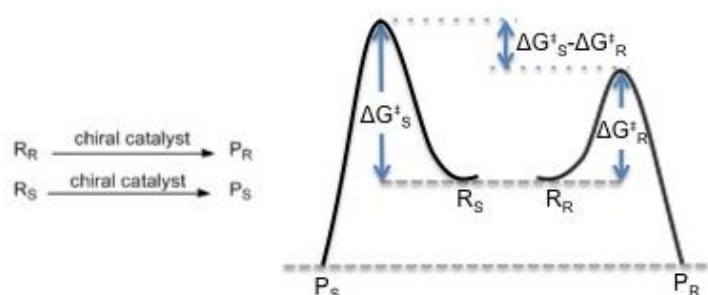
Figure 2: Energy profile diagram for a theoretical kinetic resolution where $\Delta G^{\ddagger}$ is the Gibbs energy of activation. Enantiomers are equivalent in energies, but the diastereomeric substrate-catalyst transition states have distinct energies. This produces different rates of reaction for each enantiomer.

Jacobsen demonstrated that the step of the salen ligand is crucial to the stereoselectivity of the HKR process. These stepped, chiral ligands are readily synthesised from the desired corresponding salicyaldehydes and diamines, enabling easy modification of their electronic and steric properties.[41] Careful selection of the desired synthon allows functional groups to be tacked onto the phenyl rings or the diamine bridge, with immobilisation onto solid supports as a further option.[42-46] A variety of metals also readily undergo complexation with salen ligands in a tetradentate fashion, to form monometallic, bimetallic, and polymetallic complexes.[34,43,47]

Our initial plan was to synthesise a variety of metal(salen) complexes (Figure 3) which preserve the ligand structure to determine how the identity of the metal affects the kinetic resolution of terminal epoxides. The activity and enantioselectivity of catalysts **2a** to **4c** was then investigated to study the relevance of the two hypotheses discussed earlier.

2a: M = Al, X = Cl
2b: M = Al, X = OAc
2c: M = Al, X = OTs
3a: M = Co, X = Cl
3b: M = Co, X = OAc
3c: M = Co, X = OTs
3d: M = Co, X = Br
4a: M = Cr, X = Cl
4b: M = Cr, X = OAc
4c: M = Cr, X = OTs
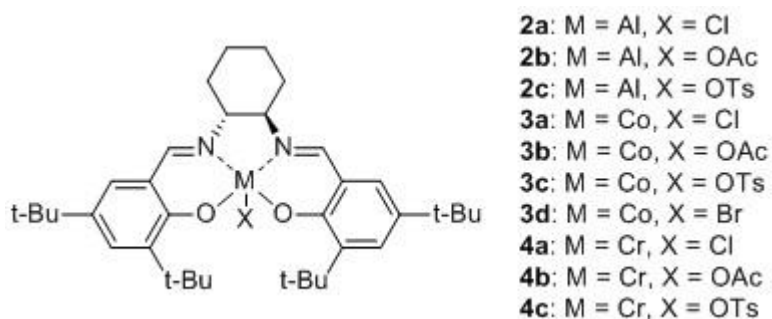
Figure 3: Structures of metal(salen) complexes

1.5. Literature Precedent

Until recently, researchers in the field have utilised either styrene oxide or propylene oxide as substrates. Examples of literature precedent have been limited to the use of propylene oxide as substrate where possible. However, aluminium(salen) complexes studied by the North group have utilised styrene oxide as substrate instead.[6,34,43] Similarly, phenyl glycidyl ether has been used as an alternative substrate for metal-free catalysis in recent years.[48-50] Nonetheless, the research presented herein retains relevance as this thesis makes use of both styrene oxide and phenyl glycidyl ether.

1.5.1. Aluminium(salen) complexes

North *et al.* demonstrated *ca.* 10 % conversion of styrene oxide to styrene carbonate using catalyst **5a** under solvent-free conditions (1 atm CO_2, 25 °C, 400 min, 2.5 mol % **5a** w.r.t. epoxide, 2.5 mol % tetrabutylammonium bromide w.r.t. epoxide). In contrast, bimetallic aluminium(salen) complex **5b** afforded *ca.* 50 % conversion under identical conditions. After 24 h at room temperature, catalyst **5b** at 2.5 mol % catalyst loading afforded 98 % conversion of styrene oxide using 1 atm of CO_2 when used in combination with tetrabutylammonium bromide (1:1 ratio).[34] Optimal yields were obtained using monosubstituted epoxides. 77 % yield of propylene carbonate was obtained after 3 h (1 atm CO_2, 0 °C, 2.5 mol % **5b** w.r.t. propylene oxide, 2.5 mol % tetrabutylammonium bromide w.r.t. epoxide. No byproducts resulting from polymer formation, epoxide hydrolysis, or epoxide rearrangement were detected.

5a   **5b**
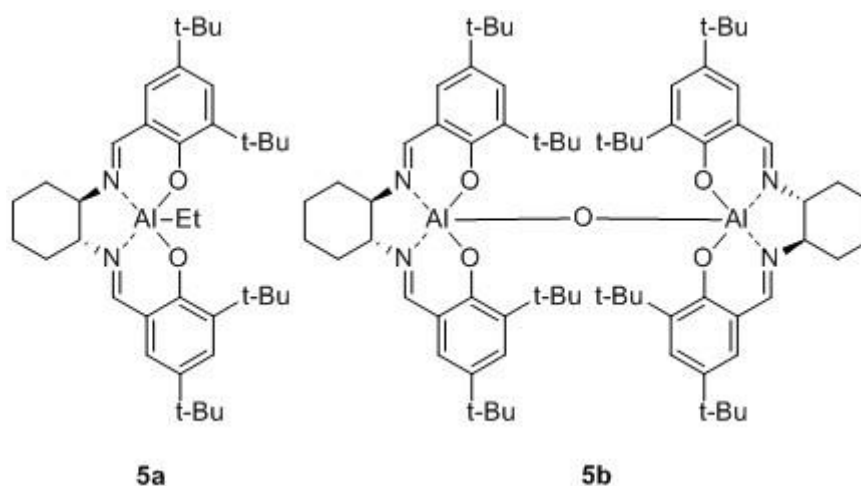
Since the reaction was carried out without solvent, propylene carbonate was purified by distillation from the reaction flask. Catalyst reusability was demonstrated for 60 consecutive runs by replenishing the vessel containing catalyst residue with fresh propylene oxide and CO_2. Any loss of activity was attributed to decomposition of tetrabutylammonium bromide. Addition of fresh tetrabutylammonium bromide co-catalyst restored activity.

Mechanistic studies showed that two molecules of tetrabutylammonium bromide are involved in the reaction (Scheme 4). The first generates a tributylamine molecule to be used in the activation of carbon dioxide, while the second

molecule ring-opens the terminal end of the coordinated epoxide. The coordination of the bimetallic complex to both the epoxide and the activated CO_2 in the rate-determining step then sets up an intramolecular reaction to form the carbonate.[6] Although reactions using only *(R)*-styrene oxide afforded enantiomerically pure styrene carbonate as assessed by chiral HPLC,[34] indicating retention of the stereocentre, kinetic resolution of styrene carbonate was not observed.
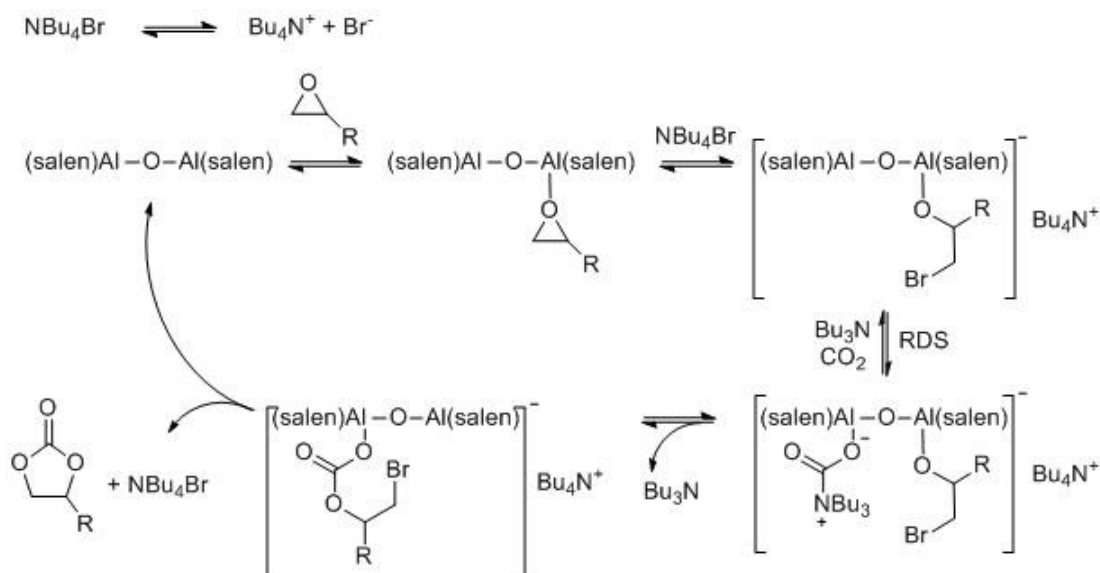
Scheme 4: Proposed mechanism for the formation of cyclic carbonate from epoxides and CO_2 using catalyst 5b adapted from Clegg *et al*.[34] Notably, only one molecule of catalyst is proposed to be involved in the rate-determining step.

A single-component catalyst (**5c**) containing both Lewis acid and quaternary ammonium bromide elements produced 97 % conversion of styrene oxide under ambient conditions (1 atm CO_2, 25 °C, 6 h, 2.5 mol % **5c** w.r.t. styrene oxide).[43] Catalytic activity was proven for nine additional terminal epoxides and retained the stereochemistry of the substrate. Having eliminated the need for a separate addition of tetrabutylammonium bromide, immobilisation on various supports was performed to facilitate application in continuous flow reactors. Using catalyst **5c** immobilised on polystyrene, 100 % yield to styrene carbonate was obtained in an initial run, which decreased to 70 % after three consecutive runs.[43]

A modified version of complex **5c** immobilised on amorphous silica (**5d**) was then packed into a column which was installed in a gas-phase continuous flow reactor. Thee conversion of waste CO_2 into cyclic carbonates using this single-

component immobilised catalyst in simulated flue gas streams was then investigated. Using a gas stream of 21 % CO_2 at 60 °C, catalyst **5d** converted 97 % of the CO_2 introduced into ethylene carbonate over 7 h. Further testing demonstrated that the catalyst was robust enough to withstand exposure to typical flue gas components such as NO (661 ppm), NO_2 (36 ppm), and SO_2 (1700 ppm). In comparison, flue gas streams of power stations powered by 1 % sulphur bituminous coal are usually about 90 % of those levels.[43] Given the near-complete consumption of CO_2, the ability of the catalyst to tolerate exposure to flue gas contaminants, and the widespread availability of inexpensive aluminium supplies, scale-up of this technology would be a highly promising alternative to carbon-capture.

5c

5d
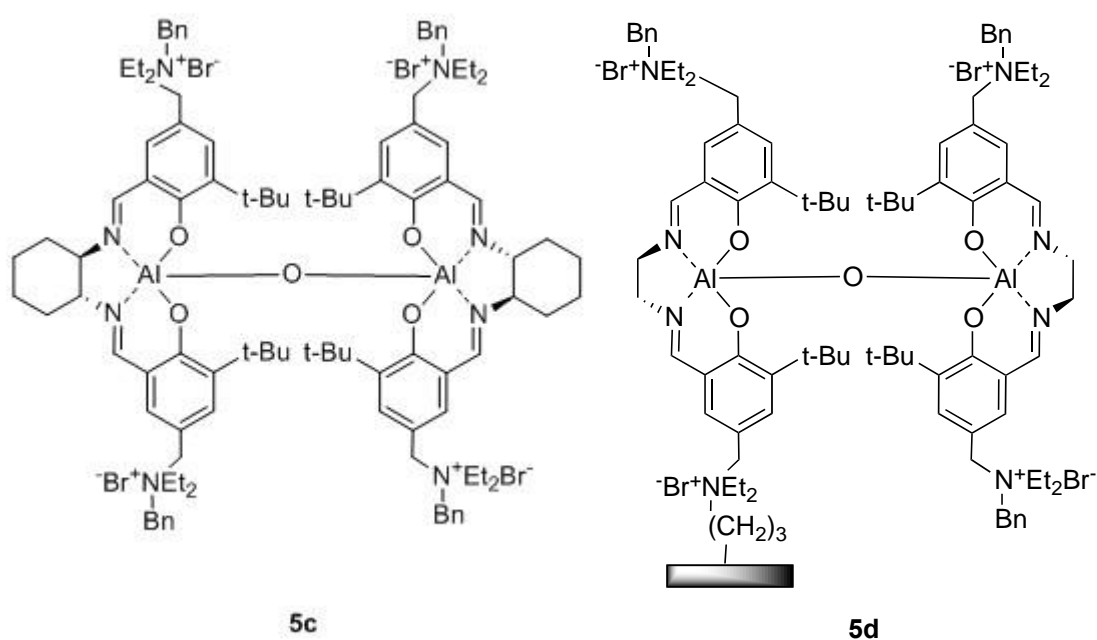
Alternatively, aluminium(salen) complexes containing phosphonium salts instead of quaternary ammonium halides may be used as single-component catalysts with enhanced thermal and moisture stability. This enabled experiments to be carried out at temperatures of up to 120 °C, which afforded turnover frequencies of 1760 h^{-1}. However, there was an upper limit of 140 °C, after which catalyst decomposition occurred as evidenced by decreased conversion and turnover frequency. The best runs using catalyst **5e** were performed at 100 °C, producing 88.6 % conversion (19.7 atm CO_2, 4 h, 0.025 mol % Al(III) w.r.t propylene oxide).[7]

5e
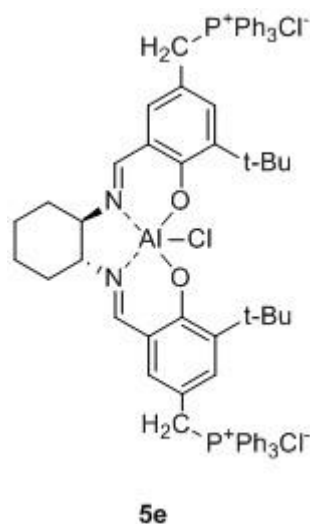
1.5.2. Cobalt(salen) complexes

Unlike aluminium(salen) complexes, cobalt(salen) complexes are known to be capable of carrying out a kinetic resolution of epoxides. In 2004, Lu *et al.* reported that complex **6a** gave up to 70.2 % ee propylene carbonate in favour of the *(S)*-isomer at 40 % conversion in the presence of tetrabutylammonium chloride as co-catalyst (k_{rel} = 8.99). Good conversions ranging from 48.2 % to 52.4 % were obtained (11.8 - 14.8 atm CO_2, 0 °C, 15 h, 0.1 mol % Co(III) w.r.t. epoxide, 0.2 mol % tetrabutylammonium chloride w.r.t. epoxide). Further experiments revealed that bulkier counterions on Co(III) enhanced enantioselectivity. Higher yields but lower enantioselectivities were observed at higher temperatures.[2] Berkessel and Brandenburg later used the same catalyst to obtain 65 % ee of propylene carbonate with a 36 % yield with a k_{rel} of 6.69 (1.0 atm CO_2, -20 °C, 18 h, 0.1 mol % Co(III) w.r.t. epoxide, 0.5 mol % tetrabutylammonium chloride w.r.t. epoxide).[3]

A similar multi-chiral Co(III)salen catalyst (**6b**) in conjunction with bis(triphenylphosphine)iminium-2,4-dinitrophenoxide (PPN$^+$DNP$^-$) later elevated enantioselectivity to an unprecedented 97.1 %. Using racemic propylene oxide as substrate, **6b** afforded 10 % conversion to *(S)*-propylene carbonate (8.2 atm CO_2, - 25 °C, 12 h, 0.05 mol % Co(III) w.r.t. epoxide, 25.0 mol % PPN$^+$DNP$^-$ w.r.t. epoxide), giving a k_{rel} of 75.58. The amount of co-catalyst used was deliberately increased to favour the formation of cyclic carbonate over polycarbonate. The presence of a bulky cation and an anion with poor leaving

ability were found to be crucial factors in maximising the extent of kinetic resolution.[4]

6a

6b: X = 2,4,-dinitrophenoxy
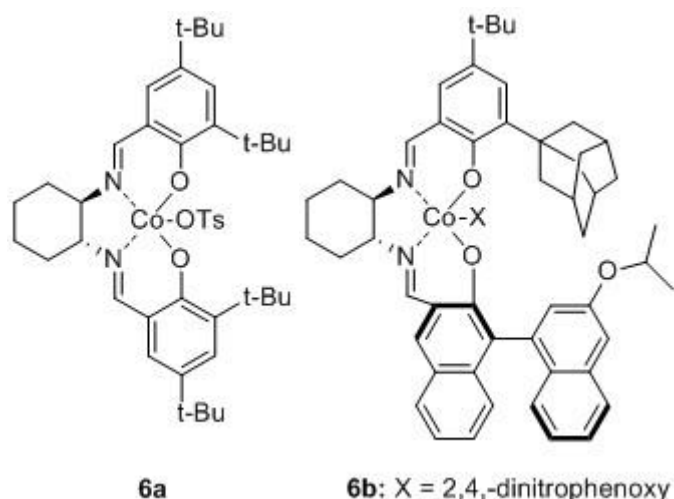
Application of a related chiral salen catalyst **6c** to racemic propylene oxide and carbon dioxide afforded 83 % ee of propylene carbonate in 45 % yield (k_{rel} = 21.79) in favour of the *(S)*-isomer (5 atm CO_2, 25 °C, 3 h, 0.1 mol % Co(III) w.r.t. epoxide, 0.01 mol % 1-butyl-3-methylimidazolium hydroxide w.r.t. epoxide). Both enantioselectivity and activity were improved by lowering catalyst loading or by adding an inorganic base such as KOH, K_2CO_3 or $KHCO_3$. The effect was more pronounced with stronger bases, which facilitated CO_2 adsorption onto the base.[51]

In continued research, Jang, Jang, Kim, and Kim reported that the enantioselectivity of a chiral Co(III)-Co(BF$_4$)$_2$ salen catalyst could be enhanced by immobilisation. Immobilisation was achieved by a straightforward reflux of the homogeneous Co(III)-Co(BF$_4$)$_2$ salen catalyst with the silica-alumina support in THF for 5 h. The resultant heterogeneous system (**6d**) afforded up to 65 % ee of *(S)*-propylene carbonate (10.0 atm CO_2, 25 °C, 14 h, 1.0 mol % Co(III) w.r.t. epoxide) in *ca.* 25 % conversion (k_{rel} = 5.39). The proximity of the support hinders the approach of the reactant epoxide to the Co(III) centre, which was confirmed by a decreased enantioselectivity of 45 % ee using the homogeneous catalyst (k_{rel} = 3.09).

Despite the non-covalent nature of the catalyst-support bonds, multiple washes with polar solvents did not detach catalyst from the support. Catalyst recycling was proven for up to three times - any loss of enantioselectivity was attributed to the detachment of the metal from the support and could be easily restored by attaching more homogeneous catalyst. Furthermore, the system was responsive to only *(S)*-propylene oxide, leaving *(R)*-propylene oxide largely unchanged at the end of the run.[5]

6c   **6d**
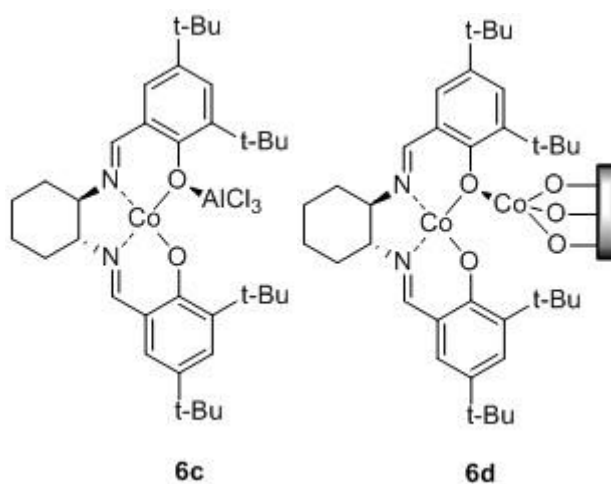
Interestingly, this sense of chiral discrimination is largely true for the complexes described in this section – (*R,R*)-cobalt(salen) complexes favour the formation of the *(S)*-propylene carbonate over the other isomer. Jacobsen observed the same phenomenon in the conversion of epoxides to diols as the bimetallic nature of the putative transition structure and the step of the salen ligand causes coordination of the mismatched enantiomer to be energetically unfavourable. The literature precedent for cobalt(salen) catalysts in the conversion of epoxides to cyclic carbonates reinforces the notion that both mechanisms are intrinsically linked.

1.5.3. Chromium(salen) complexes

The ability of chromium complexes to convert terminal epoxides to cyclic carbonates was first demonstrated by Kruper and Dellar.[52] Turnover numbers of 10,000 were observed for terminal epoxides as substrate at 50 atm CO_2 and temperatures of 60 to 80 °C for 16 to 48 h. Paddock and Nguyen later designed chromium(salen) catalysts, which could be produced in improved yields in

comparison with the chromium(porphyrin) complexes. It was noted that the performance of *meso* complex **7a** was significantly superior to that of the racemic anagolue (*trans* complex **7b**). A turnover number of 507 was obtained after 2 h (7.0 atm CO_2, 75 °C, 1.0 mol % **7a** w.r.t. propylene oxide, 1.0 mol % (4-dimethylamino)pyridine w.r.t propylene oxide, 0.5 mL dichloromethane as solvent). In contrast, the racemic *trans* complex **7b** afforded a lower turnover number of 253 as the coordination site was less accessible than in the *meso* complex. A 100 % yield of propylene carbonate was obtained under optimized conditions (3.5 atm CO_2, 75 °C, 1.5 h, 1.0 mol % **7a** w.r.t. propylene oxide, 1.0 mol % (4-dimethylamino)pyridine w.r.t. propylene oxide).[8]

7a   7b
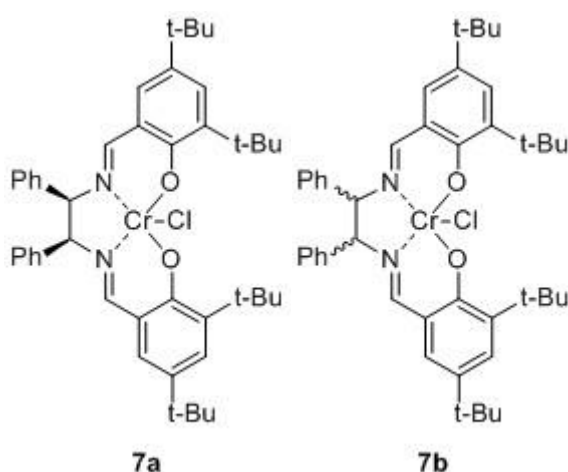
Undesirable polycarbonate formation may be avoided by judicious selection of reaction conditions, such as increasing the amount of co-catalyst present. By using a 2:1 ratio of (4-dimethylamino)pyridine: Cr(III), Chen *et al.* obtained only monomeric propylene carbonate (92.7 % yield, 14.8 atm CO_2, 40 °C, 3 h, 0.05 mol % **7c** w.r.t. propylene oxide, 0.1 mol % (4-dimethylamino)pyridine w.r.t. propylene oxide). The authors postulated that initial polymer formation is followed by depolymerisation *via* back-biting on coordination of (4-dimethylamino)pyridine to the Cr(III) centre.[53]

A variation on the ligand involved putting a bulky nucleophile on the diimine bridge of the salen ligand to produce a single-component catalyst **7d**. Under optimum conditions, **7d** produced a 42.4 % yield of propylene carbonate (19.7 atm CO_2, 80 °C, 1 h, 0.02 mol % Cr(III) w.r.t. epoxide). However, the presence of *N*-methylimidazole, whether covalently attached to the salen ligand *via* a

flexible arm or added separately, suppressed catalytic activity. This decrease in activity was attributed to competitive coordination of *N*-methylimidazole to the central Cr(III) ion thus hindering approach of the epoxide. As such, bulky co-catalysts are necessary to ensure high activity. In addition, like the aluminium(salen) complexes discussed briefly under Section 1.5.1, the chromium(salen) catalysts were able to preserve the stereochemistry of the substrate, but were unsuccessful in producing enantiopure cyclic carbonates from racemic epoxides.[54]

7c   7d
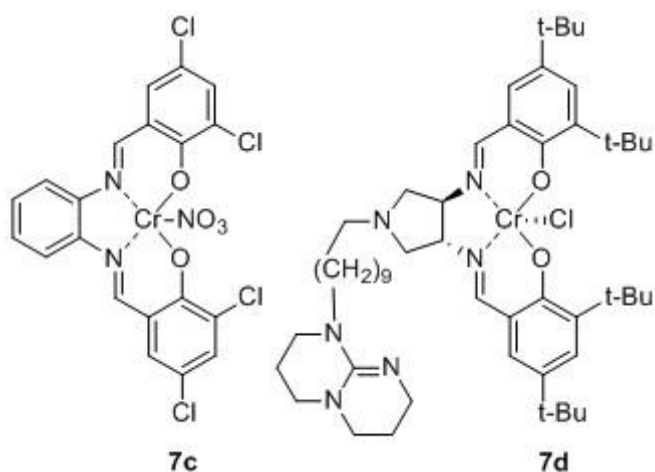
However, chromium(salen) catalysts have been reported to kinetically resolve epoxides using trimethylsilyl azide as the ring-opening agent, with a second-order rate dependence on catalyst. One chromium(salen) molecule coordinates to the ring-opening azide anion while the other activates the epoxide. Jacobsen *et al.* obtained 76 % conversion of styrene oxide to several side products, presumably including azido silyl ethers (Scheme 5). Although undesirable decomposition of the substrate was also observed, the e.e. of remaining substrate was an excellent 98 % in favour of the *(R)*-isomer. Studies carried out on the remaining catalyst residue showed that the active catalyst (**7f**) was generated *in situ*.[55]
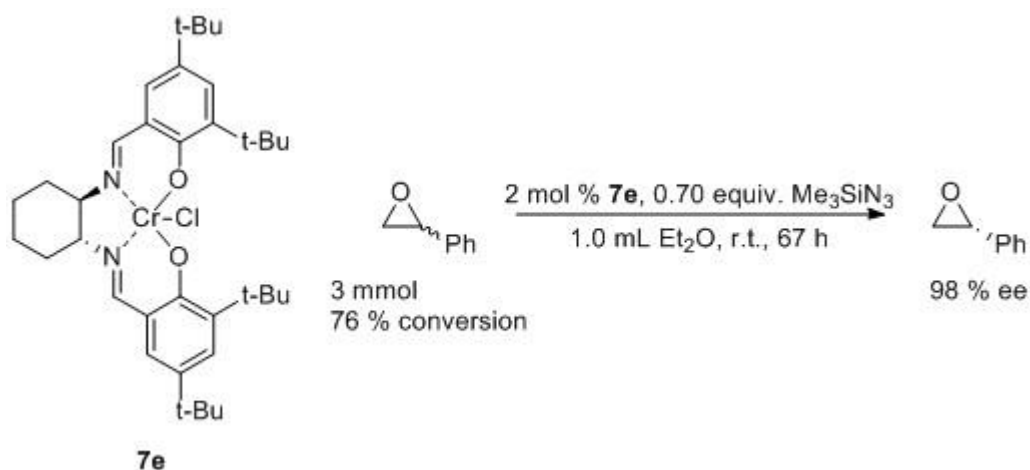
Scheme 5: Kinetic resolution of styrene oxide *via* ring-opening with trimethylsilyl azide using pre-catalyst 7e by Jacobsen *et al*.[55]

Jacobsen then extended this methodology to the kinetic resolution of propylene oxide. The use of active catalyst **7f** instead of pre-catalyst **7e** afforded the ring-opened product in much-improved yield and selectivity (98 % and 97 % respectively) with a k_{rel} of 230 (Scheme 6). It is implicit that the unreacted propylene oxide removed by rotary evaporation was the *(R)*-isomer.[56]
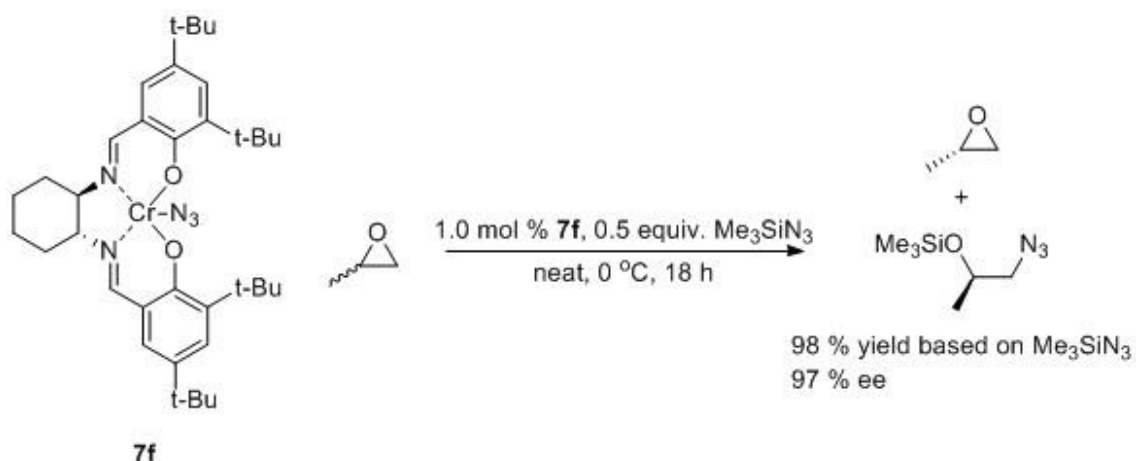
Scheme 6: Kinetic resolution of propylene oxide *via* ring-opening with trimethylsilyl azide using active catalyst 7f by Jacobsen *et al*.[56]

Although kinetic resolution of epoxides using trimethylsilyl azides in the presence of chromium(salen) catalysts has been successfully demonstrated, kinetic resolution using carbon dioxide as the ring-opening agent has yet to be established.

1.5.4. Metal-free catalysts for the conversion of epoxides to cyclic carbonates

Although tetrabutylammonium halides are usually used as co-catalysts,[2,3,6] they do exhibit catalytic activity when used alone. Caló et al. demonstrated that using molten **8a** as solvent effectively converts mono-substituted epoxides to cyclic carbonate (Scheme 7). (Phenoxymethyl)-ethylene carbonate was obtained in 90 % yield in one hour (1.0 atm CO_2, 120 °C, 20 g substrate, 50 g tetrabutylammonium halide). The bromide anion is thought to attack the less hindered end of the epoxide, generating an activated oxo-species which then reacts with CO_2 and ring-closes to afford cyclic carbonate product (Scheme 8).[48]
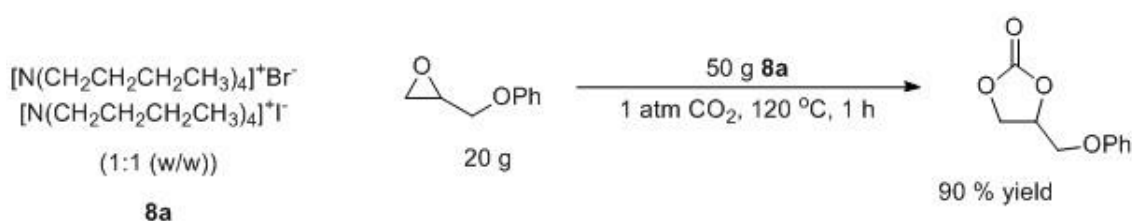
Scheme 7: Synthesis of (phenoxymethyl)ethylene carbonate by Caló et al.[48]
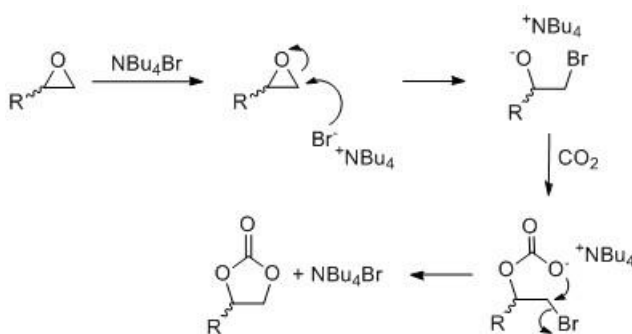
Scheme 8: Postulated mechanism for the formation of cyclic carbonate from epoxides and CO_2 using molten tetrabutylamonium halides as catalyst, showing nucleophilic attack at the unsubstituted position of the epoxide.[48]

Aoyagi, Furusho, and Endo later demonstrated the synthesis of cyclic carbonates under ambient conditions using ammonium iodide **8b** in the presence of 1-methyl-2-pyrrolidone as solvent (Scheme 9). (Phenoxymethyl)-ethylene carbonate was obtained in 85 % yield (1 atm CO_2, 25 °C, 24 h, 5 mol % **8b** w.r.t. epoxide, 0.2 mL 1-methyl-2-pyrrolidone as solvent). The yield was increased to 97 % at 45 °C.[49]
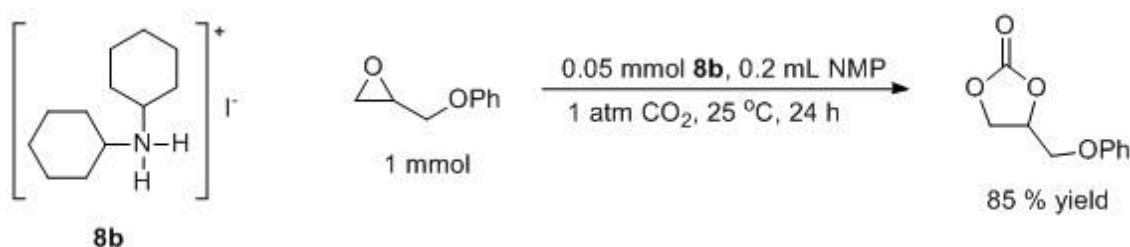
Scheme 9: Synthesis of (phenoxymethyl)ethylene carbonate by Aoyagi, Furusho, and Endo.[49]

Continuation of the above work showed that when secondary alcohols were used as solvent instead of 1-methyl-2-pyrrolidone, phosphonium iodide **8c** performed better than ammonium iodide **8b**. The catalytic system was remarkably active even under ambient conditions (Scheme 10). The use of 2-propanol and 1-methoxy-2-propanol as solvent produced optimal conversions to cyclic carbonate (97 % and 99 % yield of (phenoxymethyl)ethylene carbonate respectively, 1 atm CO_2, 25 °C, 24 h, 5.0 mol % **8c** w.r.t. epoxide, 0.2 mL solvent). In contrast, the yield of (phenoxymethyl)ethylene carbonate dropped drastically to 2 % when 1-methyl-2-pyrrolidone was used as solvent instead. Thus the authors postulated that the solvent activates the epoxide *via* hydrogen bonding. Meanwhile, the identity of the halide anion was demonstrated to be crucial to catalyst activity since it was responsible for both epoxide activation and leaving during the ring-closing step.[50]
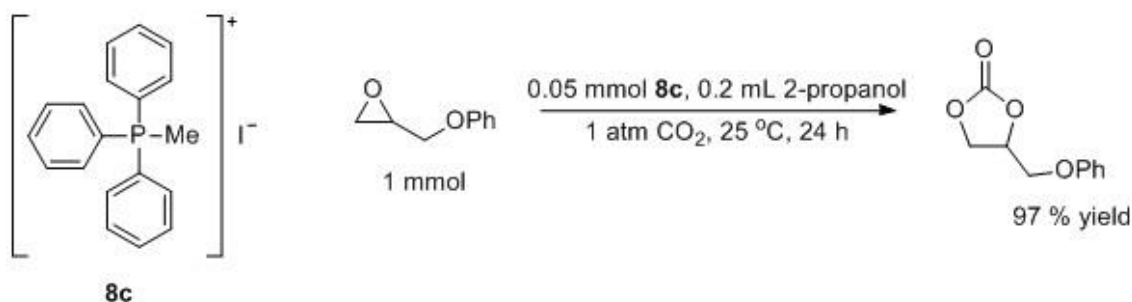
Scheme 10: Synthesis of (phenoxymethyl)ethylene carbonate by Aoyagi, Furusho, and Endo.[50]

It is unclear if kinetic resolution is possible with metal-free catalysts since no mention is made of enantioselectivity. However, the lack of chirality in ammonium and phosphonium salts studied to date forbids the formation of a diastereomeric catalyst-substrate transition state and therefore discrimination between enantiomers would be impossible.

1.5.5. Summary of literature precedent

Table 1 provides a summary of selected literature prior to the start of this project. We postulate that the ability of cobalt(salen) complexes to carry out a kinetic resolution may be caused by two fundamental differences - thus leading to our two hypotheses as given on page 3. Following synthesis and characterisation of the proposed metal(salen) complexes shown on page 7, we will make use of kinetic analyses and X-ray structure analysis to test the two hypotheses. Greater understanding of the subject will facilitate later enhanced catalyst design.

Table 1: Synthesis of cyclic carbonates from epoxides and CO_2 using aluminium, cobalt, chromium, zinc, and alternative metal-free catalysts.

Entry	Catalyst ([mol %])	Co-catalyst ([mol %])	Pressure (atm)	Temperature (°C)	t (h)	Conversion (%) (product)	% ee of cyclic carbonate	k_{rel}	Reference
1	**5a** (2.5)	TBAB (2.5)	1.0	25	6.7	*ca.*10 (SC)	-		[6]
2	**5b** (2.5)	TBAB (2.5)	1.0	25	6.7	*ca.* 50 (SC)	-		[6]
3	**5c** (2.5)	-	1.0	25	6	97 (SC)	-		[43]
4	**5d** (NA)	-	1.0	25	20	69 (SC)	-		[46]
5	**5e** (0.025)	-	19.7	100	4	89 (PC)	-		[7]
6	**6a** (0.1)	TBAC (0.2)	15.0	0	15	40 (PC)	70	8.99	[2]
7	**6a** (0.1)	TBAC (0.5)	1.0	-20	18	36 (PC)	65	6.69	[3]
8	**6b** (0.05)	PPN+DNP- (25.0)	8.2	-25	12	10 (PC)	97	75.58	[4]
9	**6c** (0.1)	BMIOH (0.01)	5.0	25	3	45 (PC)	83	21.79	[51]
10	**6d** (1.0)	-	10.0	25	14	65 (PC)	25	3.09	[5]
11	**7a** (1.0)[a]	DMAP (1.0)	3.5	75	1.5	100 (PC)	-		[8]
12	**7b** (0.075)[a]	DMAP (0.075)	6.8	75	2	19 (PC)	-		[8]
13	**7c** (0.05)	DMAP (0.1)	14.8	40	3	93 (PC)	-		[53]
17	**7d** (0.02)	-	19.7	80	1	42 (PC)	-		[54]
18	**8a** (bulk)	-	1.0	120	1	90 (PMEC) 84 (SC)	-		[48]
19	**8b** (5.0)	-	1.0	45	24	97 (PMEC)	-		[49]
20	**8c** (5.0)	-	1.0	25	24	97 (PMEC)	-		[50]

[a]0.5mL of CH_2Cl_2 added to solubilise catalyst.

2. Results and Discussion

2.1. Hypothesis 1: The rate is second-order w.r.t. enantioselective metal(salen) catalysts only

Jacobsen observed a second-order rate dependence with the studied cobalt(salen) catalysts (as well as good fit to assumed first-order dependence on substrate) from which it was deduced that the transition state involved two catalyst molecules.[1,9] Given the similarities between the hydrolytic kinetic process and the ring-opening of epoxides to form cyclic carbonates, we hypothesised that cobalt(salen) catalysts exhibit stereoselectivity due to a similar stepped *bimetallic transition structure*, which would present as a second-order rate dependence on catalyst. Meanwhile, we would expect first-order rate dependence on non-enantioselective catalysts. This hypothesis is dependent on the assumption that the rate-determining step is the ring-opening of the epoxide using carbon dioxide as the ring-opening agent.

2.1.1. Enantioselectivity of aluminium(salen) catalysts

Our initial plan was to study both propylene oxide and styrene oxide as substrates in accordance with much of the available literature. However, propylene oxide (b.p. 34 °C) was quickly lost during sampling. On the other hand, while styrene oxide performed well as substrate in previous studies by the group in Newcastle University, the reactivity was inexplicably much decreased in our facilities in York (Table 2, Entry 1 and 2). ^{1}H NMR analysis showed that our substrate had not decomposed, and distillation of styrene oxide in order to remove any impurities did not improve conversions. The reaction was then repeated with both freshly purchased substrate (Table 2, Entry 3 and 4), and a second batch of catalyst **5b** (Table 2, Entry 5 and 6) with no success. Photolysis of styrene carbonate back to the epoxide at 254 nm, previously reported by White and Ma, was dismissed when the exclusion of light did not increase conversions (Table 2, Entry 7).[57]

Since we could not explain the loss of activity for styrene oxide as substrate, we proceeded to screen different substrates (Table 2). As the reaction was performed neat, in each case the epoxide acts not only as substrate but also as

solvent, at least when epoxide is present in excess in the initial stages. For convenience, we desired to obtain 50 % conversion to cyclic carbonate in 3 h, which would enable us to monitor the reaction to completion over the course of a day. The substrate phenyl glycidyl ether (Table 2, Entry 18) was eventually identified as being suitable for further kinetic runs.
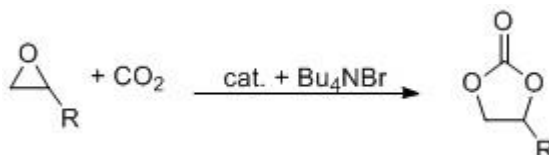
Figure 4: General scheme for the conversion of epoxides to cyclic carbonates.

Table 2: Synthesis of cyclic carbonates catalysed by 5b (2.5 mol % w.r.t. substrate) and tetrabutylammonium bromide (2.5 mol % w.r.t. substrate) at 25 °C and 1 atm CO_2.

Entry	R	Conversion to cyclic carbonate (%)[a]	
		3 h	24 h
1	Ph	23[b]	72[c]
2	Ph	17[d]	70[d]
3	Ph	21[e]	-
4	Ph	21[f]	-
5	p-ClC$_6$H$_5$	27	68
6	p-BrC$_6$H$_5$	28	70
7	CH$_2$CH$_3$	100	-
8	CH$_2$Cl	61	93
9	CH$_2$OH	39	85
10	CH$_2$OPh	51	75
11	C$_4$H$_9$	78	100
12	C$_8$H$_{17}$	14	80
13	C$_{10}$H$_{23}$	9	100

[a]Conversions to cyclic carbonate were obtained by ^{1}H NMR.

[b]The yield previously reported in the group (1 atm CO_2, 26 °C, 2.5 mol % Al(III) w.r.t. epoxide, 2.5 mol % tetrabutylammonium bromide w.r.t. epoxide) was 62 %.

[c]The yield previously reported in the group (1 atm CO_2, 26 °C, 2.5 mol % Al(III) w.r.t. epoxide, 2.5 mol % tetrabutylammonium bromide w.r.t. epoxide) was 98 %.

[d]New substrate was purchased from Sigma Aldrich.

[e]Second batch of catalyst **5b**.

[f]Reaction vessel was covered in foil to prevent photolysis.

Enantioselectivity testing was carried out using the selected substrate to establish the ability of aluminium(salen) catalysts to carry out a kinetic resolution. Since cyclic carbonate formation is performed neat, the composition of the reaction mixture changes from being largely epoxide to being largely cyclic carbonate over the course of the reaction. This drastic change in composition may affect rate dependence on substrate.[58] As such a k$_{rel}$ value has been calculated for each sample taken.

We confirmed that aluminium(salen) complexes are unable to kinetically resolve styrene oxide, in agreement with previous research (Table 3, Entries 1 to 4).[34,59] To our surprise, however, our aluminium(salen) complexes (Figure 5) demonstrated enantioselectivity with phenyl glycidyl ether (Table 3, Entries 5 to 12). Encouraged by this result, we tested *N*-(2,3-epoxypropyl)diphenylamine, which until then had been unexplored within the group. Despite a significant improvement in enantioselectivity with *N*-(2,3-epoxypropyl)diphenylamine (Table 3, Entries 13 to 20), further studies were performed with phenyl glycidyl ether due to its commercial availability at low cost.

2a: X = Cl
2b: X = OAc
2c: X = OTs

5b
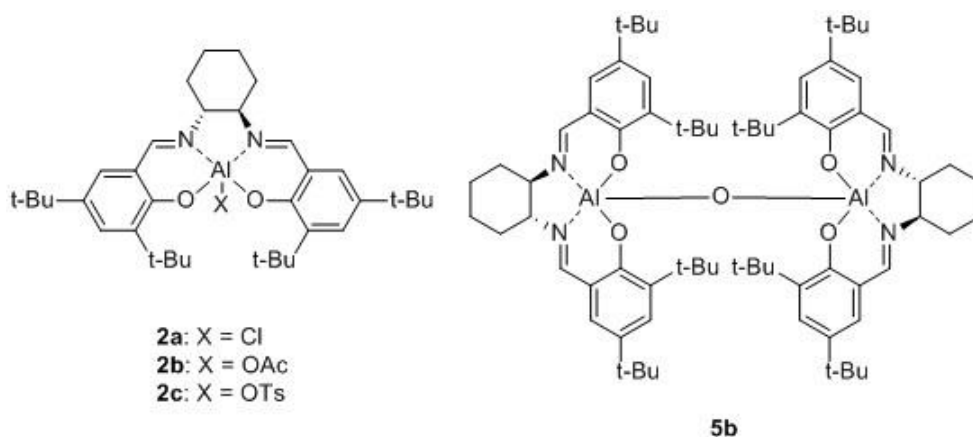
Figure 5: Structures of aluminium(salen) complexes 2a to 2c and 5b.

We consistently found that all catalysts produced cyclic carbonate in favour of the second peak eluted by chiral HPLC (Table 3, enantiomeric ratios). In addition, catalyst **2a** gave the highest conversions without sacrificing enantioselectivity (Table 3, Entries 6, 10, 14, and 18). Meanwhile, catalyst **2c** had the lowest level of activity and extended running times were sometimes required in order to obtain significant conversion (Table 3, Entries 3, 7, 11, 15, and 19). In addition, lowered reaction temperatures decreased conversions but successfully improved enantioselectivity across both phenyl glycidyl ether and *N*-(2,3-epoxypropyl)diphenylamine and across all catalysts (Table 3, Entries 5 to 20). This is expected of a typical kinetic resolution as lower temperatures decrease the energy available for activation of the disfavoured enantiomer to a greater extent compared to the favoured enantiomer.

Table 3: Activity and enantioselectivity of aluminium(salen) catalysts, 2a, 2b, 2c and 5b, (2.5 mol %) and tetrabutylammonium bromide (2.5 mol %) under solvent-free conditions.

Entry	Catalyst	R	Time (h)	Temp (°C)	Conversion (%)	% ee of epoxide	e.r. of cyclic carbonate[c]	% ee of cyclic carbonate	k_{rel}^d
1	2a	Ph[a]	3	25	21.4	NA[e]	47: 53	5	1.13
2	2b	Ph	3	25	28.0	NA[e]	50: 50	0	1.01
3	2c	Ph	3	25	6.6	NA[e]	47: 53	6	1.14
4	5b	Ph	3	25	21.0	NA[e]	48: 52	4	1.08
5	2a	CH_2OPh[b]	1	25	34.8	7.0	42: 58	17	1.52
6	2b	CH_2OPh	1	25	40.7	NA[f]	39: 61	22	1.82
7	2c	CH_2OPh	1	25	3.7	NA[f]	32: 68	37	2.18
8	5b	CH_2OPh	1	25	33.5	NA[f]	40: 60	20	1.66
9	2a	CH_2OPh	24	0	17.2	10.2	25: 75	49	3.26
10	2b	CH_2OPh	24	0	35.5	NA[f]	23: 77	53	4.32
11	2c	CH_2OPh	72	0	8.2	NA[f]	21: 78	56	3.77
12	5b	CH_2OPh	42	0	25.1	NA[f]	25:75	51	3.63
13	2a	CH_2NPh_2[b]	4	25	35.5	NA[e]	16: 84	69	7.73
14	2b	CH_2NPh_2	4	25	55.8	NA[e]	23: 77	53	6.43
15	2c	CH_2NPh_2	18	25	19.0	NA[e]	21: 79	58	4.32
16	5b	CH_2NPh_2	4	25	58.6	NA[e]	27: 73	47	5.27
17	2a	CH_2NPh_2	24	0	11.2	NA[e]	8: 92	85	13.70
18	2b	CH_2NPh_2	24	0	14.8	NA[e]	7: 93	86	15.38
19	2c	CH_2NPh_2	64	0	13.9	NA[e]	10: 90	80	10.70
20	5b	CH_2NPh_2	24	0	2.9	NA[e]	8: 92	84	11.63

[a]Conversions to cyclic carbonate were obtained by ^{1}H NMR.

[b]Conversions to cyclic carbonate were obtained by HPLC.

[c]e.r. values were obtained by chiral HPLC and correspond to area under first peak: area under second peak. [d]k_{rel} is calculated as $\frac{\ln[1-c(1+ee)]}{\ln[1-c(1-ee)]}$. [e]The epoxide could not be resolved on our existing HPLC columns. [f]The substrate was not detected due to decomposition in the time taken for HPLC analysis.

The inability of our aluminium(salen) complexes to kinetically resolve styrene oxide may be attributed to the proximity of the phenyl functional group. Although the prevailing theory is that terminal epoxides undergo attack at the unhindered end (Figure 6, route A),[59] this may not hold true for styrene oxide. Nucleophilic attack at the CH site, which is more electrophilic, may be favoured over attack at the CH_2 site (Figure 6, route B), thus producing a conjugated intermediate. Since the intermediate formed from phenyl glycidyl ether lacks the stabilising effect of such conjugation, we might expect differences in mechanism between the two substrates. Since earlier research indicates a first-order dependence on styrene oxide, which was not kinetically resolved, we decided to determine if a second-order rate-dependence on phenyl glycidyl ether would be observed.
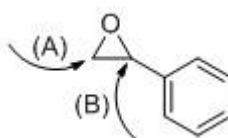
Figure 6: Two possible routes for nucleophilic attack on styrene oxide.

It is also plausible that catalyst-substrate interaction may be influenced by steric effects. In phenyl glycidyl ether, the bulky phenyl group projects further out than in styrene oxide. In *N*-(2,3-epoxypropyl)diphenylamine, the presence of two phenyl groups would further increase steric hindrance during epoxide activation. Alternatively, the presence of a heteroatom may be sufficient to induce a kinetic resolution.

We then carried out an experiment investigating the variation of ee against conversion using the conditions used for Table 3, Entry 16, for which the catalyst (**5b**) was determined to have a k_{rel} of 5.27. The calculations for the theoretical curve are based on the assumption that the system exhibits a first-order rate dependence on substrate. Although the determination of k_{rel} from known conversions and ee values is elementary, calculations to obtain conversion or ee values from a known k_{rel} value are by no means as simple and require the help of an online graphing calculator (Figure 7, in green). Our data obtained from experiments done in duplicate (Figure 7, in blue and red) fits well to the calculated data. We therefore report the first instance of catalyst **5b** successfully demonstrating the ability to carry out a classical kinetic resolution.
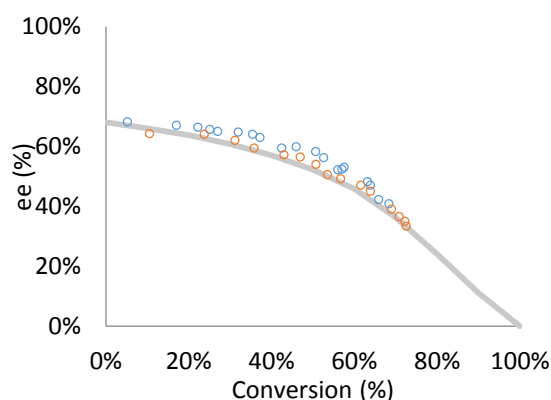
Figure 7: Observed ee of 4-*(N,N*-diphenylaminomethyl)-1,3-dioxolan-2-one against conversion for two separate runs (blue and red). Both reactions were carried out using catalyst 5b (k_{rel} 5.27, 2.5 mol %) and tetrabutylammonium bromide (2.5 mol %) under solvent-free conditions. The reactions were carried out at 25 °C and 1 atm CO_2 and monitored over 8 h by HPLC. The theoretical ee against conversion for a catalyst with k_{rel} 5.27 is shown in green and is obtained by plotting $5.27 = \frac{\ln(1-c(1+ee))}{\ln(1-c(1-ee))}$ on the Desmos Graphing Calculator.[60]

2.1.2. Order of reaction w.r.t. aluminium(salen) catalysts

In kinetic analyses, we began with the rate equation (Eqn. 1) given as follows, where the orders of reaction *a*, *b*, *c*, and *d* are unknown. This assumes that there is no back reaction which is consistent with experimental findings and the highly negative heat of reaction.[6,61]

$$rate \; = \; k[epoxide]^a[CO_2]^b[catalyst]^c[Bu_4NBr]^d \; - \; \text{Eqn. 1}$$

Since CO_2 is present in large excess, the concentration of CO_2 remains unchanged over the course of a reaction. Catalyst and Bu_4NBr concentrations also remain constant throughout the run. We thus have a simplified rate equation that is applicable for each catalyst screened.

$$rate \; = \; k_{obs}[epoxide]^a, where \; k_{obs} \; = \; k[CO_2]^b[catalyst]^c[Bu_4NBr]^d$$

The application of logarithms to both sides gives Eqn. 2 below.

$$\ln k_{obs} \; = \; \ln k \; + \; b\ln[CO_2] \; + \; c\ln[catalyst] \; + \; d\ln[Bu_4NBr] \; - \; \text{Eqn. 2}$$

By keeping $[Bu_4NBr]$ constant and under the assumption that carbon dioxide diffuses into the bulk solution at a much faster rate than the rate of cyclic carbonate formation, Eqn. 2 simplifies to Eqn. 3, where the unknown constant *c* is the order of reaction w.r.t. catalyst.

$$\ln k_{obs} \; = \; c\ln[catalyst] + k',$$
$$where \; k' \; = \; \ln k + \; b\ln[CO_2] \; + \; d\ln[Bu_4NBr] \; - \; \text{Eqn. 3}$$

A plot of ln k_{obs}, which is experimentally derived, against ln[catalyst], gives the constant *c* (order of reaction w.r.t. catalyst) as the gradient of the resultant line. As kinetic analyses using catalyst **5b**, and styrene oxide as substrate have already been performed,[34,59] we decided to carry out our kinetic analysis with catalyst **5b**, and with phenyl glycidyl ether as substrate.

Unlike our substrate screening where the bulk of the reaction mixture changes drastically from epoxide to cyclic carbonate, in performing kinetic runs a solvent is necessary. Solvents were chosen according to literature precedent showing

that solvents containing carbonyl functional groups were better able to solubilise CO_2.[62] Preliminary screening for the conversion of phenyl glycidyl ether to cyclic carbonate in ethyl acetate (0.5 mL) showed significant solvent loss *via* evaporation. As such, ethylene carbonate (b.p. 248 °C)[10] (Figure 8, blue) and propylene carbonate (b.p. 242-243 °C)[10] (Figure 8, red) were tested as solvent. As ethylene carbonate is a solid, the corresponding reaction was carried out at 45 °C. Since both reactions failed to reach completion in a suitable timescale, we then tested the use of propylene carbonate at 45 °C as well (Figure 8, green), which was found agreeable as approximately three half-lives could be observed over 8.5 h. These reactions were performed in open 28 mL borosilicate glass vials in a water bath.

Reaction performed in 0.5 mL propylene carbonate, 25 °C
Reaction performed in 0.5 mL ethylene carbonate, 45 °C
Reaction performed in 0.5 mL propylene carbonate, 45 °C
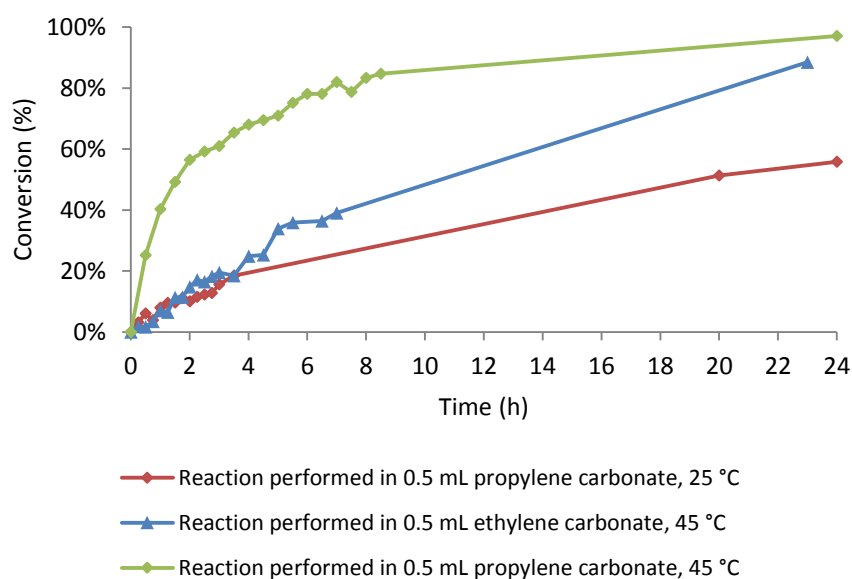
Figure 8: Addition of carbon dioxide to phenyl glycidyl ether catalysed by complex 5b (2.5 mol %)[6] and tetrabutylammonium bromide (2.5 mol %) in solvent. The reaction was monitored by ^{1}H NMR.

In order to determine k_{obs}, we needed to first determine the order of reaction w.r.t. epoxide. From Figure 8 it is evident that order of reaction w.r.t. epoxide (the constant *a*) is not zero since a linear fit is not observed. Assuming a first-order rate dependence on epoxide, the differential rate law (Eqn. 4) follows:

$$rate = k_{obs}[epoxide]^1 = -\frac{d[epoxide]}{dt}$$

$$\text{Hence,} \quad \frac{d[epoxide]}{[epoxide]} = -k_{obs}dt \quad - \text{ Eqn. 4}$$

Integration on both sides gives:

$$\int \frac{1}{[epoxide]} d[epoxide] = -\int k_{obs} dt$$
$$\ln[epoxide] = -k_{obs}t + C$$

At t = 0, $\ln[epoxide]_0 = C$.
Hence, $\ln epoxide = \ln[epoxide]_0 - k_{obs}t$

The plot of ln[epoxide], which was experimentally derived, against time, closely approximated first-order rate dependence on substrate as indicated by the R^2 value of 0.9929 (Figure 9). In contrast, the R^2 values for the zero- and second-order rate dependence on epoxide indicated considerably poorer fit. Further information about duplicate runs may be found in Appendix A.
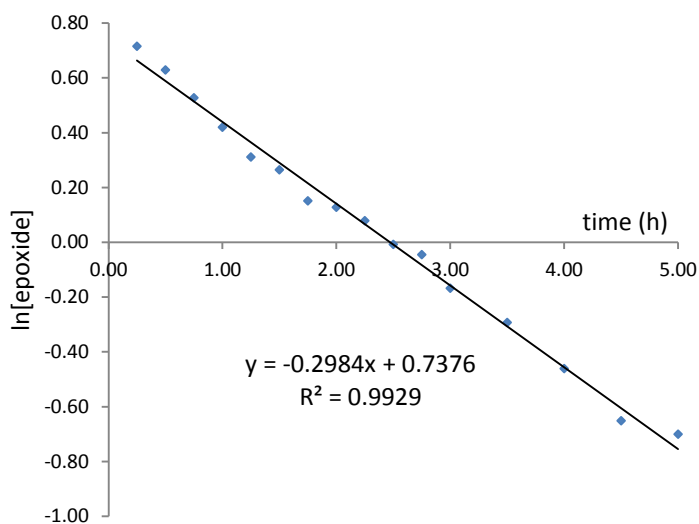
R^2	Order of reaction
0.9320	0
0.9929	1
0.9638	2

y = -0.2984x + 0.7376
R^2 = 0.9929

Figure 9: Plot of ln[epoxide] against time for the addition of carbon dioxide to phenyl glycidyl ether (1.66 mmol) catalysed by complex 5b (2.5 mol %) and tetrabutylammonium bromide (2.5 mol %) in propylene carbonate as solvent (0.5 mL). The reaction was carried out at 45 °C and 1 atm CO_2 and monitored over 5 h by HPLC.

As previous research within the group showed a first-order rate dependence on catalyst **5b** using styrene oxide as substrate and propylene carbonate (5 equiv. v/v) as solvent,[59] our preference would have been to use parallel conditions in the conversion of phenyl glycidyl ether. Unfortunately, although our initial screening in propylene carbonate produced strong evidence for the first-order rate dependence on substrate (Figure 9), reproducibility was problematic. Runs performed under the same conditions (1.66 mmol of phenyl glycidyl ether, 2.5

mol % catalyst **5b**, 2.5 mol % tetrabutylammonium bromide in 0.5 mL propylene carbonate at 45 °C and 1 atm CO_2) gave a range of k_{obs} values ranging from 0.3742 to 0.2173 mol dm^{-3} h^{-1} (Figure 10).

[5b]/mol dm^{-3}	k_{obs}/mol dm^{-3} h^{-1}
0.02875	0.2940
0.05761	0.3742
0.05761	0.2173
0.05761	0.2977
0.08648	0.1847
0.1152	0.3539
0.1152	0.2290

Figure 10: Double logarithmic plot to determine order of reaction w.r.t. catalyst 5b. (2.5 mol % tetrabutylammonium bromide, 1 atm CO$_2$, 25 °C, 2 vol. equivalents of propylene carbonate as solvent). As the reaction mixture was not homogeneous, the data was not reproducible.

The lack of reproducibility was attributed to the incomplete dissolution of catalyst **5b** even at elevated temperatures (45 °C, 25 mg of catalyst in 1.0 mL of propylene carbonate). Addition of more solvent only served to slow reaction rates. Replacement of propylene carbonate with conventional solvents with good solvating power such as dichloromethane and ethyl acetate were also found to be unsuitable due to volatility issues. The use of condensation apparatus in a conventional setup with round-bottomed flasks was also ineffective due to a number of reasons. In comparison to the volume of solvent itself (2 mL), the volume of the entire setup was still too large to eliminate significant solvent loss over the course of the reaction. Furthermore, the use of low volumes in round-bottomed flasks made sampling very difficult.

We therefore resorted to using stoppered 28 mL borosilicate glass vials as reaction vessels, and selected *p*-cymene (b.p. 176 °C)[63] as solvent although the temperature had to be increased to 75 °C in order to perform kinetics in 8 hours. Despite the high b.p. of the solvent and the use of septa to prevent solvent loss, a steady decrease in solvent levels over 8 h was still observed. As such, only initial rates were used in further kinetic analysis.
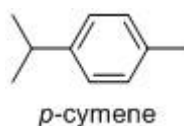
p-cymene

The final conditions were 1 atm CO_2, 75 °C, 20 vol. equivalents of *p*-cymene as solvent and 2.5 mol % of tetrabutylammonium bromide. By varying catalyst loading (2.5 mol %, 3.0 mol %, 4.0 mol % and 5.0 mol % of **5b** w.r.t substrate) a straight line with gradient 1.0628 was obtained. Since we had observed enantioselectivity with phenyl glycidyl ether (albeit under solvent-free conditions), we had expected a bimetallic transition state similar to Jacobsen's computation model, which would present as second-order rate dependence on catalyst. Instead, the gradient indicates first-order rate dependence on catalyst **5b**. This was in agreement with the rate against [**5b**] plot which approximated a straight line passing through the origin (Figure 11).
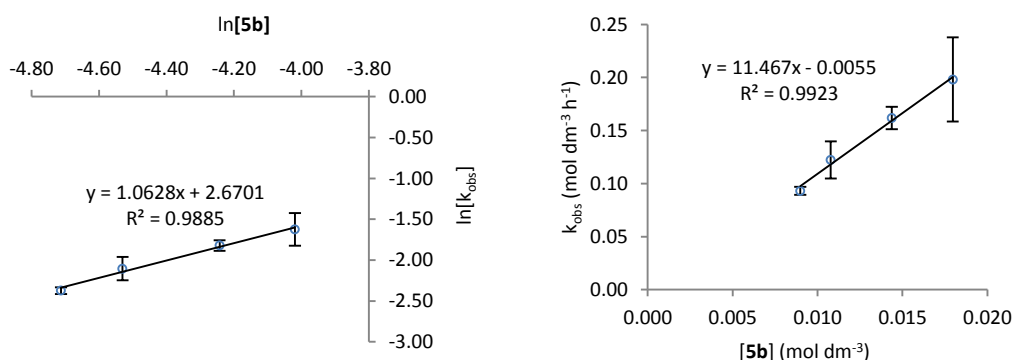
Figure 11: (*left*) Double logarithmic plot to determine order of reaction w.r.t catalyst 5b. (*right*) Linear plot to demonstrate first-order rate dependence on catalyst 5b. (2.5 mol % tetrabutyl-ammonium bromide, 1 atm CO_2, 75 °C, 20 vol. equivalents of *p*-cymene as solvent). Error bars are within a 95 % confidence interval. Each point shown is the mean of experiments done in duplicate.

Assuming that the addition of a solvent does not change the rate-determining step or the rate dependence on catalyst, the first-order rate dependence on **5b** indicated that the HKR process was not an accurate model for the synthesis of cyclic carbonate from epoxides and CO_2. Furthermore, while the aluminium-(salen) catalysts demonstrated enantioselectivity only with selected substrates, the cobalt(salen) complexes were enantioselective for all epoxides tested (Section 2.1.3). Evidently, our aluminium(salen) catalysts are dissimilar to Jacobsen's cobalt(salen) complexes.

29

2.1.3 Enantioselectivity of cobalt(salen) catalysts

Literature precedent has shown that cobalt(salen) catalysts are enantioselective for propylene oxide.[2-5,51] Our priority was therefore to establish enantioselectivity for phenyl glycidyl ether, which has a much bulkier functional group, using cobalt(salen) catalysts **3a** to **3d** (Figure 12). Figure 4 (General scheme for the conversion of epoxides to cyclic carbonates.) has been reproduced for easy reference. Although tetrabutylammonium bromide is active for the formation of cyclic carbonate, only racemic product was produced. No cyclic carbonate was observed in the absence of tetrabutylammonium bromide.

Unlike the aluminium(salen) catalysts, the cobalt(salen) catalysts did not produce a marked improvement in k_{rel} in changing the substrate from styrene oxide to phenyl glycidyl ether (Table 4, Entries 1 to 16). The increase in k_{rel} when the substrate was changed to *N*-(2,3-epoxypropyl)diphenylamine (Table 4, Entries 17 to 24) was also much smaller than that observed using our aluminium(salen) complexes. The cobalt(salen) system consistently produced cyclic carbonate in favour of the second isomer of 4-*(N,N*-diphenylamino-methyl)-1,3-dioxolan-2-one by chiral HPLC (Table 4, Entries 17 to 24), but the trend was less clear for styrene carbonate and (phenoxymethyl)ethylene carbonate.

Conversions were on the whole rather comparable across both classes of catalysts. Meanwhile, lowering the temperature to 0 °C decreased conversions, but did not significantly improve k_{rel} values. It appears that the cobalt(salen) complexes are indeed dissimilar to the aluminium(salen) complexes in that the aluminium(salen) complexes were more dependent on both substrate and temperature. However, given literature precedent it is unexpected that our cobalt(salen) complexes were considerably less enantioselective than the aluminium counterparts in the conversion of phenyl glycidyl ether and *N*-(2,3-epoxypropyl)diphenylamine.

30
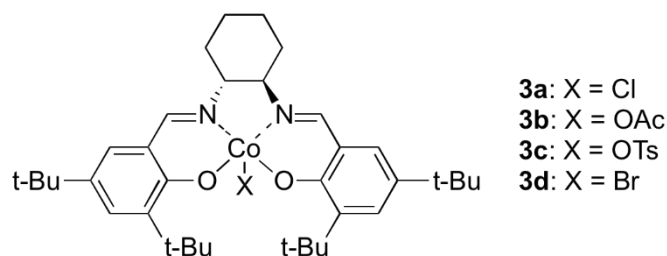
Figure 12: Structures of cobalt(salen) complexes 3a to 3d.

3a: X = Cl
3b: X = OAc
3c: X = OTs
3d: X = Br
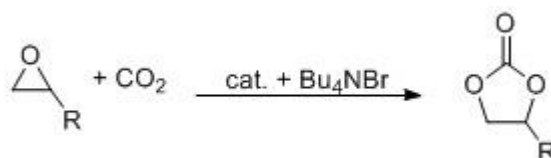
Figure 4: General scheme for the conversion of epoxides to cyclic carbonates.

Table 4: Activity and enantioselectivity of cobalt(salen) catalysts 3a to 3d (2.5 mol %) and tetrabutylammonium bromide (2.5 mol %) under solvent-free conditions.

Entry	Catalyst	R	Time (h)	Temp (°C)	Conversion (%)	e.r. of cyclic carbonate[c]	% ee of cyclic carbonate	k_{rel}[d]
1	3a	Ph[a]	6	25	66.8	45: 55	10	1.43
2	3b	Ph	6	25	69.3	56: 44	11	1.53
3	3c	Ph	6	25	24.0	48: 52	4	1.10
4	3d	Ph	6	25	68.0	53: 47	7	1.28
5	3a	Ph	24	0	59.0	48: 52	4	1.13
6	3b	Ph	24	0	46.3	52: 48	4	1.13
7	3c	Ph	24	0	31.0	53: 47	6	1.16
8	3d	Ph	24	0	47.1	53: 47	6	1.19
9	3a	CH$_2$OPh[b]	3	25	22.7	51: 49	1	1.03
10	3b	CH$_2$OPh	3	25	72.8	53: 47	7	1.32
11	3c	CH$_2$OPh	3	25	29.9	57: 43	14	1.41
12	3d	CH$_2$OPh	3	25	72.4	55: 45	11	1.56
13	3a	CH$_2$OPh	24	0	20.7	52: 48	4	1.09
14	3b	CH$_2$OPh	24	0	17.3	48: 52	3	1.08
15	3c	CH$_2$OPh	24	0	55.1	56: 44	11	1.42
16	3d	CH$_2$OPh	24	0	56.1	53: 47	7	1.23
17	3a	CH$_2$NPh$_2$[b]	6	25	36.1	41: 59	18	1.59
18	3b	CH$_2$NPh$_2$	6	25	49.5	43: 57	15	1.52
19	3c	CH$_2$NPh$_2$	6	25	29.8	41: 59	18	1.54
20	3d	CH$_2$NPh$_2$	6	25	44.1	36: 64	27	2.13
21	3a	CH$_2$NPh$_2$	24	0	8.3	32: 68	36	2.20
22	3b	CH$_2$NPh$_2$	24	0	21.0	33: 67	35	2.26
23	3c	CH$_2$NPh$_2$	64	0	16.5	39: 61	21	1.61
24	3d	CH$_2$NPh$_2$	24	0	34.2	41: 59	19	1.60

[a]Conversions to cyclic carbonate were obtained by ^{1}H NMR.

[b]Conversions to cyclic carbonate were obtained by HPLC.

[c]e.r. values were obtained by chiral HPLC and correspond to area under first peak: area under second peak.

[d]k_{rel} is calculated as $\frac{\ln[1-c(1+ee)]}{\ln[1-c(1-ee)]}$.

2.1.3. Order of reaction w.r.t. cobalt(salen) catalysts

The rate equation for the conversion of epoxides to cyclic carbonates in the presence of cobalt(salen) catalysts may be given as

$$\ln k_{obs} = c \ln[catalyst] + k', \qquad where\ k' = \ln k + b \ln[CO_2] + d \ln[Bu_4NBr]$$

As shown in Section 2.1.2, a plot of ln k_{obs}, which is experimentally derived, against ln[catalyst], gives the constant c (i.e. order of reaction w.r.t. catalyst) as the gradient. We attempted to preserve reaction conditions used in Section 2.1.2, Figure 11 (1 atm CO_2, 75 °C, and 20 vol. equivalents of p-cymene as solvent). However, catalyst **3c** failed to fully dissolve under the same conditions. Additionally, the epoxide was prone to ring-opening with water as shown in Figure 13.
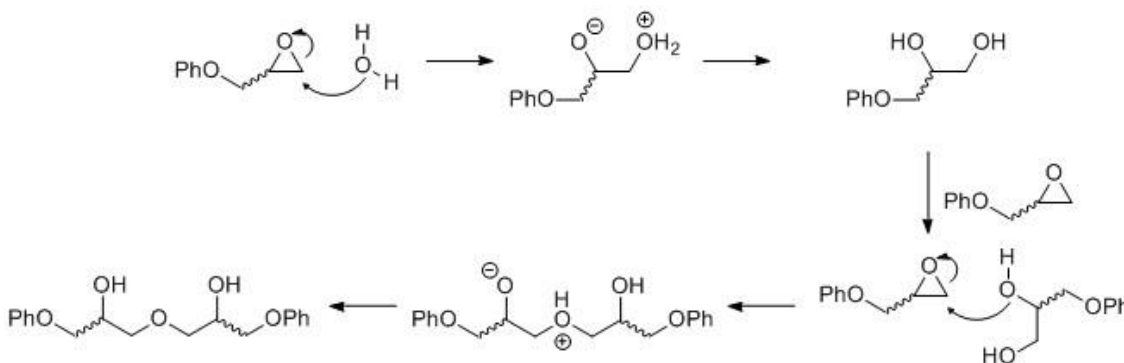
Figure 13: Possible mechanism for the ring-opening of phenyl glycidyl ether in the presence of a small amount of water. Product and possible isomers have been isolated and identified by ESI-MS, ^{1}H NMR, and ^{13}C NMR.

As such alternative conditions of 1 atm CO_2, 25 °C, and 20 vol. equivalents of ethyl acetate as solvent had to be selected. Care was taken to exclude moisture from the experimental setup. A plot of ln[epoxide] against time showed good approximation to first-order rate dependence on substrate (Figure 14). We thus used first-order rate constants to determine order of reaction with respect to catalyst.
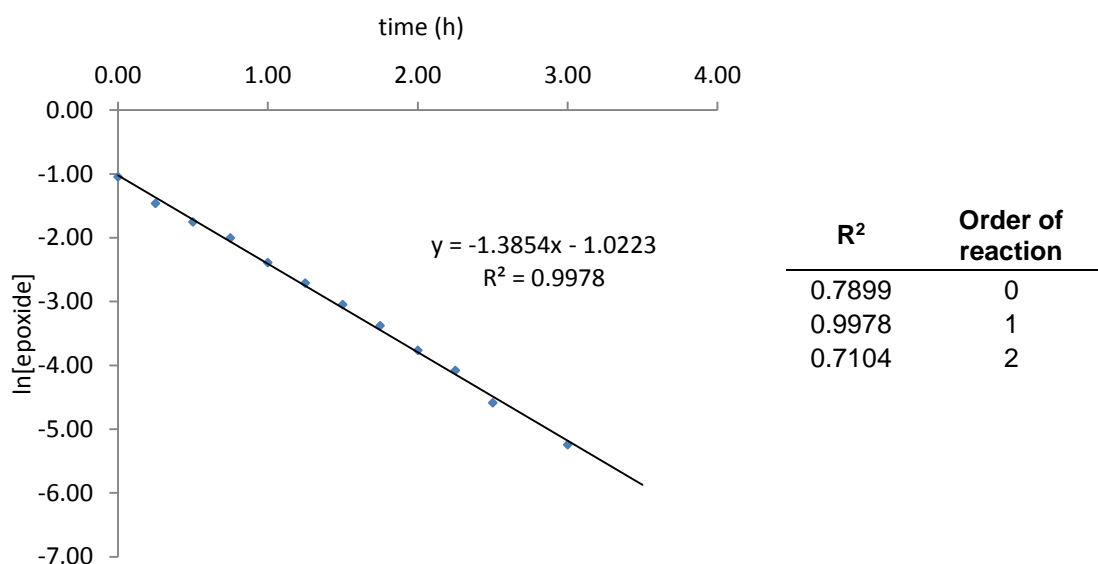
Figure 14: Plot of ln[epoxide] against time for the addition of carbon dioxide to phenyl glycidyl ether (0.83 mmol) catalysed by complex 3c (2.5 mol %) and tetrabutylammonium bromide (10.0 mol %) in ethyl acetate as solvent (2.2 mL). The reaction was carried out at 25 °C and 1 atm CO_2 and monitored over 4 h by HPLC. A duplicate run gave a gradient of 1.4216 with an R^2 value of 0.9978, proving good reproducibility between runs.

However, when the co-catalyst was present in less than equimolar amounts w.r.t. **3c**, e.g. 3.75 mol % **3c** and 2.5 mol % co-catalyst, no conversion was observed. Therefore, in order to facilitate variation in catalyst loading, the amount of co-catalyst had to be increased to 10.0 mol %. We then performed kinetic analyses for 1.0 mol %, 2.5 mol % and 5.0 mol % **3c** w.r.t substrate to obtain the plot shown in Figure 15, which gave reproducible results, but not a straight line.
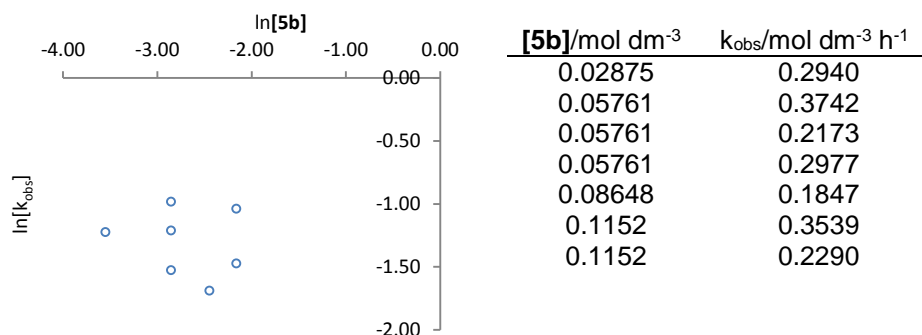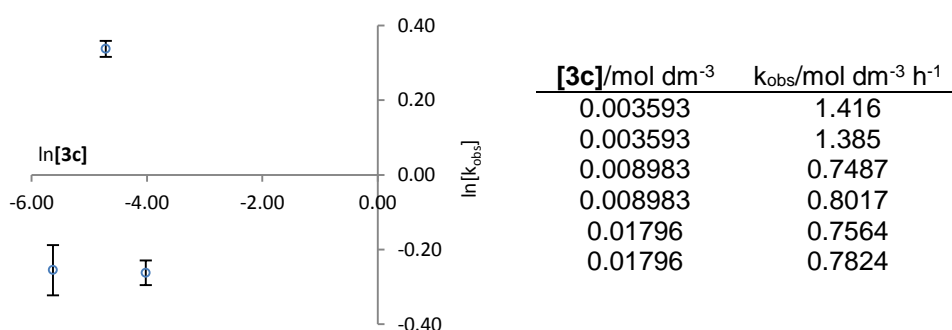

Figure 15: Double logarithmic plot to determine order of reaction w.r.t. catalyst 3c. (10.0 mol % tetrabutylammonium bromide, 1 atm CO_2, 25 °C, 20 vol. equivalents of ethyl acetate as solvent). Error bars are within a 95 % confidence interval. Each point shown is the mean of experiments done in duplicate.

As such we investigated the possible anion exchange of catalyst **3c** with tetrabutylammonium bromide to form potentially active species **3d**, which might

explain the inactivity of the catalyst system when the co-catalyst was the limiting reagent. Unfortunately, catalyst **3d** was inactive when used in the absence of co-catalyst. Nonetheless, we carried out further investigation with catalyst **3d** to eliminate the possibility of the OTs⁻ anion being active for cyclic carbonate formation.

Reactions with catalyst **3d** exhibited the same approximation to first-order rate dependence on epoxide (Figure 16). We carried out the same kinetic analyses for 1.0 mol %, 2.5 mol % and 5.0 mol % **3d** w.r.t substrate as we did with catalyst **3c** (Figure 17). However, despite the good reproducibility of the points as demonstrated in Figure 17, a good linear fit was still not established.
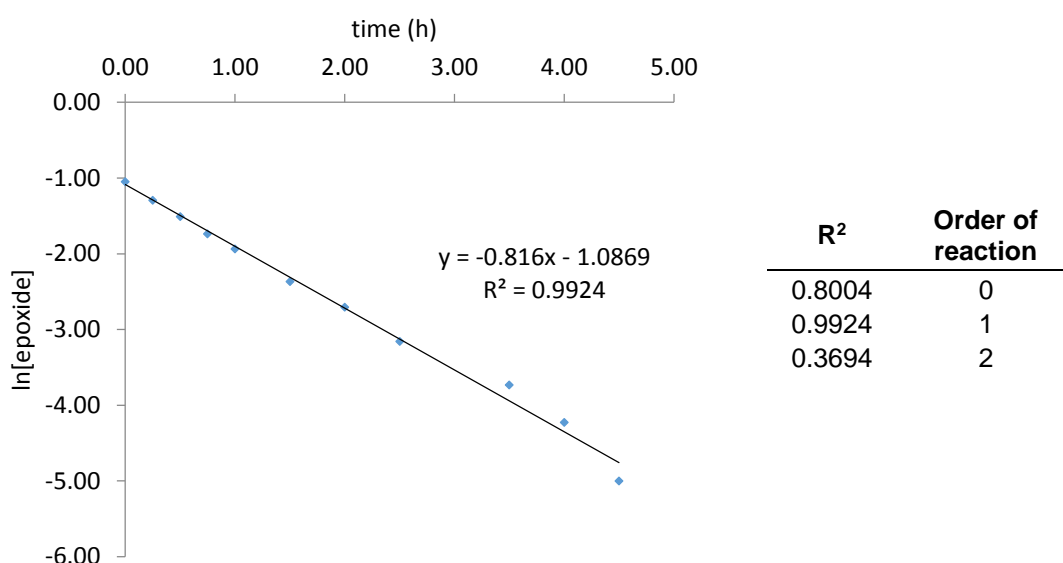
Figure 16: Plot of ln[epoxide] against time for the addition of carbon dioxide to phenyl glycidyl ether (0.83 mmol) catalysed by complex 3d (2.5 mol %) and tetrabutylammonium bromide (10.0 mol %) in ethyl acetate as solvent (2.2 mL). The reaction was carried out at 25 °C and 1 atm CO_2 and monitored over 4.5 h by HPLC. A duplicate run gave a gradient of 0.8909 with an R^2 value of 0.9836, proving good reproducibility between runs.

[3d]/mol dm^{-3}	k$_{obs}$/mol dm^{-3} h^{-1}
0.003593	0.27838
0.003593	0.24613
0.008983	0.89089
0.008983	0.81599
0.01796	0.79917
0.01796	0.91502
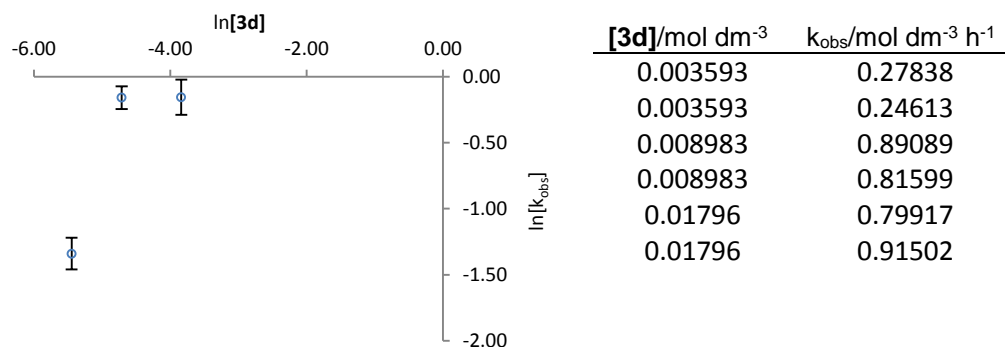
Figure 17: Double logarithmic plot to determine order of reaction w.r.t. catalyst 3d. (10.0 mol % tetrabutylammonium bromide, 1 atm CO$_2$, 25 °C, 20 vol. equivalents of ethyl acetate as solvent). Error bars are within a 95 % confidence interval. Each point shown is the mean of experiments done in duplicate.

Our next step was to treat the [**3d** + tetrabutylammonium bromide] system as one such that $\ln k_{obs} = c' \ln[3d + TBAB] + k''$, where the unknown constant c' now refers to the combined order of reaction for both components of the catalyst system. By subtracting the order of reaction w.r.t. tetrabutylammonium bromide only (to be found separately) from c', the order of reaction w.r.t. catalyst **3d** only can be obtained.

Catalyst **3d** loading was fixed at 2.5 mol % for the following kinetic runs at 2.5, 5.0, 10.0, and 15.0 mol % of tetrabutylammonium bromide. Excellent fit was observed for both the double logarithmic plot and the linear plot, indicating a first-order rate dependence on tetrabutylammonium bromide (Figure 18).
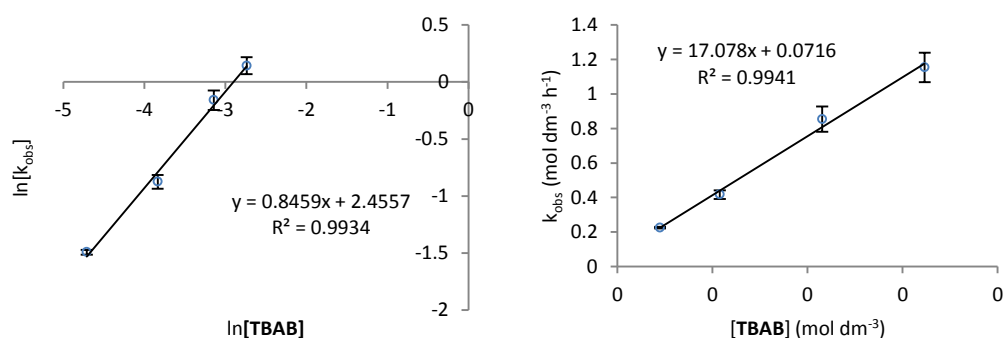
Figure 18: *(left)* Double logarithmic plot to determine order of reaction w.r.t tetrabutylammonium bromide. (*right*) Linear plot to demonstrate first-order rate dependence on tetrabutylammonium bromide. (1 atm CO$_2$, 25 °C, 20 vol. equivalents of ethyl acetate as solvent). Error bars are within a 95 % confidence interval. Each point shown is the mean of experiments done in duplicate.

Since the optimum rate was observed at 2.5 mol % of **3d** and 15.0 mol % of tetrabutylammonium bromide, this ratio was preserved when varying both **3d** and tetrabutylammonium bromide. Kinetics were then run using a 1:6 ratio of **3d** to co-catalyst (2.5 mol %, 3.3 mol %, and 5.0 mol % of **3d**). Once again, an

excellent fit was observed for both the double logarithmic plot and the linear plot, indicating that the combined order of reaction closely approximates 1 (Figure 19).
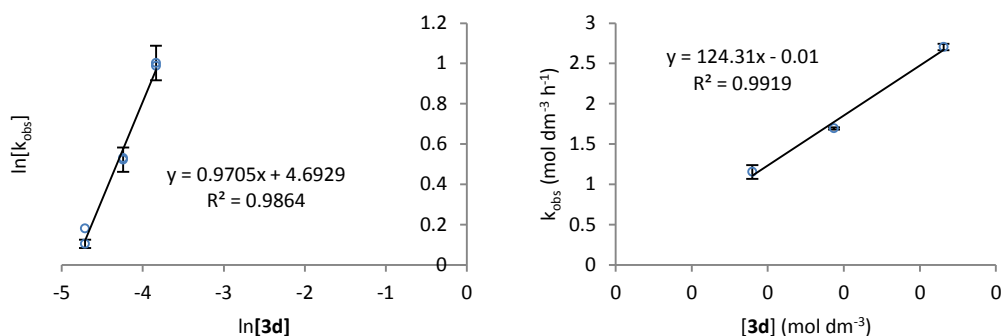
Figure 19: *(left)* **Double logarithmic plot to determine order of reaction w.r.t [3d + tetrabutylammonium bromide]. (***right***) Linear plot to demonstrate first-order rate dependence on the combined catalyst system. (1 atm CO$_2$, 25 °C, 20 vol. equivalents of ethyl acetate as solvent). Error bars are within a 95 % confidence interval. Each point shown is the mean of experiments done in duplicate.**

Since both the combined order and the order of reaction w.r.t. tetrabutylammonium bromide is 1, the order of reaction w.r.t. **3d** alone would appear to be **0**. However, we note that a 1:6 ratio of **3d** to tetrabutylammonium bromide may have saturated the system with co-catalyst, producing pseudo first-order kinetics.

To determine if this was the case, a fourth set of kinetics were performed. A constant 30.0 mol % of tetrabutylammonium bromide was used while varying catalyst **3d** (2.0 mol %, 3.0 mol %, 4.0 mol %, and 5.0 mol %). As tetrabutylammonium bromide is known to be active for the non-enantioselective ring-opening of epoxides,[48] a control was first performed, giving 6.0 % of (phenoxymethyl)ethylene carbonate after 24 h (30.0 mol % tetrabutylammonum bromide, 20 vol. equivalents of EtOAc, 25 °C, 1 atm anhydrous CO$_2$). This level of activity was deemed negligible.

Kinetic analysis afforded good linear approximation showing that the order of reaction w.r.t. catalyst **3d** is **1** (Figure 20), and that pseudo first-order kinetics had indeed been observed at 1:6 ratio of **3d** to co-catalyst. Therefore although cobalt(salen) catalysts are enantioselective for phenyl glycidyl ether, we were unable to demonstrate a second-order rate dependence on catalyst.

y = 0.8789x + 4.3024
R² = 0.99661

y = 110.94x + 0.1704
R² = 0.99797

ln[3d]

[3d] (mol dm⁻³)
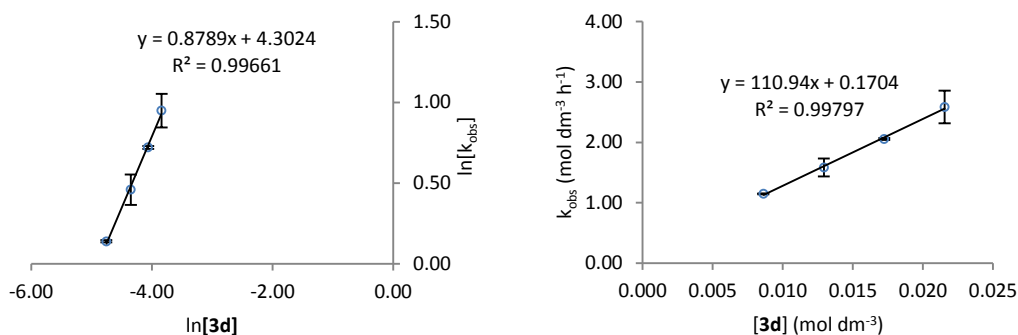
Figure 20: *(left)* **Double logarithmic plot to determine order of reaction w.r.t catalyst 3d. (*right*) Linear plot to demonstrate first-order rate dependence on catalyst 3d. (1 atm CO_2, 25 °C, 20 vol. equivalents of ethyl acetate as solvent). Error bars are within a 95 % confidence interval. Each point shown is the mean of experiments done in duplicate.**

2.1.4. Nature of the active cobalt(salen) catalyst

From kinetic experiments it is apparent that the cobalt(salen) system required tetrabutylammonium bromide (at least 1 equivalent) in the conversion of terminal epoxides to cyclic carbonates. However, the active catalyst is not formed from a simple anion displacement as evidenced by the inactivity of catalyst **3d** in the absence of tetrabutylammonium bromide. Kinetic analysis has also shown that the order of reaction w.r.t. tetrabutylammonium bromide is 1 (Figure 18, page 35).

Darensbourg and Moncada have unequivocally proven by X-ray crystallography that chromium(salen)Cl forms six-coordinate complexes in the presence of two equivalents of anions such as CN^-, N_3^-, and NCO^-.[64] By extending this reasoning to our cobalt(salen) system, tetrabutylammonium bromide could act as an anion source to form a theoretical six-coordinate cobalt(salen)Br_2^- complex (Scheme 11). This would explain the need for excess tetrabutylammonium bromide in our cobalt(salen)/co-catalyst system.
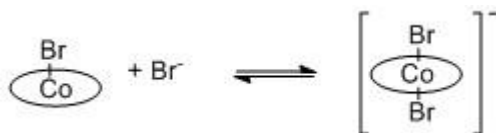
Scheme 11: Formation of postulated Co(III)salenBr₂⁻ active catalyst in the presence of excess bromide anions.

As suspected, the ¹H NMR spectrum of cobalt(salen)bromide catalyst **3d** with excess tetrabutylammonium bromide exhibits a shift in the aryl region. In the

37

presence of 15 equivalents of tetrabutylammonium bromide, the singlet at 8.35 ppm shifts to 8.20 ppm while the doublets at 7.35 ppm and 7.02 ppm shift to 7.20 ppm and 6.88 ppm respectively. The changes in the cyclohexyl region, if any, are swamped by the signals from tetrabutylammonium bromide (Figure 21, top).
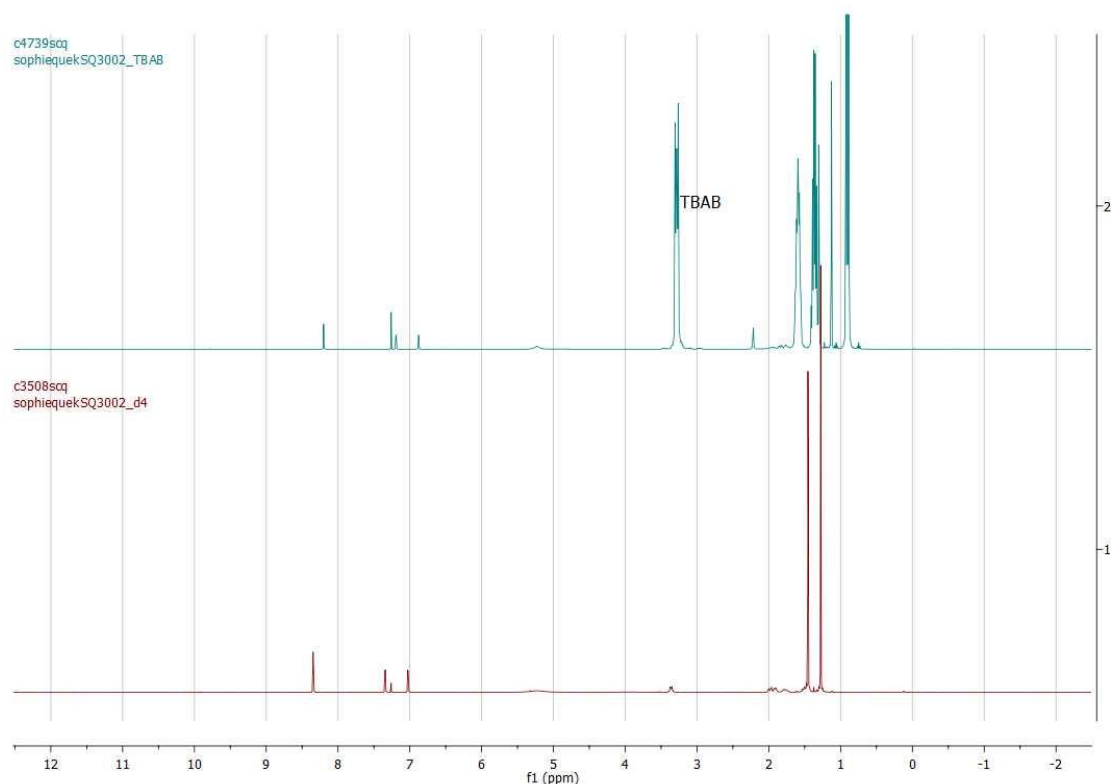
Figure 21: ^{1}H NMR spectrum of catalyst 3d in the presence of 15 equivalents of tetrabutylammonium bromide in CDCl$_3$ (top, blue), and ^{1}H NMR spectrum of catalyst 3d alone in CDCl$_3$ (bottom, red).

However, there were no differences in the ^{13}C NMR spectra. Furthermore, electrospray ionisation mass spectrometry did not produce the desired peak, which we predicted to be a [**3d**+Br]$^-$ ion at 761.1733. The observed species were instead a major peak at m/z 402.1180 and a minor peak corresponding to [**3d**]$^-$.

The UV spectrum of catalyst **3d** in a large excess of tetrabutylammonium bromide also failed to show either a shift in wavelength, or the presence of a new peak. The resultant spectrum (Figure 22, red) appears to be the sum spectrum of catalyst **3d** (Figure 22, green) and tetrabutylammonium bromide (Figure 22, blue).
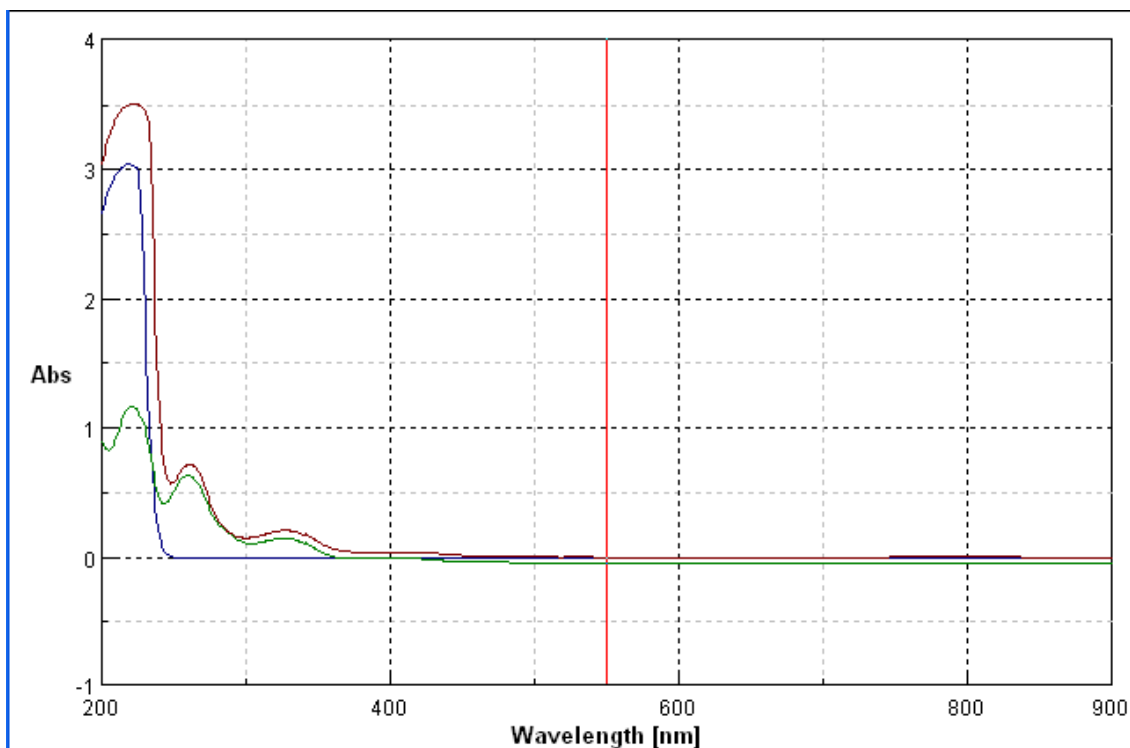
Figure 22: UV spectra of catalyst 3d in acetonitrile (green), tetrabutylammonium bromide in acetonitrile (blue), and catalyst 3d in the presence of 100 equiv. of tetrabutylammonium bromide in acetonitrile (red).

Although ^{1}H NMR analysis appears to indicate formation of a new complex *in situ*, the shifts in signals may also be attributed to the addition of tetrabutylammonium bromide, which would alter solvent polarity. We also attempted crystal growth of **3d** in the presence of tetrabutylammonium bromide. The resultant crystal structure was shown to contain **3d** alone. In the absence of further evidence we were unable to ascertain the formation of Co(III)salenBr$_2^-$ by adding tetrabutylammonium bromide to **3d**.

At the beginning of the project we had a pre-conceived belief that cobalt(salen) catalysts were unique in producing enantio-enriched cyclic carbonates from epoxides and carbon dioxide. However, our work on aluminium(salen) (Section 2.1.1) and chromium(salen) complexes (Section 0) proves otherwise. We therefore opted out of further investigating the properties of the active cobalt(salen) catalysts.

2.1.5. Enantioselectivity of chromium(salen) catalysts

Since chiral chromium(salen) catalysts have demonstrated enantioselectivity for the ring-opening of epoxides, they therefore have the potential to produce enantio-enriched cyclic carbonates. Indeed, we observed enantioselectivity in the production of cyclic carbonates from racemic epoxides using our chromium(salen) catalysts with a range of co-catalysts (Figure 23, Table 5). With the exception of Entry 32, the catalysts favoured production of the second enantiomer of cyclic carbonate by chiral HPLC.
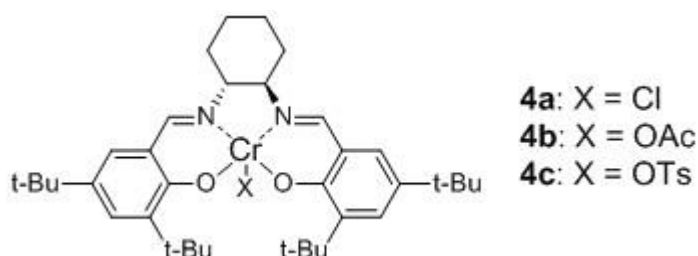
Figure 23: Structures of chromium(salen) catalysts 4a to 4c.

Due to the presence of side products when phenyl glycidyl ether was used as substrate, our standard quantification method based on HPLC response factors was rendered inaccurate. The presence of paramagnetic chromium(III) also complicated ^{1}H NMR analysis due to peak broadening. As most of the peak area may be assigned to either substrate or product, which have similar response factors (923109 and 901514 respectively), area % by HPLC was considered sufficient for quantitative analysis.

Controls performed in the absence of co-catalysts showed conversions that were too low to be viable (Table 5, Entries 1, 18, and 23). In addition, much like the aluminium(salen) catalysts, catalyst **4a** was less enantioselective for styrene oxide even at doubled catalyst loading (Table 5, Entry 15) but more enantioselective for *N*-(2,3-epoxypropyl)diphenylamine (Table 5, Entry 16). Furthermore, the enantioselectivity of the chromium(salen) catalysts surpassed that of the cobalt(salen) catalysts.

Co-catalyst testing with **4a** and **4c** showed that amongst the tetrabutyl-ammonium halide catalysts, the bromide salt consistently produced the highest % ee values (Table 5, Entries 2 to 9 and 25 to 31). Using phenyl glycidyl ether as substrate, we then tested a range of alternative co-catalysts, (Table 5,

Entries 10 to 13, 17, and 18). Since the highest k_{rel} value of 3.10 was observed using bis(triphenylphosphine)iminium chloride (Table 5, Entry 13), further optimisation was performed with that co-catalyst. Doubling the catalyst loading successfully produced an increase of ee values to 43 % (Table 5, Entry 14).

Table 5 Activity and enantioselectivity of chromium(salen) catalysts 4a to 4c (2.5 mol %) and various co-catalysts using phenyl glycidyl ether as substrate under solvent-free conditions at 25 °C.

Entry	Catalyst	Co-catalyst	Time (h)	Conversion to cyclic carbonate (%)	e.r. of cyclic carbonate	% ee of cyclic carbonate	k_{rel}^{α}
1	4a	-	24	6.1	34: 66	31	1.94
2	4a	NBu4F	6	Not detected	NA	NA	-
3	4a	NBu4F	24	63.4	43: 57	13	1.57
4	4a	NBu4Cl	6	4.6	36: 65	29	1.84
5	4a	NBu4Cl	24	89.2	44: 56	12	2.92
6	4a	NBu4Br	6	61.8	49: 51	2	1.07
7	4a	NBu4Br	24	86.5	48: 52	4	1.30
8	4a	NBu4I	6	43.4	49: 52	3	1.08
9	4a	NBu4I	24	88.6	47: 53	5	1.45
10	4a	4-dimethylaminopyridine	6	9.8	40: 60	21	1.57
11	4a	4-dimethylaminopyridine	24	61.5	39: 62	23	2.20
12	4a	PPN+Cl-ε	6	16.5	37: 63	27	1.83
13	4a	PPN+Cl-	24	84.3	42: 58	16	3.10
14	4aβ	PPN+Cl-	3	16.8	29: 71	43	2.72
15	4aβ, γ	PPN+Cl-	4	13.0	47: 54	7	1.16
16	4aδ	PPN+Cl-	3	20.9	14: 86	72	7.32
17	4a	Guanidinium chloride	6	8.3	33: 67	33	2.04
18	4a	Guanidinium chloride	24	17.4	45: 55	11	1.28
19	4b	-	24	6.5	44: 56	12	1.28
20	4b	NBu4Br	6	77.7	49: 51	1	1.05
21	4b	NBu4Br	24	91.2	46: 54	8	2.29
22	4b	4-dimethylaminopyridine	6	2.7	39: 61	21	1.54
23	4b	4-dimethylaminopyridine	24	52.2	46: 55	9	1.31
24	4c	-	24	5.2	40: 60	21	1.55
25	4c	NBu4F	6	11.0	38: 63	25	1.72
26	4c	NBu4F	24	18.2	38: 62	24	1.72
27	4c	NBu4Cl	6	17.0	41: 59	18	1.49
28	4c	NBu4Cl	24	31.5	40: 60	21	1.68
30	4c	NBu4Br	24	23.0	37: 63	25	1.86
31	4c	NBu4I	24	7.9	42: 58	15	1.38
32	4c	4-dimethylaminopyridine	24	6.1	53: 47	6	1.12
33	4c	PPN+Cl-	6	11.0	40: 60	20	1.54
34	4c	PPN+Cl-	24	21.5	37: 63	24	1.74

[α]k_{rel} is calculated as $\frac{\ln[1-c(1+ee)]}{\ln[1-c(1-ee)]}$. [β]Reaction was carried out using 5.0 mol % of **4a** and 5.0 mol % of co-catalyst. [γ]Styrene oxide as substrate, conversion obtained by ^{1}H NMR. [δ]N-(2,3-Epoxypropyl)diphenylamine as substrate, conversion obtained by HPLC. [ε]PPN+: Bis(triphenylphosphine)iminium.

Section 2.1.3 (page 32) disproves the hypothesis that the reaction is second-order w.r.t. cobalt(salen) catalysts. Consequently, we worked on improving k_{rel} values by varying ligand design (Figure 24, Table 6) instead of performing kinetic analyses on our chromium(salen) complexes. Indeed, our k_{rel} values were only modest at best. In comparison, Jacobsen and co-workers reported k_{rel} values ranging from 49 to 500 for the hydrolytic kinetic resolution of epoxides.[1]

Chromium(salen) complexes **4d** to **4j** (Figure 24) were selected with our optimal results in mind (Table 5, Entries 13 and 14), i.e. the chromium(salen)chloride in combination with bis(triphenylphosphine)iminium salts. Insolubility issues with the bis(triphenylphosphine)iminium co-catalysts were rectified by a pre-treatment step reported by Darensbourg and Moncada. This step involved dissolving both the chromium(salen) complex and the PPN⁺X⁻ salts in dichloromethane, or any suitable solvent, followed by solvent removal *in vacuo* and finally substrate introduction.[64]

Pretreatment was ineffective as it produced an increase in activity but a corresponding decrease in k_{rel} (Table 6, Entries 7 to 12, and 15 to 16), as did the use of PPN⁺Br⁻ (Table 6, Entries 13 and 14) instead of PPN⁺Cl⁻ (Table 6, Entries 7 and 8). The presence of t-Bu groups enhanced solubility and increased conversions, but likewise did little to increase enantioselectivity (Table 6, Entries 3 to 8, 17 and 18). The presence of electron-donating groups were likewise largely detrimental to enantioselectivity (Table 6, Entries 19 to 22). The presence of electron-withdrawing Br substituents slightly increased k_{rel} values, but conversions were decreased (Table 6, Entries 23 to 26). In summary, the variation of R groups on the phenyl rings did not significantly change the enantioselectivity of the reaction.

We then investigated the effect of the diimine backbone on enantioselectivity. Since the enantioselectivity of the reaction is dependent on the "step" of the ligand, we reasoned that the presence of bulky phenyl groups on the backbone might improve enantioselectivity. As the optimum ee values were observed when R_2 = H and R_3 = t-Bu (Table 6, Entries 7 and 8), we selected 3-*tert*-butyl-2-hydroxybenzaldehyde, and *(R,R)*-1,2-diphenyl-1,2-ethanediamine as the

42

desired synthons. However, the increased cost of the ligand was not justified as the complex was barely enantioselective (Table 6, Entries 27 and 28).

4a: R_1 = -(CH$_2$)$_4$-, R_2 = t-Bu = R_3
4d: R_1 = -(CH$_2$)$_4$-, R_2 = H = R_3
4e: R_1 = -(CH$_2$)$_4$-, R_2 = H, R_3 = t-Bu
4f: R_1 = -(CH$_2$)$_4$-, R_2 =t-Bu, R_3 = H
4g: R_1 = -(CH$_2$)$_4$-, R_2 = OMe, R_3 = H
4h: R_1 = -(CH$_2$)$_4$-, R_2 = OMe, R_3 = t-Bu
4i: R_1 = -(CH$_2$)$_4$-, R_2 = Br, R_3 = H
4j: R_1 = -(CH$_2$)$_4$-, R_2 = Br, R_3 = t-Bu
4k: R_1 = Ph, R_2 = H, R_3 = t-Bu
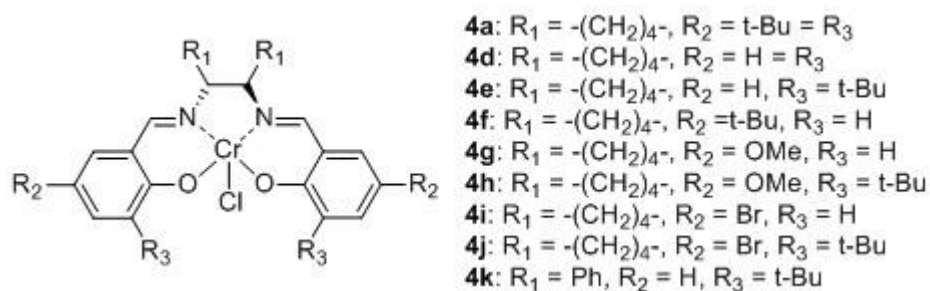
Figure 24: Variants of Cr(III)(salen) complexes 4a to 4k.

Table 6: Activity and enantioselectivity of chromium(salen) chloride catalysts 4a to 4k (2.5 mol % loading, 1: 1 Cr to PPN+X- salts) using phenyl glycidyl ether as substrate.

Entry	Catalyst	Co-catalyst	Pretreatment	Temp. (°C)	Time (h)	Area% of cyclic carbonate (%)	% ee of cyclic carbonate	k_{rel}
1	-	PPN+Cl-	No	25	24	12.6	2.0	-
2	-	PPN+Br-	No	25	24	17.9	0.2	-
3	4a	PPN+Cl-	No	25	6	16.5	27	1.83
4	4a	PPN+Cl-	No	25	24	84.3	16	3.10
5	4d	PPN+Cl-	No	25	6	19.7	31	2.04
6	4d	PPN+Cl-	No	25	24	36.1	22	1.76
7	4e	PPN+Cl-	No	25	6	28.0	36	2.43
8	4e	PPN+Cl-	No	25	24	51.0	15	1.55
9	4e	PPN+Cl-	Yes	25	6	57.4	9	1.31
10	4e	PPN+Cl-	Yes	25	24	61.3	8	1.29
11	4e	PPN+Cl-	No	0	72	1.3	44	2.60
12	4e	PPN+Cl-	Yes	0	72	4.1	32	1.97
13	4e	PPN+Br-	No	25	6	49.3	4	1.13
14	4e	PPN+Br-	No	25	24	69.0	4	1.17
15	4e	PPN+Br-	No	0	72	11.9	29	1.90
16	4e	PPN+Br-	Yes	0	72	21.0	25	1.79
17	4f	PPN+Cl-	No	25	6	26.2	26	1.86
18	4f	PPN+Cl-	No	25	24	54.2	20	1.85
19	4g	PPN+Cl-	No	25	6	23.3	28	1.93
20	4g	PPN+Cl-	No	25	24	54.1	18	1.73
21	4h	PPN+Cl-	No	25	6	52.3	14	1.52
22	4h	PPN+Cl-	No	25	24	65.2	9	1.38
23	4i	PPN+Cl-	No	25	6	16.8	28	1.88
24	4i	PPN+Cl-	No	25	24	41.8	24	1.91
25	4j	PPN+Cl-	No	25	6	17.3	32	2.08
26	4j	PPN+Cl-	No	25	24	36.7	19	1.63
27	4k	PPN+Cl-	No	25	6	20.3	30	1.98
28	4k	PPN+Cl-	No	25	24	43.3	15	1.50
29	4k	TBAB	No	25	6	74.4	0	1.02
30	4k	TBAB	No	25	24	89.7	4	1.35

2.2. Hypothesis 2: Cobalt(salen) catalysts exhibit the most stepped conformation

If the ring-opening of epoxides is truly similar to Jacobsen's hydrolytic kinetic resolution, the cobalt(salen) complexes would exhibit a more stepped conformation than similar metal(salen) complexes which exhibit lesser stereoselectivity. To verify this hypothesis we examined crystal structures of aluminium, cobalt, and chromium complexes obtained from the Cambridge Structural Database. Attempts at crystal growth were also successful in yielding a crystal structure (Table 7, Entry 8). Details of the crystal structure, including acquisition data, may be found in Appendix B.

We first limited the search to complexes containing the *(R,R)*-N,N′-bis(3,5-di-*tert*-butylsalicylidene)-1,2-cyclohexanediamine ligand. The step was then approximated by measuring the angle between two planes. The first plane was drawn using the four donor atoms of the ligand (Figure 25, red plane) and the second plane was extended from the aryl rings (Figure 25, green plane). However, the angles proved to be different for each aryl ring even within the same molecule (Figure 26, blue and green planes). The differences between the two tilts for each molecule ranged from 0.18 ° to a significant 10.89 ° (CSD reference – ZUQCIX)[65] even in a single crystal structure containing two complexes which may have been caused by crystal-packing forces.
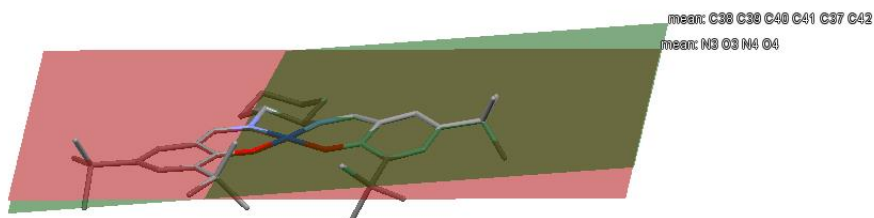
Figure 25: Approximation of step in (*(R,R)*-(-)-N,N'-bis(3,5-Di-t-butylsalicylidene)-1,2-cyclohexanediamino)-cobalt(II) chloroform solvate, CSD reference – ZUQCIX.[65] Hydrogen atoms, solvent molecules, and the second complex molecule have been omitted for clarity. The red plane is extended from the four donor atoms surrounding the cobalt centre. The green plane is extended from the aryl ring on the left.
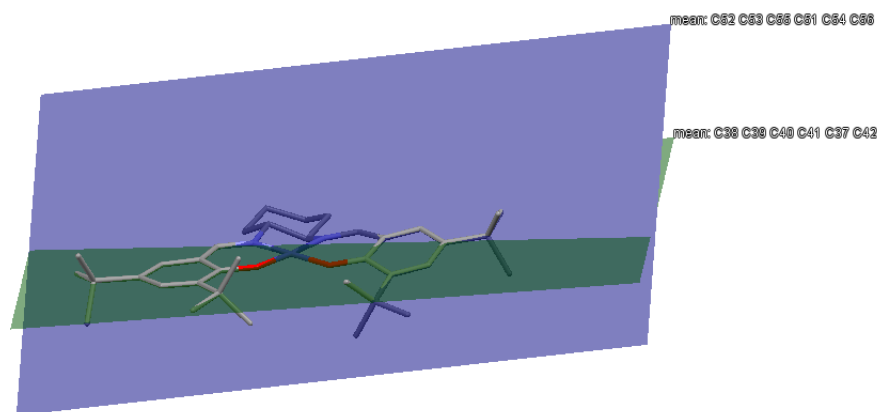
Figure 26: Planes extended from the aryl rings in (*(R,R)*-(-)-N,N'-bis(3,5-Di-t-butylsalicylidene)-1,2-cyclohexanediamino)-cobalt(II) chloroform solvate, CSD reference – ZUQCIX.[65] Hydrogen atoms, solvent molecules, and the second complex molecule have been omitted for clarity. The green plane is extended from the aryl ring on the left. The blue plane is extended from the aryl ring on the right, and is clearly not parallel to the green plane.

Since each crystal exhibits signs of distortion from crystal packing, the scope of comparison was extended to include the range of steps for each aryl ring. Even then, the available data was fairly restricted. Consequently, complexes with differing R groups on the 5 and 5' positions (Figure 27) were included with the view that the diamine backbone dictates the step of the complex and that the distance at the 5 and 5' positions from the metal centre would minimise effects on the step.

While this assumption holds true for the 4-coordinate cobalt(salen) complexes which are expected to remain relatively planar (Table 7, Entries 3 to 5), there is a significant increase in step when the R-group is changed from MeO to a bulky t-Bu in the 6-coordinate cobalt(salen) complexes (Table 7, Entries 9 and 10). It appears that the combined bulk of both the axial ligands and the t-Bu functional groups may be sufficient to induce distortion.

Although the smallest angle measured for the 4-coordinate cobalt(salen) complexes was considerably less than that of the 5-coordinate cobalt(salen) complexes, there was little change in the maximum angle measured. (Table 7, Entries 3 to 8). However, the 6-coordinate cobalt(salen) complexes showed drastically different angles dependent on the identity of the axial ligands (Table 7, Entries 10 and 11). The same may be said for the 6-coordinate chromium(salen) complexes (Table 7, Entries 12 and 13).
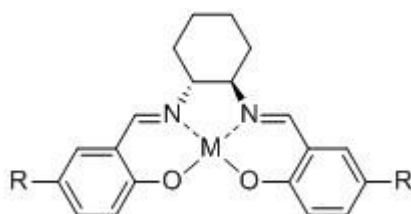
Figure 27: General structure of crystal structures examined in Table 7.

Table 7: Range of angles obtained for various metal(salen) complexes containing a 1,2-cyclohexanediamine backbone. The angles are approximated using the two corresponding planes in Figure 25 for each crystal structure.

Entry	M	R	No. of coordination sites	Ligands present	Smallest angle measured (°)	Largest angle measured (°)
1	Al	t-bu	5	(S)-chloropropanol	2.34[66]	14.25[66]
2	Al	t-bu	5	Bis(trimethylsilyl)amide	22.42[67]	31.56[67]
3	Co	H	4	-	2.42[47]	18.04[47]
4	Co	MeO	4	-	2.32[68]	19.48[68]
5	Co	t-bu	4	-	4.29[65]	15.18[65]
6	Co	t-bu	5	1,3-butadien-2-yl	2.81[69]	17.19[69]
7	Co	t-bu	5	Cl$^-$	8.91[70]	18.89[70]
8	Co	t-bu	5	Br$^-$	8.27	17.41
9	Co	MeO	6	1-methyl-1H-imidazole, 1-methyl-1H-imidazole	1.01[68]	7.42[68]
10	Co	t-bu	6	1-methyl-1H-imidazole, 1-methyl-1H-imidazole	7.29[71]	9.74[71]
11	Co	t-bu	6	(2R,3S)-2-Phenyl-3-methylaziridine-N, (2R,3S)-2-Phenyl-3-methylaziridine-N	18.79[72]	28.66[72]
12	Cr	t-bu	6	N$_3^-$, THF	4.13[73]	10.23[73]
13	Cr	t-bu	6	Cl$^-$, Cl$^-$	6.10[74]	15.56[74]

Our hypothesis was that cobalt(salen) complexes exhibit the largest step, thus resulting in high enantioselectivity for a broad range of substrates. However, given the unpredictability of angles observed in the cobalt(salen) complexes and the fact that the largest tilt was observed in an aluminium(salen) complex (Table 7, Entry 1), we were unable to unequivocably prove our hypothesis. Extensive distortion from crystal packing forces may have rendered the data irrelevant. Alternative justifications include the failure of the premise that cobalt(salen) complexes are unique in producing enantio-enriched product for which our work on aluminium(salen) complexes (Section 2.1.1) and chromium(salen) complexes (Section 2.1.5) provides corroborating evidence

3. Conclusion

The two hypotheses put forward were based on the assumption that only cobalt(salen) catalysts are able to kinetically resolve cyclic carbonates. Our work on enantioselective aluminium(salen) and chromium(salen) complexes has shown that this assumption is false. Furthermore, first-order rate dependence on catalyst was observed for catalysts affording enantioselectivity, in contrast with our expectations of a second-order rate dependence. Examination of the crystal structures of similar metal(salen) catalysts showed little correlation between the "step" of the catalyst and the extent of enantioselectivity. Therefore we were unable to prove either hypothesis.

Furthermore, unlike the HKR process where enantioselectivity is largely substrate-independent, we have evidence that enantioselective cyclic carbonate formation from epoxides is reliant on the substrate across all tested catalysts. While we were limited by the inability of our current equipment to analyse other substrates, it is clear that the HKR process is an unlikely model for the synthesis of cyclic carbonates from epoxides and CO_2.

Without doubt, the most intriguing results were the unexpected enantioselectivities of aluminium(salen) and chromium(salen) complexes, where none had been expected. The enantioselectivity of the reaction may be improved by substrate choice, and by lowering the temperature, but not by pre-treatment with compatible solvents or by varying ligand design for the chromium(salen) catalysts. Both aluminium(salen) and chromium(salen) complexes exhibited stronger substrate-dependence than the cobalt(salen) catalysts. In the cases where enantioselectivity was observed, the k_{rel} values obtained using aluminium(salen) and chromium(salen) catalysts surpassed that obtained using the cobalt(salen) catalysts.

4. Future Work

The range of epoxides for which aluminium(salen) and chromium(salen) complexes are enantioselective needs to be fully established. Investigations using a series of epoxides containing alkyl chains of differing lengths such as butylene oxide, hexylene oxide, and decylene oxide, should reveal if the enantioselectivity is dependent on steric factors alone. Substrate screening using substituted styrene oxide such as *p*-chlorostyrene oxide and *p*-bromostyrene oxide would likewise reveal any influence arising from inductive effects.

It would be enlightening to examine how functional groups on the salen ligand of our aluminium(salen) complexes would affect enantioselectivity, particularly as the aluminium(salen) complexes afforded the highest k_{rel} values observed thus far. In hindsight, greater effort needed to be expended in increasing k_{rel} values for aluminium(salen) complexes as opposed to the chromium(salen) complexes, particularly as chromium is a relatively scarce resource[75] and aluminium is the most abundant metal in the Earth's crust.[76]

In order to increase the green credentials of aluminium(salen) complexes, alternative sources of aluminium should be explored. From an industrial viewpoint, there is a need to investigate opportunities for catalyst recycling and immobilisation onto heterogeneous supports. Furthermore, development of a single-component aluminium(salen) catalyst would be desirable. However, these investigations should be carried out only after ascertaining that kinetic resolution using aluminium(salen) catalysts is viable i.e. k_{rel} values approaching 50.

Since we were unable to vastly improve ee and k_{rel} values by varying ligand design, better enantioselectivity may be observed with other metal centres such as iron, a cheap and readily abundant material.[76]

Finally, due to the short duration of this project we found it unnecessary to continue performing kinetics on the chromium(salen) complexes. Nonetheless a kinetic study carried out using chromium(salen) complexes would be useful in

elucidating if the ring-opening step is homologous to the corresponding step in the HKR process.

5. Preparation of catalysts, co-catalysts, and reagents

General experimental procedures. Reactions were carried out in oven-dried round bottomed flasks, unless otherwise noted. Commercially available reagents were purchased from *Aldrich*, *Fluka*, *Acros*, and *Alfa Aesar*. Commercial-grade solvents were used as received unless otherwise noted.

Instrumentation. ^{1}H and ^{13}C NMR spectra were recorded on a Jeol ECX400 or Jeol ECS400 spectrometer at 400 MHz and 101 MHz respectively unless otherwise noted. All spectra were recorded at room temperature unless otherwise stated in a suitable solvent that is reported in parentheses. Chemical shifts for protons are reported in parts per million and are referenced to residual protons in the NMR solvent (CHCl$_3$: δ = 7.26). Chemical shifts for carbon are reported in parts per million and are referenced to the carbon resonances of the solvent (CDCl$_3$: δ = 77.16). Data are represented as follows: chemical shift, multiplicity, integration. Abbreviations for NMR spectral multiplicities are as follows: br = broad, s = singlet, d = doublet, t = triplet, q = quartet, m = multiplet.

Infrared (IR) spectra were obtained on a Bruker Vertex 700 spectrometer using a range between 600 cm^{-1} and 4000 cm^{-1} using attenuated total reflectance. Data are represented as follows: frequency of absorption (cm^{-1}), intensity of absorption (s = strong, m = medium, w = weak, br = broad). UV-vis spectra were obtained on a JASCO V-550 spectrophotometer. Optical rotations were measured using a 2 mL cell with a 100 mm path length on a JASCO DIP-370 digital polarimeter at the sodium D-line in a suitable solvent that is reported in parentheses (concentration given in g/100 mL). Melting points were measured on a Stuart SMP3 melting point machine.

High resolution mass spectra were recorded on a Bruker microTOF operating in positive electrospray ionisation mode unless stated otherwise. Low resolution mass spectra were recorded on a Waters Micromass GCT Premier orthogonal time-of-flight instrument using liquid injection field desorption/ionization.

X-ray analysis was carried out using a Oxford Diffraction SuperNova equipped with a 4-circle goniometer, microfocus Mo X-ray source and CCD detector. The

crystal was kept at 110.00(14) K during data collection. Details of the crystal structures obtained are given in Appendix B.

Crystallographic Data. The crystal structures of metal(salen) complexes were downloaded from the Cambridge Structural Database[77] if they were already available. Mercury[78] was used to analyse the crystallographic information.

5.1.   Preparation of aldehydes

3,5-Di-*tert*-butyl-2-hydroxybenzaldehyde:
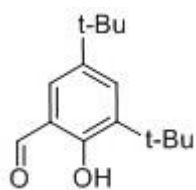
Synthesis was carried out according to a reported literature procedure.[79] Et_3N (2.64 mL, 19.38 mmol) was added dropwise to a suspension of 2,4-di-*tert*-butylphenol (2.00 g, 9.69 mmol), $MgCl_2$ (1.84 g, 19.38 mmol), and paraformaldehyde (0.64 g, 21.33 mmol) in THF (50 mL). The mixture was refluxed at 70 °C for 20 h to give a yellow suspension. The reaction was quenched with water (60 mL) and extracted with CH_2Cl_2 (2 x 100 mL). The combined organic extracts were washed with brine (2 x 100 mL), dried ($MgSO_4$) and the solvent removed *in vacuo*. The yellow residue was purified by flash chromatography using petroleum ether/$CHCl_3$ (7:1) as eluent to give a pale yellow solid, R_f (petroleum ether/$CHCl_3$ 7:1) 0.24. Yield: 1.43 g, 27 %. M.P: 58.5 -59.7 °C (lit. 59 - 61 °C).[80] ^{1}H NMR (400 MHz, $CDCl_3$) δ: 11.64 (s, 1H), 9.87 (s, 1H), 7.59 (d, J = 2.5 Hz, 1H), 7.35 (d, J = 2.5 Hz, 1H), 1.43 (s, 9H), 1.33 (s, 9H). ^{13}C NMR (101 MHz, $CDCl_3$) δ: 197.7, 159.4, 141.9, 137.9, 132.2, 128.1, 120.3, 35.3, 34.5, 31.6, 29.6. FT-IR (ATR): υ [cm^{-1}] = 2959 (s), 2872 (m), 2361 (w), 1648 (s), 1614 (m), 1441 (s), 1363 (m), 1271 (m), 1171 (s), 1027 (m), 896 (m), 770 (m), 715 (s). HRMS (EI): Calculated for [$C_{15}H_{22}O_2$] ([M]$^+$): 234.1620; Found: 234.1619.

5-*Tert*-butyl-2-hydroxybenzaldehyde:
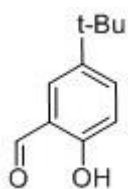
t-Bu Synthesis was carried out following the procedure for 3,5-di-*tert*-butyl-2-hydroxybenzaldehyde, refluxing overnight. Et$_3$N (12.99 mL, 93.19 mmol) was added dropwise to a suspension of 4-*tert*-butylphenol (7.00 g, 46.59 mmol), MgCl$_2$ (8.87 g, 93.19 mmol), and paraformaldehyde (3.07 g, 102.5 mmol) in THF (200mL). The mixture was refluxed at 70 °C overnight to give a yellow suspension. The reaction was quenched with water (150 mL) and extracted with CH$_2$Cl$_2$ (2 x 100 mL). The combined organic extracts were washed with brine (2 x 100 mL), dried (MgSO$_4$) and the solvent removed *in vacuo*. A brown oil was obtained, which was purified by flash chromatography using petroleum ether/EtOAc (5:1) as eluent to yield a yellow oil, R$_f$ (petroleum ether/EtOAc 5:1) 0.44. Yield: 4.49 g, 54 %. ^{1}H NMR (400 MHz, CDCl$_3$) δ: 10.87 (s, 1H), 9.89 (s, 1H), 7.59 (dd, J = 8.8 Hz, 2.5 Hz, 1H), 7.52 (d, J = 2.5 Hz, 1H), 6.94 (d, J = 8.8 Hz, 1H), 1.33 (s, 9H). ^{13}C NMR (101 MHz, CDCl$_3$) δ: 196.9, 159.6, 142.8, 134.8, 129.9, 120.1, 117.3, 34.2, 31.3. FT-IR (ATR): υ [cm^{-1}] = 2962 (m), 1652 (s), 1484 (s), 1264 (s), 1229 (s), 924 (m), 833 (s), 600 (s). HRMS (ESI): Calculated for [C$_{12}$H$_{18}$NaO$_3$] ([M+Na+MeOH]$^+$): 233.1154; Found: 233.1141.

3-*Tert*-butyl-2-hydroxybenzaldehyde:
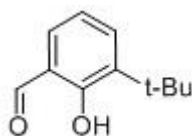
t-Bu Synthesis was carried out following the procedure for 3,5-di-*tert*-butyl-2-hydroxybenzaldehyde. Et$_3$N (7.26 mL, 52.07 mmol) was added dropwise to a suspension of 3-*tert*-butylphenol (4.0 mL, 26.04 mmol), MgCl$_2$ (4.96 g, 52.07 mmol), and paraformaldehyde (1.72 g, 57.29 mmol) in THF (100mL). The pink mixture was refluxed at 70 °C overnight to give a brown suspension. The reaction was quenched with water (50 mL) and extracted with CH$_2$Cl$_2$ (3 x 100 mL). The combined organic extracts were washed with brine (3 x 80 mL), dried (MgSO$_4$) and the solvent removed *in vacuo*. A dark green oil was obtained on standing, which was purified by flash chromatography using petroleum ether/EtOAc (25:1) as eluent to yield an orange oil, R$_f$ (petroleum ether/EtOAc 25:1) 0.26. Yield: 2.70 g, 58 %. ^{1}H NMR (400 MHz, CDCl$_3$) δ: 11.77 (s, 1H), 9.87 (s, 1H), 7.52 (dd, J = 7.5 Hz, 1.7 Hz, 1H), 7.38 (dd, J = 7.5 Hz, 1.7 Hz, 1H), 1.41 (s, 9H). ^{13}C NMR (101 MHz, CDCl$_3$)

δ: 197.2, 161.2, 138.3, 134.1, 132.0, 120.7, 34.9, 29.2. FT-IR (ATR): υ [cm⁻¹] = 2959 (m), 1650 (s), 1431 (s), 1311 (s), 1196 (s), 750 (s). HRMS (EI): Calculated for [$C_{11}H_{14}O_2$] ([M]⁺): 178.0994; Found: 178.0992.

3-*Tert*-butyl-5-bromo-2-hydroxybenzaldehyde:
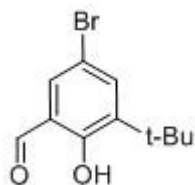
Synthesis was carried out according to a literature procedure.[81] A round-bottomed flask was charged with 3-*tert*-butyl-2-hydroxybenzaldehyde (0.29 g, 1.65 mmol) in 15 mL of glacial acetic acid. A solution of bromine (0.09 mL, 1.70 mmol) in 30 mL of glacial acetic acid was then added dropwise. The resulting brown solution was stirred at r.t. for 18 h. The solution was diluted to 100 mL with CH_2Cl_2 and washed with water (100 mL), $Na_2S_2O_5$ (100 mL), $NaHCO_3$ (100 mL), and brine (100 mL). After drying over $MgSO_4$, the solvent was removed *in vacuo* to yield a yellow solid which was used without further purification. Yield: 0.36 g, 86 %. ¹H NMR (400 MHz, CDCl₃) δ: 11.73 (s, 1H), 9.81 (s, 1H), 7.58 (d, J = 2.3 Hz, 1H), 7.52 (d, J = 2.3 Hz, 1H), 1.40 (s, 9H). ¹³C NMR (101 MHz, CDCl₃) δ: 196.1, 160.3, 141.2, 137.1, 133.7, 121.7, 111.2. FT-IR (ATR): υ [cm⁻¹] = 3088 (w), 2957 (m), 1657 (s), 1427 (s), 1302 (s), 1271 (s), 1165 (s), 867 (s), 700 (s). HRMS (EI): Calculated for [$C_{11}H_{13}{}^{79}BrO_2$] ([M]⁺): 256.0099; Found: 256.011.

5.2. Preparation of salen ligands

(R,R)-N,N'-Bis(3,5-di-*tert*-butylsalicylidene)-1,2-cyclohexanediamine:
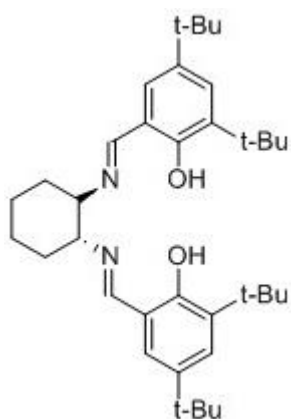
Synthesis was carried out according to a literature procedure.[82] 3,5-Di-*tert*-butyl-2-hydroxybenzaldehyde (18.59 g, 79.3 mmol) was added to a round-bottomed flask and dissolved in EtOH (200 mL) to give a pale yellow solution. A solution of K_2CO_3 (12.06 g, 87.3 mmol) and *(R,R)*-1,2-diaminocyclohexane tartrate (9.77 g, 39.7 mmol) in EtOH/water (1:1, 200 mL) was added to the 3,5-di-*tert*-butyl-2-hydroxybenzaldehyde solution, giving a bright yellow suspension. The mixture was refluxed for 18 h, quenched with

water (150 mL), and extracted with CH_2Cl_2 (2 x 200 mL). The organic extracts were washed with brine (200 mL), and dried ($MgSO_4$). Solvent was removed *in vacuo* to yield a yellow solid, which was purified by washing with ethanol. Yield: 14.5 g, 69 %. M.P: 206.0 – 206.5 °C (lit. 201 - 204 °C).[82] ^{1}H NMR (400 MHz, $CDCl_3$) δ: 13.72 (s, 2H), 8.30 (s, 2H), 7.30 (d, J = 2.5 Hz, 2H), 6.98 (d, J = 2.5 Hz, 2H), 3.33 – 3.30 (m, 2H), 1.96 – 1.72 (m, 2H), 1.41 (s, 18H), 1.23 (s, 18H). ^{13}C NMR (101 MHz, $CDCl_3$) δ: 165.93, 158.1, 140.0, 136.4, 126.8, 126.8, 117.9, 72.5, 35.0, 34.1, 33.4, 31.5, 29.5, 24.5. FT-IR (ATR): υ [cm^{-1}] 2951 (s), 2907 (m), 2865 (m), 2361 (w), 2324 (w), 1630 (s), 1391 (m), 828 (m), 772 (m), 644 (m). HRMS (ESI): Calculated for [$C_{36}H_{55}N_2O_2$] ([M+H]$^+$): 547.4258; Found: 547.4262. [α]$_D$ -288 (c = 0.9, CH_2Cl_2) (lit. -315).[82]

(R,R)-N,N'-Bis(salicylidene)-1,2-cyclohexanediamine:
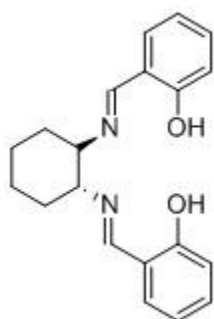
Synthesis was carried out according to a literature procedure.[83] K_2CO_3 (0.69 g, 5.0 mmol) and *(R,R)*-1,2-diaminocyclohexane tartrate (1.17 g, 4.76 mmol) were added to a two-necked round-bottomed flask. Water (10 mL) was added to the mixture, which was heated at 60 °C until complete dissolution. EtOH (30 mL) was added and the mixture heated to reflux. Salicyaldehyde was dissolved in EtOH (30 mL) and added dropwise to give a bright yellow solution. The solution was refluxed for 1 h. The solvent was reduced to half the volume *in vacuo*, and extracted with CH_2Cl_2 (50 mL). The organic phase was washed with water (50 mL) and dried ($MgSO_4$). The solvent was removed *in vacuo* to yield a yellow glass which crystallised on standing. The solid was used without further purification. Yield: 1.34 g, 88 %. ^{1}H NMR (400 MHz, $CDCl_3$) δ: 13.31 (s, 2H), 8.26 (s, 2H), 7.22 (m, 2H), 7.13 (dd, J = 7.3, 1.4 Hz, 2H), 6.86 (d, J = 7.4 Hz, 2H), 6.80 – 6.75 (m, 2H), 3.38 – 3.26 (m, 2H), 1.99 – 1.82 (m, 4H), 1.82 – 1.65 (m, 2H), 1.52 – 1.40 (m, 2H). ^{13}C NMR (101 MHz, $CDCl_3$) δ: 164.77, 161.0, 132.2, 131.6, 118.7, 118.6, 116.8, 33.2, 24.3. FT-IR (ATR): υ [cm^{-1}] 2931 (m), 2858 (m), 1626 (s), 1496 (m), 1276 (s), 1150 (m), 847 (m), 751 (s).HRMS (ESI): Calculated for [$C_{20}H_{23}N_2O_2$] ([M+H]$^+$): 323.1754; Found: 323.1761.

(R,R)-N,N'-Bis(3-*tert*-butylsalicylidene)-1,2-cyclohexanediamine:
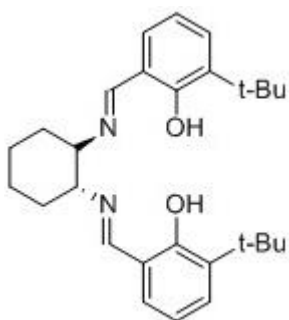
Synthesis was carried out according to a literature procedure.[84] K_2CO_3 (0.40 g, 2.86 mmol) was added to a solution of *(R,R)*-1,2-diaminocyclohexane tartrate (0.35 g, 1.43 mmol) in EtOH (100 mL) and water (5 mL). The mixture was heated at 60 °C for 10 minutes. 3-*Tert*-butyl-2-hydroxybenzaldehyde was dissolved in EtOH (30 mL) and added dropwise. The yellow solution was then refluxed for 1 h. After cooling to r.t., the solvent was removed *in vacuo*. The resulting residue was taken up in CH_2Cl_2 (80 mL) and washed with brine (80 mL), water (80 mL) and dried (Na_2SO_4). Solvent was removed *in vacuo* to yield a yellow solid which was used without further purification. Yield: 0.57 g, 91 %. ^{1}H NMR (400 MHz, CDCl$_3$) δ: 8.29 (s, 2H), 7.24 (dd, J = 7.9, 1.5 Hz, 2H), 7.0 (dd, J = 7.6, 1.6 Hz, 2H), 6.70 (t, J = 8.0 Hz, 2H), 3.40 – 3.26 (m, 2H), 2.0 – 1.93 (m, 2H), 1.93 – 1.83 (m, 2H), 1.79 – 1.67 (m, 2H), 1.53 – 1.45 (m, 2H), 1.41 (s, 18H). ^{13}C NMR (101 MHz, CDCl$_3$) δ: 165.6, 160.4, 137.1, 129.8, 129.3, 118.6, 117.8, 72.4, 34.8, 33.2, 31.0, 29.4, 24.4. FT-IR (ATR): υ [cm^{-1}] 2937 (m), 2861 (m), 1627 (s), 1484 (s), 1265 (m), 1145 (m), 1084 (m), 851 (m), 749 (s). HRMS (ESI): Calculated for [$C_{28}H_{39}N_2O_2$] ([M+H]$^+$): 435.3006; Found: 435.3009.

(R,R)-N,N'-Bis(5-*tert*-butylsalicylidene)-1,2-cyclohexanediamine:
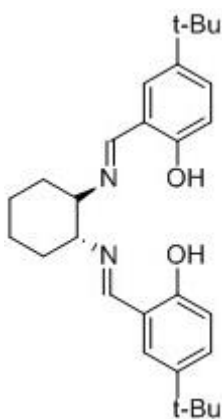
Synthesis was carried out according to a literature procedure.[85] K_2CO_3 (0.28 g, 2.04 mmol) was added to a solution of *(R,R)*-1,2-diaminocyclohexane tartrate (0.25 g, 1.02 mmol) in EtOH (20 mL) and water (10 mL). The mixture was heated to reflux for 10 minutes. 5-*Tert*-butyl-2-hydroxybenzaldehyde was dissolved in EtOH (40 mL) and added dropwise. The yellow solution was then refluxed for 2 h. After cooling to r.t., the solvent was removed *in vacuo*. The resulting residue was taken up in CH_2Cl_2 (50 mL) and washed with water (2 x 25 mL), brine (20 mL) and dried (Na_2SO_4). Solvent was removed *in vacuo* to yield a yellow solid which was used without further purification. Yield: 0.35 g, 79 %. ^{1}H NMR (400 MHz, CDCl$_3$) δ: 13.10 (br, 2H), 8.25 (s, 2H), 7.27 (dd, J =

8.5, 2.8 Hz, 2H), 7.0 (d, J = 2.8 Hz, 2H), 6.82 (d, J = 8.5 Hz, 2H), 3.36 – 3.25 (m, 2H), 2.0 – 1.82 (m, 4H), 1.80 – 1.65 (m, 2H), 1.53 – 1.38 (m, 2H). ^{13}C NMR (101 MHz, CDCl$_3$) δ: 165.11, 158.7, 141.3, 129.5, 128.0, 118.0, 116.3, 72.9, 33.9, 33.3, 31.5, 24.3. FT-IR (ATR): υ [cm^{-1}] 2956 (m), 2865 (m), 1633 (s), 1493 (s), 1268 (s), 1045 (w), 825 (s). HRMS (ESI): Calculated for [C$_{28}$H$_{39}$N$_2$O$_2$] ([M+H]$^+$): 435.3006; Found: 435.3016.

(R,R)-N,N′-Bis(5-methoxysalicylidene)-1,2-cyclohexanediamine:
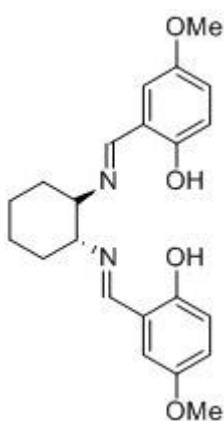
Synthesis was carried out following the procedure for *(R,R)*-N,N′-bis(5-*tert*-butylsalicylidene)-1,2-cyclohexanediamine. K$_2$CO$_3$ (0.45 g, 3.29 mmol) was added to a solution of *(R,R)*-1,2-diaminocyclohexane tartrate (0.40 g, 1.64 mmol) in EtOH (25 mL) and water (10 mL). The mixture was heated to reflux for 10 minutes. 5-Methoxy-2-hydroxybenzaldehyde was dissolved in EtOH (25 mL) and added dropwise. The yellow solution was then refluxed for 2 h. After cooling to r.t., the solvent was removed *in vacuo* to half the original volume. The resulting solution was diluted to 100 mL with water and extracted with CH$_2$Cl$_2$ (2 x50 mL). The organic phase was washed with brine (50 mL) and dried (Na$_2$SO$_4$). Solvent was removed *in vacuo* to yield a brown sticky solid which crystallised on standing. The crude product was purified by washing with hexane. Yield: 0.32 g, 51 %. ^{1}H NMR (400 MHz, CDCl$_3$) δ: 12.80 (br, 2H), 8.19 (s, 2H), 6.85 - 6.82 (m, 4H), 6.65 (dd, J = 2.4, 0.9 Hz, 2H), 3.70 (s, 6H), 3.55 – 3.23 (m, 2H), 2.00 – 1.83 (m, 4H), 1.81 – 1.56 (m, 2H), 1.54 – 1.41 (m, 2H). ^{13}C NMR (101 MHz, CDCl$_3$) δ: 164.5, 155.1, 152.0, 119.5, 118.3, 117.5, 114.9, 72.8, 55.9, 33.1, 24.2. FT-IR (ATR): υ [cm^{-1}] 2942 (m), 1954 (m), 1631 (s), 1590 (s), 1491 (s), 1268 (s), 1095 (m), 1035 (s), 809 (s). HRMS (ESI): Calculated for [C$_{22}$H$_{27}$N$_2$O$_4$] ([M+H]$^+$): 383.1965; Found: 383.1974.

(R,R)-N,N′-Bis(3-tert-butyl-5-methoxysalicylidene)-1,2-cyclohexanediamine:
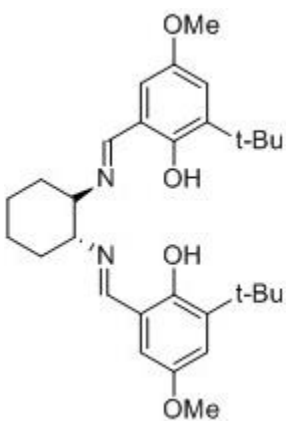
Synthesis was carried out according to a literature procedure.[84] K_2CO_3 (0.43 g, 3.12 mmol) was added to a solution of *(R,R)*-1,2-diaminocyclohexane tartrate (0.38 g, 1.56 mmol) in water (15 mL). The mixture was heated to reflux for 10 minutes. 3-*Tert*-butyl-5-methoxy-2-hydroxybenzaldehyde was dissolved in EtOH (75 mL) and added dropwise. The yellow solution was then refluxed for 1 h. After cooling to r.t., the solvent was removed *in vacuo*. The residue was taken up in CH_2Cl_2 (80 mL) and washed with water (50 mL) and brine (50 mL). The organic phase was dried (Na_2SO_4). Solvent was removed *in vacuo* to yield a yellow solid which was used without further purification. Yield: 0.67 g, 86 %. ^{1}H NMR (400 MHz, $CDCl_3$) δ: 8.23 (s, 2H), 6.89 (d, J = 3.2 Hz, 2H), 6.47 (d J = 3.3 Hz, 2H), 3.68 (s, 6H), 3.36 – 3.26 (m, 2H), 2.00 – 1.90 (m, 2H), 1.93 – 1.83 (m, 2H), 1.82 – 1.67 (m, 2H), 1.52 – 1.42 (m, 2H), 1.39 (s, 18H). ^{13}C NMR (101 MHz, $CDCl_3$) δ: 165.5, 154.9, 151.2, 138.7, 118.3, 117.9, 111.4, 72.5, 55.8, 35.0, 33.2, 29.3, 24.4. FT-IR (ATR): υ [cm^{-1}] 2936 (m), 2861 (m), 1632 (s), 1597 (s), 1429 (s), 1330 (s), 1097 (s), 782 (s).HRMS (ESI): Calculated for [$C_{30}H_{43}N_2O_4$] ([M+H]$^+$): 495.3217; Found: 495.3234.

(R,R)-N,N′-Bis(5-bromosalicylidene)-1,2-cyclohexanediamine:
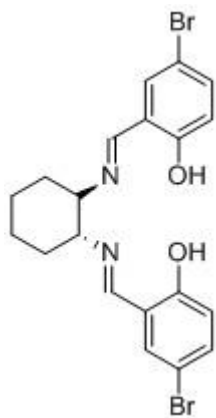
Synthesis was carried out following the procedure for *(R,R)-N,N′*-Bis(5-*tert*-butylsalicylidene)-1,2-cyclohexanediamine. K_2CO_3 (0.21 g, 1.50 mmol) was added to a solution of *(R,R)*-1,2-diaminocyclohexane tartrate (0.18 g, 0.75 mmol) in EtOH (20 mL) and water (2 mL). The mixture was heated to reflux for 10 minutes. 5-Bromo-2-hydroxybenzaldehyde (0.3 g, 1.5 mmol) was dissolved in EtOH (50 mL) and added dropwise. The yellow solution was then refluxed for 2 h. After cooling to r.t., the solution was diluted to 50 mL with CH_2Cl_2 and washed with water (50 mL). The organic phase was washed with brine (3 x 50 mL) and dried ($MgSO_4$). Solvent was removed *in vacuo* to yield an orange solid which was used without

further purification. Yield: 0.33 g, 91 %. ^{1}H NMR (400 MHz, CDCl$_3$) δ: 13.23 (br, 2H), 8.16 (s, 2H), 7.31 (d, J = 8.3 Hz, 1H), 7.30 (d, J = 8.3 Hz, 1H), 7.24 (d, J = 2.3 Hz, 2H), 6.78 (d, J = 8.9 Hz, 2H), 3.27 – 3.25 (m, 2H), 1.98 – 1.80 (m, 4H), 1.79 – 1.61 (m, 2H), 1.50 – 1.40 (m, 2H). ^{13}C NMR (101 MHz, CDCl$_3$) δ: 163.6, 160.1, 135.0, 133.6, 120.0, 119.0, 72.8, 33.0, 24.1. FT-IR (ATR): υ [cm^{-1}] 2919 (m), 2854 (m), 1631 (m), 1474 (s), 1280 (s), 1184 (s), 827 (s). HRMS (ESI): Calculated for [C$_{20}$H$_{21}$^{79}Br$_2$N$_2$O$_2$] ([M+H]$^+$): 478.9964; Found: 478.9978

(R,R)-N,N'-Bis(3-tert-butyl-5-bromosalicylidene)-1,2-cyclohexanediamine:
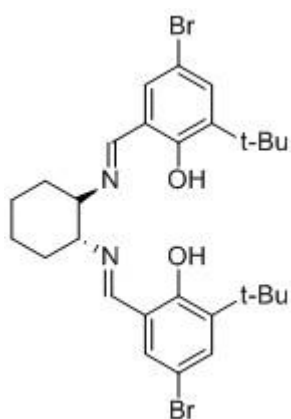
Synthesis was carried out following the procedure for *(R,R)-N,N'-*Bis(5-*tert*-butylsalicylidene)-1,2-cyclohexanediamine. K$_2$CO$_3$ (0.11 g, 0.78 mmol) was added to a solution of *(R,R)-*1,2-diaminocyclohexane tartrate (0.10 g, 0.39 mmol) in EtOH (5 mL) and water (1 mL). The mixture was heated to reflux for 10 minutes. 3-*Tert*-butyl-5-bromo-2-hydroxybenzaldehyde (0.20 g, 0.78 mmol) was dissolved in ethanol (20 mL) and added dropwise. The yellow solution was then refluxed for 1.5 h. After cooling to r.t., the solution was diluted to 50 mL with CH$_2$Cl$_2$ and washed with water (3 x50 mL). The organic phase was washed with brine (50 mL) and dried (MgSO$_4$). Solvent was removed *in vacuo* to yield a yellow solid which was used without further purification. Yield: 0.20 g, 88 %. ^{1}H NMR (400 MHz, CDCl$_3$) δ: 8.17 (s, 2H), 7.32 – 7.30 (m, 2H), 7.08 (d, J = 2.5 Hz, 2H), 3.37 – 3.20 (m, 2H), 2.04 – 1.94 (m, 2H), 1.93 – 1.83 (m, 2H), 1.82 – 1.75 (m, 2H), 1.53 – 1.42 (m, 2H). ^{13}C NMR (101 MHz, CDCl$_3$) δ: 164.5, 159.4, 139.9, 132.4, 131.6, 119.8, 109.8, 72.4, 35.1, 32.9, 29.2, 24.3. FT-IR (ATR): υ [cm^{-1}] 2936 (m), 2861 (m), 1629 (s), 1428 (s), 1302 (s), 1201 (s), 867 (s), 705 (s). HRMS (ESI): Calculated for [C$_{28}$H$_{37}$^{79}Br$_2$N$_2$O$_2$] ([M+H]$^+$): 591.1216; Found: 591.1202.

(R,R)-N,N'-Bis(3-*tert*-butylsalicylidene)-1,2-diphenyl-1,2-ethanediamine:
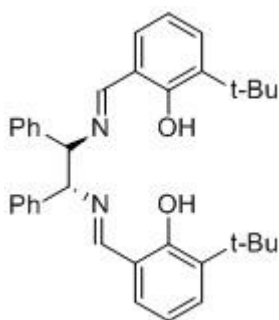
Synthesis was carried out following a literature procedure.[86] *(1R, 2R)*-(+)-1,2-Diphenyl-1,2-ethanediamine (0.12 g, 0.56 mmol) was dissolved in EtOH (15 mL) and added to a solution of 3-*tert*-butyl-2-hydroxybenzaldehyde (0.20 g, 1.12 mmol) in EtOH (5 mL). The solution immediately turned yellow. The mixture was heated to reflux for 18 h. After cooling to r.t., the solvent was removed *in vacuo* to yield a yellow solid which was used without further purification. Yield: 0.29 g, 99 %. ^{1}H NMR (400 MHz, CDCl$_3$) δ: 8.35 (s, 2H), 7.28 – 7.13 (m, 12H), 7.00 (d, J = 7.0 Hz, 1.8 Hz, 2H), 6.70 (t, J = 7.7 Hz, 2H), 4.71 (s, 1H), 1.41 (s, 18H). ^{13}C NMR (101 MHz, CDCl$_3$) δ: 166.9, 160.3, 139.6, 137.2, 129.7, 128.4, 128.1, 127.6, 118.6, 117.9, 80.2, 34.9, 29.4. FT-IR (ATR): υ [cm^{-1}] 2958 (m), 1625 (s), 1494 (s), 1266 (m), 1203 (m), 751 (s), 700 (s). HRMS (ESI): Calculated for [C$_{36}$H$_{41}$N$_2$O$_2$] ([M+H]$^+$): 533.3163; Found: 533.3159.

5.3. Preparation of aluminium(salen) complexes

Riccardo's catalyst (**5b**):
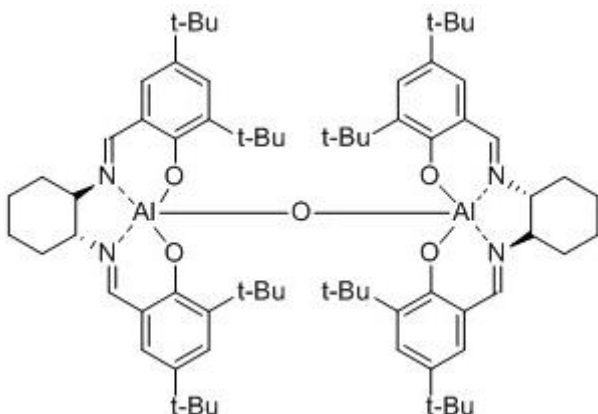
Synthesis was carried out according to a literature procedure.[87] Shredded aluminium foil (0.85 g, 31.64 mmol) was added to EtOH/MePh (400 mL, 3:1 ratio). A crystal of I$_2$ was added and the mixture was refluxed for 1.5 h, during which the aluminium was seen to disintegrate into a grey precipitate. A solution of *(R,R)-N,N'*-bis(3,5-di-*tert*-butylsalicylidene)-1,2-cyclohexanediamine (8.65 g, 15.82 mmol) in MePh was added and the resulting mixture was refluxed for 20 h. After cooling to r.t., the suspension was filtered through celite and the solvent removed *in vacuo*. The residue was taken up in CH$_2$Cl$_2$ (200 mL), washed with water (3 x 200 mL) and brine (200 mL), and dried (Na$_2$SO$_4$). Solvent was removed *in vacuo* to yield

a grey-yellow solid which was washed with hexanes to afford a light yellow precipitate. Yield: 3.64 g, 40 %. ^{1}H NMR (400 MHz, CDCl$_3$) δ: 8.09 (s, 4H), 7.46 (s, 4H), 7.03 (s, 4H), 2.88-3.54 (m, 4H), 1.66-2.44 (m, 16H), 1.42 (s, 36H), 1.30 (s, 36H) FT-IR (ATR): υ [cm^{-1}] = 2951 (s), 2866 (m), 1625 (s), 1354 (m), 1175 (m), 1026 (m), 865 (m), 753 (m). HRMS (ESI): Calculated for [C$_{72}$H$_{105}$AlN$_4$O$_5$] ([M+H]$^+$): 1159.7719; Found: 1159.7710.

(R,R)-N,N′-Bis(3,5-di-*tert*-butylsalicylidene)-1,2-cyclohexanediaminoaluminium(III) chloride (**2a**):
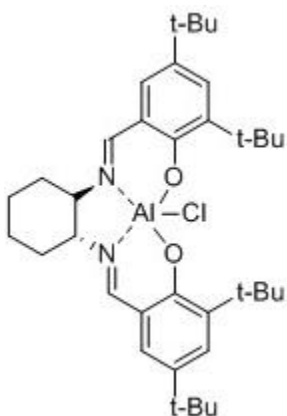
Synthesis was carried out according to a reported literature procedure.[59] Diethylaluminium chloride solution (0.9 M in MePh, 4.10 mL, 3.69 mmol) was added dropwise *via* syringe to a solution of *(R,R)*-N,N′-bis(3,5-di-tert-butylsalicylidene)-1,2-cyclohexanediamine (2.00 g, 3.66 mmol) in dry MePh. The resulting solution was stirred under nitrogen for 24 h. Solvent was removed *in vacuo* to yield a yellow solid which was used without further purification. Yield: 2.20 g, 99 %. ^{1}H NMR (400 MHz, CDCl$_3$) δ: 8.37 (s, 2H), 8.18 (s, 2H), 7.54 (s, 2H), 3.17-3.92 (m, 2H), 2.08-2.58 (m, 8H), 1.54 (s, 18H), 1.30 (18H). FT-IR (ATR): υ [cm^{-1}] = 2952 (m), 2867 (w), 1615 (s), 1542 (m), 1315 (m), 1178 (m), 865 (m). HRMS (ESI): Calculated for [C$_{37}$H$_{56}$AlN$_2$O$_3$] ([M-Cl+MeOH]$^+$): 603.4106; Found: 603.4117. [α]$_D$ -580 (c = 0.1, CHCl$_3$) (lit. -503)[59]

*(R,R)-N,N'-*Bis(3,5-di-*tert*-butylsalicylidene)-1,2-cyclohexanediaminoaluminium(III) acetate (**2b**):

Synthesis was carried out according to a modified literature procedure.[88] Silver(I) acetate (0.35 g, 2.12 mmol) was added to a solution of *(R,R)-N,N'-*bis(3,5-di-*tert*-butylsalicylidene)-1,2-cyclohexanediamino-aluminium(III) chloride (1.28 g, 2.12 mmol) in methyl *tert*-butyl ether (25 mL). The resultant solution was stirred at r.t. overnight in darkness and filtered over celite. The celite was flushed with methyl *tert*-butyl ether (15 mL) and the solvent was removed *in vacuo* to yield a yellow solid. The solid was used without further purification. Yield: 0.97 g, 72 %. ^{1}H NMR (400 MHz, CDCl$_3$) δ: 8.37 (s, 1H), 8.18 (s, 1H), 7.52 (br, 2H), 7.11 (m, 1H), 7.03 (m, 1H), 4.00 (br, 1H), 3.11 (m, 1H), 2.57 (s, 2H), 2.42 (s, 2H), 2.06 (s, 4H), 1.76 (m, 3H), 1.50 (s, 18H), 1.31 (s, 9H), 1.29 (s, 9H). ^{13}C NMR (101 MHz, CDCl$_3$) δ: 165.9, 158.1, 140.8, 139.9, 136.4, 126.8, 126.1, 117.9, 72.5, 35.6, 35.0, 34.1, 33.4, 31.5, 29.7, 29.5, 24.5. FT-IR (ATR): υ [cm^{-1}] = 2952 (m), 2867 (w), 2164 (w), 1625 (s), 1464 (s), 1441 (s), 1359 (s), 1174 (s), 1051 (m), 846 (s), 787 (s), 731 (s). HRMS (ESI): Calculated for [C$_{37}$H$_{56}$AlN$_2$O$_3$] ([M-OAc+MeOH]$^+$): 603.4106; Found: 603.4107. LRMS (LIFDI): Calculated for [C$_{38}$H$_{58}$AlN$_2$O$_4$] ([M]$^+$): 630.3977. Found: 630.40.

*(R,R)-N,N'-*Bis(3,5-di-*tert*-butylsalicylidene)-1,2-cyclohexanediaminoaluminium(III) tosylate (**2c**):

Synthesis was carried out according to a literature procedure.[3] To a solution of silver(I) tosylate (0.63 g, 2.27 mmol) in MeCN (50 mL) was added a solution of *(R,R)-N,N'-*bis(3,5-di-*tert*-butylsalicylidene)-1,2-cyclohexanediamino-aluminium(III) chloride (1.30 g, 2.14 mmol) in MeCN (3 mL) under nitrogen. The mixture was stirred at r.t for 16 h in darkness. The resultant suspension was filtered over celite and the absorbent flushed with MeCN (15

mL). The solvent was removed *in vacuo* to yield a yellow solid. The solid was used without further purification. Yield: 1.34 g, 84 %. ^{1}H NMR (400 MHz, CDCl$_3$) δ: 8.30 (s, 2H), 7.52 (d, J= 2.5 Hz, 2H), 7.31 (d, J = 7.3 Hz, 2H), 7.09 (d, J = 2.5 Hz, 2H), 6.85 (d, J = 2.5 Hz, 2H), 2.55 (m, 2H), 2.24 (s, 3H), 2.10 (m, 2H), 1.75 (m, 2H), 1.60 – 1.45 (m, 4H), 1.39 (s, 18H), 1.33 (s, 18H). FT-IR (ATR): ʋ [cm^{-1}] = 2954 (m), 2869 (w), 2362 (w), 1625 (s), 1545 (m), 1238 (m), 1176 (s), 1037 (m), 847 (s), 819 (m), 682 (m). HRMS (ESI): Calculated for [C$_{37}$H$_{56}$AlN$_2$O$_3$] ([M-OTs+MeOH]$^+$): 603.4106; Found: 603.4117. LRMS (LIFDI): Calculated for [C$_{43}$H$_{59}$AlN$_2$O$_5$S] ([M]$^+$): 742.3960. Found: 742.40.

5.4.   Preparation of cobalt(salen) complexes

(R,R)-N,N'-Bis(3,5-di-*tert*-butylsalicylidene)-1,2-cyclohexanediaminocobalt(II) :
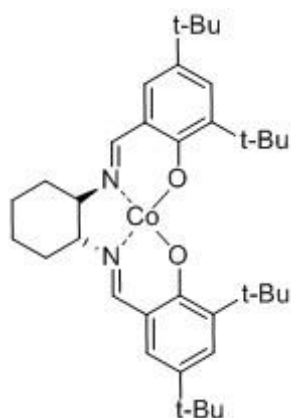
Synthesis was carried out according to a literature procedure.[89] To a solution of *(R,R)-N,N'*-bis(3,5-di-*tert*-butylsalicylidene)-1,2-cyclohexanediamine (2.00 g, 3.65 mmol) in CH$_2$Cl$_2$ (15 mL) was added a solution of cobalt(II) acetate tetrahydrate (1.09 g, 4.39 mmol) in MeOH (10 mL) under nitrogen. The mixture was stirred at r.t. for 5 minutes, then cooled to 0 °C and stirred for another 15 minutes. A red precipitate was formed which was washed with ice-cold MeOH (10 mL). Yield: 1.83 g, 83 %. M.P: > 298 °C (decomposition) (lit. >300 °C).[90] FT-IR (ATR): ʋ [cm^{-1}] = 2951 (s), 2867 (m), 1594 (s), 1526 (s), 1320 (s), 1253 (s), 1175 (s), 1049 (w), 786 (s). HRMS (ESI): Calculated for [C$_{36}$H$_{52}$CoN$_2$O$_2$] ([M]$^+$): 603.3361. Found: 603.3338. [α]$_D$ -742 (c = 0.0038, CHCl$_3$) (lit. -1145)[69]

(R,R)-N,N'-Bis(3,5-di-*tert*-butylsalicylidene)-1,2-cyclohexanediaminocobalt(III) chloride (**3a**):
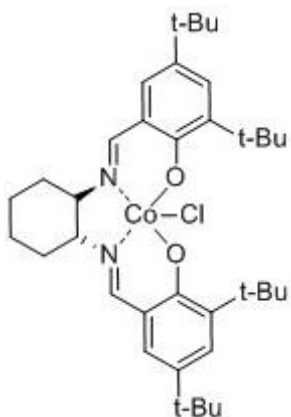
Synthesis was carried out according to a literature procedure.[91] *(R,R)-N,N'*-bis(3,5-di-*tert*-butylsalicylidene)-1,2-cyclohexanediaminocobalt(III) tosylate (1.13 g, 1.46 mmol) was dissolved in CH_2Cl_2 (40 mL) and washed with brine (3 x 40 mL). The organic phase was dried over Na_2SO_4. Solvent was removed *in vacuo* to yield a dark green powder. Yield: 0.76 g, 81 %. ^{1}H NMR (400 MHz, DMSO-d_6) δ: 7.81 (s, 2H), 7.51 (m, 2H), 7.47 (m, 2H), 3.58 - 3.68 (m, 2H), 3.04 - 3.15 (m, 2H), 1.99 - 2.11 (m, 2H), 1.89 - 1.99 (m, 2H), 1.78 (s, 18H), 1.56 - 1.67 (m, 2H), 1.34 (s, 18H). FT-IR (ATR): υ [cm^{-1}] = 2954 (m), 2866 (m), 1981 (w), 1607 (m), 1525 (m), 1360 (m), 1254 (s), 1174 (m), 1092 (m), 1011 (s), 803 (s). LRMS (LIFDI): Calculated for [$C_{36}H_{52}{}^{35}ClCoN_2O_2$] ([M]$^+$): 638.3049. Found: 638.31. [α]$_D$ -526 (c = 0.0038, $CHCl_3$)

(R,R)-N,N'-Bis(3,5-di-*tert*-butylsalicylidene)-1,2-cyclohexanediaminocobalt(III) acetate (**3b**):
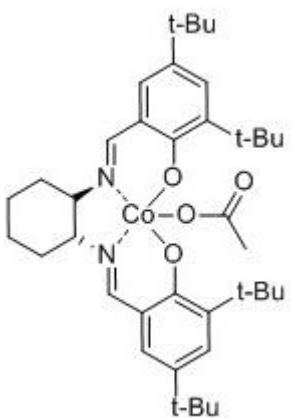
Synthesis was carried out according to a literature procedure.[91] To a solution of *(R,R)-N,N'*-bis(3,5-di-*tert*-butylsalicylidene)-1,2-cyclohexanediamine (1.69 g, 3.10 mmol) in CH_2Cl_2 (10 mL) was added a solution of cobalt(II) acetate tetrahydrate (0.93 g, 3.72 mmol) in MeOH (10 mL). The mixture was stirred at r.t. under air for 1 h. Solvent was removed *in vacuo* to yield a brown solid. The solid was redissolved in MeOH (10 mL) and precipitated by slow addition of water (10 mL). The precipitate was filtered, rinsed with water (3 x 10 mL), and dried *in vacuo* to yield a brown powder. Yield: 1.30 g, 63 %. ^{1}H NMR (400 MHz, CD_2Cl_2) δ: 7.47 (br, s, 1H), 7.30 (br, s, 1H), 7.25 (br, s, 1H), 7.20 (br, s, 1H), 7.17 (br, s, 1H), 6.70 (s, 1H), 4.4-4.6 (m, 2H), 3.2-3.4 (m, 2H), 2.7-2.8 (m, 2H), 1.9-2.0 (m, 2H), 1.8-1.9 (m, 2H), 1.67 (s, 3H), 1.49 (s, 9H), 1.36 (s, 9H), 1.31 (s, 9H), 1.22 (s, 9H); M.P: > 180 °C

(decomposition). FT-IR (ATR): υ [cm^{-1}] 3355 (br), 2950 (s), 2906 (m), 2866 (m), 2361 (w), 2163 (w), 2050 (w), 1980 (w), 1635 (s), 1528 (s), 1459 (s), 1436 (s), 1255 (s), 1169 (s), 1026 (m), 834 (m), 783 (m). HRMS (ESI): Calculated for [C$_{36}$H$_{52}$CoN$_2$O$_2$]: 603.3355; Found: 603.3338. [α]$_D$ +502 ° (c = 0.0038, CHCl$_3$)

(R,R)-N,N′-Bis(3,5-di-*tert*-butylsalicylidene)-1,2-cyclohexanediaminocobalt(III) tosylate (**3c**):
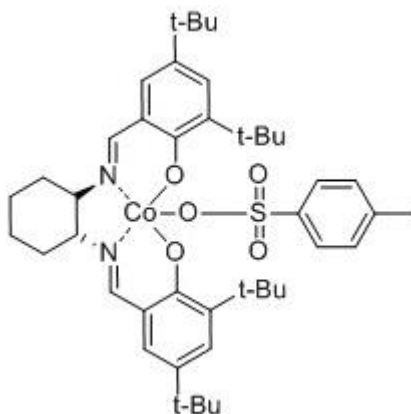
Synthesis was carried out according to a literature procedure.[3] *(R,R)-N,N′*-bis(3,5-di-*tert*-butylsalicylidene)- 1,2-cyclohexanediamino-cobalt(II) (1.83 g, 3.03 mmol) was dissolved in CH$_2$Cl$_2$ (25 mL). p-toluene sulfonic acid (0.61 g, 3.22 mmol) was added. The resultant mixture was stirred open to the atmosphere for 2 h at r.t. A colour change from orange to dark green was observed. Solvent was removed *in vacuo* to yield a dark green powder. The solid was used without further purification. Yield: 2.34 g, 99 %. ^{1}H NMR (400 MHz, DMSO-d$_6$) δ: 7.86 (s, 2H), 7.51 (m, 2H), 7.49 (m, 2H), 7.48 (m, 2H), 7.14 - 7.16 (m, 2H), 3.60 - 3.69 (m, 2H), 3.09 - 3.12 (m, 2H), 2.32 (s, 3H), 2.00 - 2.10 (m, 2H), 1.90 - 2.00 (m, 2H), 1.78 (s, 18H), 1.62 - 1.66 (m, 2H), 1.34 (s, 18H). ^{13}C NMR (101 MHz, DMSO-d$_6$) δ:165.6, 163.1, 146.8, 142.8, 138.5, 136.9, 130.3, 129.8, 129.0, 126.5, 119.6, 70.2, 36.8, 34.5, 32.5, 31.4, 30.5, 25.3, 21.8. HRMS (ESI): Calculated for [C$_{36}$H$_{52}$CoN$_2$O$_2$] ([M-OTs]$^+$): 603.3355; Found: 603.3352. [α]$_D$ -665 (c = 0.0038, CHCl$_3$)
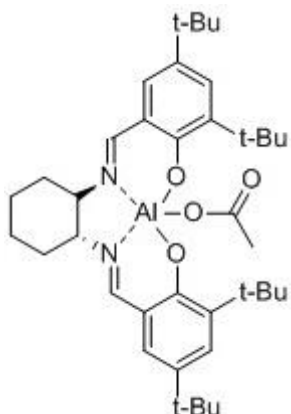
(R,R)-N,N′-Bis(3,5-di-*tert*-butylsalicylidene)-1,2-cyclohexanediaminocobalt(III) bromide (**3d**):
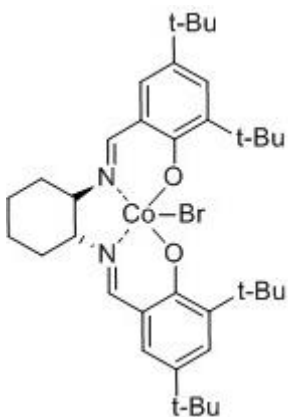
Synthesis was carried out according to a literature procedure.[92] *(R,R)-N,N′*-bis(3,5-di-*tert*-butylsalicylidene)-1,2-cyclohexanediaminocobalt(III) tosylate (1.83 g, 2.36 mmol) was dissolved in CH_2Cl_2 (80 mL) and washed with sat'd NaBr(aq) (3 x 50 mL). The organic phase was dried over Na_2SO_4. Solvent was removed *in vacuo* to yield a dark green powder. Yield: 1.38 g, 85 %. ^{1}H NMR (400 MHz, CDCl$_3$) δ: 8.32 (s, 2H), 7.31 (d, J = 2.4 Hz, 2H), 7.00 (d, J = 2.4 Hz, 2H), 3.30 - 3.40 (m, 2H), 1.82 - 2.01 (m, 4H), 1.67 - 1.82 (m, 2H), 1.44 -1.56 (m, 2H), 1.42 (s, 18H), 1.25 (s, 18H). ^{13}C NMR (101 MHz, CDCl$_3$) δ: 165.9, 158.1, 140.0, 136.6, 126.8, 126.2, 117.9, 72.6, 35.1, 34.1, 33.4, 31.6, 29.6, 24.5. FT-IR (ATR): υ [cm^{-1}] = 2953 (s), 2862 (m), 1627 (s), 1440 (s), 1391 (m), 1361 (s), 1273 (s), 1252 (s), 1203 (m), 1174 (s), 1097 (w), 877 (m), 830 (m), 772 (m), 733 (m), 713 (m). LRMS (LIFDI): Calculated for [C$_{36}$H$_{52}$^{79}BrCoN$_2$O$_2$] ([M]$^+$): 682.2544. Found: 682.25. [α]$_D$ -287 (c = 0.0132, CH_2Cl_2)
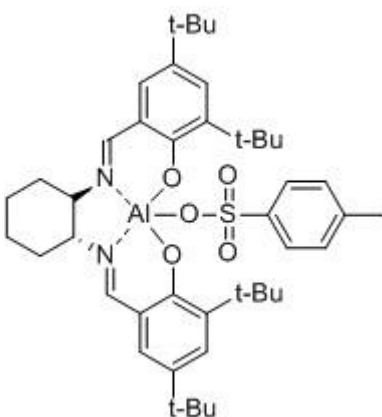
5.5. Preparation of chromium(salen) complexes

(R,R)-N,N'-Bis(3,5-di-*tert*-butylsalicylidene)-1,2-cyclohexanediaminochromium(III) chloride (**4a**):
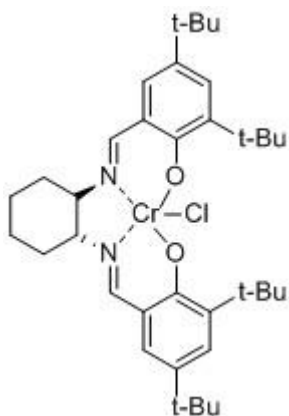
Synthesis was carried out according to a literature procedure.[55] *(R,R)-N,N'*-bis(3,5-di-*tert*-butylsalicylidene)-1,2-cyclohexanediamine (2.00 g, 3.66 mmol) was dissolved in dry, degassed THF. Chromium(II) chloride (0.49 g, 4.02 mmol) was suspended in dry, degassed THF and then added to the *(R,R)-N,N'*-bis(3,5-di-*tert*-butylsalicylidene)-1,2-cyclohexanediamine solution. The yellow solution rapidly turned brown. The solution was stirred under N_2 for 4 h, and under air for 18 h. The solution was diluted with methyl *tert*-butyl ether (50 mL) and washed with saturated NH_4Cl (aq) (3 x 100 mL) and brine (3 x 100 mL). The organic phase was dried (Na_2SO_4) and solvent removed *in vacuo* to yield a red-brown solid. The solid was used without further purification. Yield: 2.24 g, 97 %. M.P: > 222 °C (decomposition) (lit. >375-398 °C).[55] FT-IR (ATR): υ [cm^{-1}] 2951 (s), 2867 (m), 1619 (s), 1435 (m), 1361 (m), 1030 (s), 967 (m), 814 (m). HRMS (ESI): Calculated for [$C_{36}H_{52}CrN_2O_2$] ([M-Cl]$^+$): 596.3434; Found: 596.3450. [α]$_D$ -259 (c = 0.087, CHCl$_3$)

(R,R)-N,N'-Bis(3,5-di-*tert*-butylsalicylidene)-1,2-cyclohexanediaminochromium(III) acetate (**4b**):
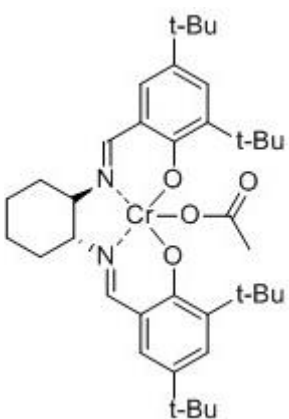
Synthesis was carried out according to a literature procedure.[93] Silver(I) acetate (0.33 g, 1.99 mmol) was added to a solution of *(R,R)-N,N'*-bis(3,5-di-*tert*-butylsalicylidene)-1,2-cyclohexanediaminochromium(III) chloride (1.26 g, 1.99 mmol) in methyl *tert*-butyl ether (20 mL). The resultant solution was stirred at r.t. overnight in darkness and filtered over celite. The celite was flushed with methyl *tert*-butyl ether (10 mL) and the solvent was removed *in vacuo* to yield a red-brown solid. The solid was used without further purification. Yield: 1.09 g, 84 %. M.P: > 148 °C (decomposition). FT-IR (ATR): υ

[cm^{-1}] 2951 (s), 2907 (m), 2866 (m), 2363 (w), 1727 (w), 1622 (s), 1530 (s), 1435 (s), 1360 (s), 1255 (s), 1200 (s), 1167 (s), 1032 (m), 1026 (m), 836 (m). HRMS (ESI): Calculated for [C$_{36}$H$_{52}$CrN$_2$O$_2$] ([M-OAc]$^+$): 596.3429; Found: 546.3431. LRMS (LIFDI): Calculated for [C$_{38}$H$_{55}$CrN$_2$O$_4$] ([M]$^+$): 655.3657. Found: 655.39. [α]$_D$ +281 ° (c = 0.07, CHCl$_3$)

(R,R)-N,N′-Bis(3,5-di-*tert*-butylsalicylidene)-1,2-cyclohexanediaminochromium(III) tosylate (**4c**):
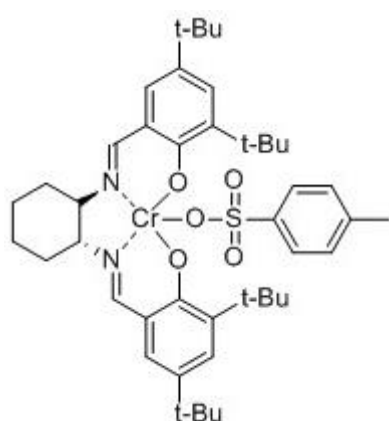
Synthesis was carried out according to a literature procedure.[3] Silver(I) p-toluenesulfonate (0.57 g, 2.03 mmol) was dissolved in dry, degassed MeCN (3 mL) under nitrogen. To this solution was added a solution of *(R,R)-N,N′*-bis(3,5-di-*tert*-butyl-salicylidene)-1,2-cyclohexanediaminochromium(III) chloride (1.20 g, 1.90 mmol) in dry, degassed MeCN (20 mL). The resultant solution was stirred at r.t. overnight in darkness and filtered over celite. The celite was flushed with MeCN (15 mL) and the solvent was removed *in vacuo* to yield a red brown solid. The solid was used without further purification. Yield: 1.42 g, 98 %. M.P: > 178 °C (decomposition). FT-IR (ATR): υ [cm^{-1}] 2952 (s), 2867 (m), 2324 (w), 2164 (w), 1981 (w), 1727 (w), 1620 (s), 1435 (s), 1235 (m), 1166 (s), 1032 (m), 1012 (m), 837 (m), 681 (m). LRMS (LIFDI): Calculated for [C$_{43}$H$_{59}$CrN$_2$O$_5$S] ([M]$^+$): 767.3550. Found: 767.36. [α]$_D$ +71 (c = 0.0626, CHCl$_3$)

(R,R)-N,N′-Bis(salicylidene)-1,2-cyclohexanediaminochromium(III) chloride (**4d**):

Synthesis was carried out following the procedure for *(R,R)-N,N′*-bis(3,5-di-*tert*-butylsalicylidene)-1,2-cyclohexanediamino-chromium(III) chloride (**4a**). *(R,R)-N,N′*-bis(salicylidene)-1,2-cyclohexanediamine (0.44 g, 1.37 mmol) was dissolved in dry, degassed THF. Chromium(II) chloride (0.18 g, 1.50 mmol) was suspended in dry, degassed THF and then added to the *(R,R)-N,N′*-bis(salicylidene)-1,2-cyclohexanediamine solution. The yellow solution rapidly turned brown. The solution was stirred under N$_2$ for 4 h, and under air

for 18 h. The solution was diluted with methyl *tert*-butyl ether (50 mL) and washed with saturated NH_4Cl (aq) (3 x 100 mL) and brine (3 x 100 mL). The organic phase was dried (Na_2SO_4) and solvent removed *in vacuo* to yield a yellow-brown solid. The solid was used without further purification. Yield: 0.33 g, 59 %. M.P: > 290 °C. FT-IR (ATR): υ [cm^{-1}] 2937 (w), 1632 (s), 1621 (s), 1469 (s), 1315 (s), 1194 (m), 1024 (m), 906 (s), 749 (s). HRMS (ESI): Calculated for [$C_{20}H_{20}CrN_2O_2$] ([M-Cl]$^+$): 372.0924; Found: 372.0924. LRMS (LIFDI): Calculated for [$C_{20}H_{20}^{35}ClCrN_2O_2$] ([M]$^+$): 407.06; Found: 407.08. [α]$_D$ -543 (c = 0.025, THF)

(R,R)-N,N'-Bis(3-*tert*-butyl-salicylidene-1,2-cyclohexanediaminochromium(III) chloride (**4e**):

Synthesis was carried out following the procedure for *(R,R)-N,N'*-bis(3,5-di-*tert*-butylsalicylidene)-1,2-cyclohexanediaminochromium(III) chloride (**4a**). *(R,R)-N,N'*-bis(3-*tert*-butyl-salicylidene)-1,2-cyclohexanediamine (0.56 g, 1.29 mmol) was dissolved in dry, degassed THF (15 mL). Chromium(II) chloride (0.17 g, 1.42 mmol) was suspended in dry, degassed THF (15 mL) and then added to the *(R,R)-N,N'*-bis(3-*tert*-butyl-salicylidene)-1,2-cyclohexanediamine solution. The yellow solution rapidly turned brown. The solution was stirred under N_2 for 4 h, and under air for 18 h. The solution was diluted with methyl *tert*-butyl ether (15 mL) and washed with saturated NH_4Cl (aq) (3 x 20 mL) and brine (3 x 20 mL). The organic phase was dried (Na_2SO_4) and solvent removed *in vacuo* to yield a red-brown solid. The solid was used without further purification. Yield: 0.63 g, 94 %. M.P: > 290 °C. FT-IR (ATR): υ [cm^{-1}] 2941 (m), 2858 (w), 1619 (s), 1532 (s), 1543 (s), 1421 (s), 1316 (m), 1190 (m), 1024 (m), 870 (s), 749 (s). HRMS (ESI): Calculated for [$C_{28}H_{36}CrN_2O_2$] ([M-Cl]$^+$): 484.2176; Found: 484.2190. LRMS (LIFDI): Calculated for [$C_{28}H_{36}^{35}ClCrN_2O_2$] ([M]$^+$): 519.19; Found: 519.20. [α]$_D$ -1285 (c = 0.040, THF)

(*R,R*)-*N,N'*-Bis(5-*tert*-butyl-salicylidene-1,2-cyclohexanediaminochromium(III) chloride (**4f**):
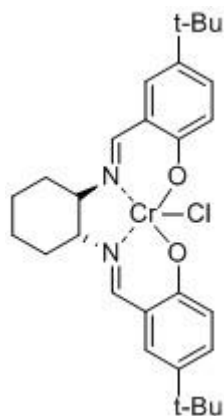
Synthesis was carried out following the procedure for (*R,R*)-*N,N'*-bis(3,5-di-*tert*-butylsalicylidene)-1,2-cyclohexanediamino-chromium(III) chloride (**4a**). (*R,R*)-*N,N'*-bis(5-*tert*-butyl-salicylidene)-1,2-cyclohexanediamine (0.56 g, 1.29 mmol) was dissolved in dry, degassed THF (25 mL). Chromium(II) chloride (0.17 g, 1.42 mmol) was suspended in dry, degassed THF (15 mL) and then added to the (*R,R*)-*N,N'*-bis(5-*tert*-butyl-salicylidene)-1,2-cyclohexanediamine solution. The yellow solution rapidly turned brown. The solution was stirred under N_2 for 4 h, and under air for 18 h. The solution was diluted with methyl *tert*-butyl ether (20 mL) and washed with saturated NH_4Cl (aq) (3 x 40 mL) and brine (3 x 40 mL). The organic phase was dried (Na_2SO_4) and solvent removed *in vacuo* to yield a brown solid. The solid was used without further purification. Yield: 0.29 g, 79 %. M.P: > 270 °C (decomposition). FT-IR (ATR): υ [cm^{-1}] 2963 (m), 2858 (w), 1621 (s), 1258 (s), 1177 (s), 1062 (m), 1033 (m), 831 (s). HRMS (ESI): Calculated for [$C_{28}H_{36}CrN_2O_2$] ([M-Cl]$^+$): 484.2176; Found: 484.2162. LRMS (LIFDI): Calculated for [$C_{28}H_{36}{}^{35}ClCrN_2O_2$] ([M]$^+$): 519.19; Found: 519.20. [α]$_D$ + 425 (c = 0.034, THF)

(*R,R*)-*N,N'*-Bis(5-methoxy-salicylidene-1,2-cyclohexanediaminochromium(III) chloride (**4g**):
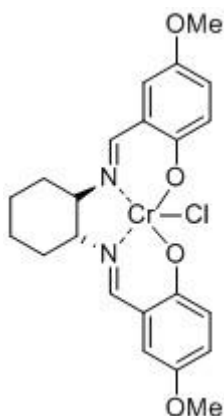
Synthesis was carried out following the procedure for (*R,R*)-*N,N'*-bis(3,5-di-*tert*-butylsalicylidene)-1,2-cyclohexanediamino-chromium(III) chloride (**4a**). (*R,R*)-*N,N'*-bis(5-methoxy-salicylidene)-1,2-cyclohexanediamine (0.25 g, 0.65 mmol) was dissolved in dry, degassed THF (5 mL). Chromium(II) chloride (88 mg, 0.72 mmol) was suspended in dry, degassed THF (15 mL) and then added to the (*R,R*)-*N,N'*-bis(5-methoxy-salicylidene)-1,2-cyclohexanediamine solution. The yellow solution rapidly turned brown. The solution was stirred under N_2 for 4 h, and under air for 18 h. The solution was diluted with methyl *tert*-butyl ether (20 mL)

and washed with saturated NH4Cl (aq) (3 x 50 mL) and brine (3 x 50 mL). The organic phase was dried (Na2SO4) and solvent removed *in vacuo* to yield a brown solid. The solid was used without further purification. Yield: 0.24 g, 78 %. M.P: > 290 °C. FT-IR (ATR): υ [cm^{-1}] 2933 (m), 1630 (m), 1543 (m), 1475 (s), 1158 (s), 1030 (s), 817 (s), 783 (m). LRMS (LIFDI): Calculated for [C22H24^{35}ClCrN2O4] ([M]$^+$): 467.08; Found: 467.08. [α]D -266 (c = 0.048, THF)

(*R,R*)-*N,N'*-Bis(3-*tert*-butyl-5-methoxy-salicylidene-1,2-cyclohexanediaminochromium(III) chloride (**4h**):
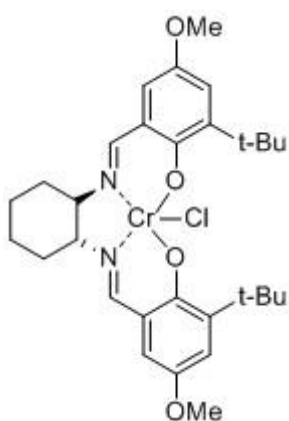
Synthesis was carried out following the procedure for (*R,R*)-*N,N'*-bis(3,5-di-*tert*-butylsalicylidene)-1,2-cyclohexanediaminochromium(III) chloride (**4a**). (*R,R*)-*N,N'*-bis(5-methoxy-3-*tert*-butyl-salicylidene)-1,2-cyclohexanediamine (0.67 g, 1.35 mmol) was dissolved in dry, degassed THF (15 mL). Chromium(II) chloride (0.18 g, 1.49 mmol) was suspended in dry, degassed THF (15 mL) and then added to the (*R,R*)-*N,N'*-bis(3-*tert*-butyl-5-methoxy-salicylidene)-1,2-cyclohexanediamine solution. The yellow solution rapidly turned brown. The solution was stirred under N2 for 4 h, and under air for 18 h. The solution was diluted with methyl *tert*-butyl ether (15 mL) and washed with saturated NH4Cl (aq) (3 x 20 mL) and brine (3 x 20 mL). The organic phase was dried (Na2SO4) and solvent removed *in vacuo* to yield a brown solid. The solid was used without further purification. Yield: 0.48 g, 61 %. M.P: > 230 °C. FT-IR (ATR): υ [cm^{-1}] 2939 (m), 1864 (w), 1622 (s), 1543 (m), 1416 (s), 1315 (s), 1209 (s), 1064 (s), 823 (s), 800 (s). HRMS (ESI): Calculated for [C30H40CrN2O4] ([M-Cl]$^+$): 544.2388; Found: 544.2381. LRMS (LIFDI): Calculated for [C30H40^{35}ClCrN2O4] ([M]$^+$): 579.21; Found: 579.21. [α]D -948 (c = 0.056, THF)

(*R,R*)-*N,N'*-Bis(5-bromo-salicylidene-1,2-cyclohexanediaminochromium(III) chloride (**4i**):
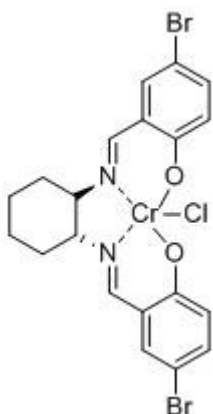
Synthesis was carried out following the procedure for (*R,R*)-*N,N'*-bis(3,5-di-*tert*-butylsalicylidene)-1,2-cyclohexanediamino-chromium(III) chloride (**4a**). A dry round-bottomed flask was charged with (*R,R*)-*N,N'*-bis(5-bromo-salicylidene)-1,2-cyclohexanediamine (0.20 g, 0.42 mmol) and chromium(II) chloride (56 mg, 0.45 mmol). Dry, degassed THF (10 mL) was syringed in to form a brown solution. The solution was stirred under N_2 for 4 h, and under air for 18 h. The resulting yellow-brown precipitate was filtered off and used without further purification. Yield: 0.12 g, 49 %. M.P: > 290 °C. FT-IR (ATR): ʋ [cm^{-1}] 2933 (m), 2867 (w), 1622 (m), 1460 (m), 1176 (s), 812 (s), 652 (s). LRMS (LIFDI): Calculated for [$C_{20}H_{18}{}^{79}Br^{81}BrCrN_2O_2$] ([M-Cl]$^+$): 529.91; Found: 529.93. [α]$_D$ -121 (c = 0.025, EtOH)
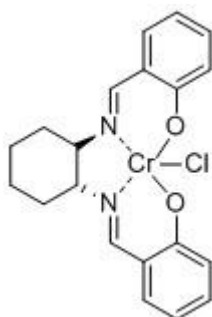
(*R,R*)-*N,N'*-Bis(5-bromo-3-*tert*-butyl-salicylidene-1,2-cyclohexanediaminochromium(III) chloride (**4j**):
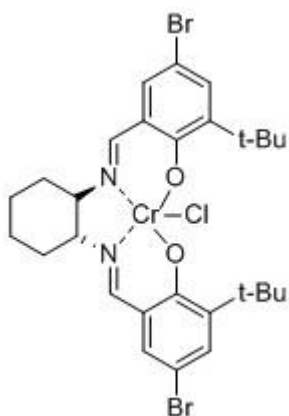
Synthesis was carried out following the procedure for (*R,R*)-*N,N'*-bis(3,5-di-*tert*-butylsalicylidene)-1,2-cyclohexanediaminochromium(III) chloride (**4a**). A dry round-bottomed flask was charged with (*R,R*)-*N,N'*-bis(3-*tert*-butyl-5-bromo-salicylidene)-1,2-cyclohexanediamine (0.15 g, 0.25 mmol) and chromium(II) chloride (34 mg, 0.28 mmol). Dry, degassed THF (10 mL) was syringed in to form a brown solution. The solution was stirred under N_2 for 4 h, and under air for 18 h. The solution was washed with saturated NH_4Cl (aq) (10 mL), dried (Na_2SO_4) and solvent removed *in vacuo* to yield a brown solid. The solid was used without further purification. Yield: 0.17 g, 99 %. M.P: > 290 °C. FT-IR (ATR): ʋ [cm^{-1}] 2943 (m), 2864 (w), 1620 (s), 1428 (m), 1316 (s), 1165 (s), 734 (s). LRMS (LIFDI): Calculated for [$C_{28}H_{34}{}^{79}Br^{81}Br^{35}ClCrN_2O_2$] ([M]$^+$): 677.01; Found: 677.02. [α]$_D$ -429 (c = 0.047, EtOH)

(*R,R*)-*N,N′*-Bis(3-*tert*-butyl-salicylidene-1,2-diphenyl-1,2-ethanediaminochromium(III) chloride (**4k**):
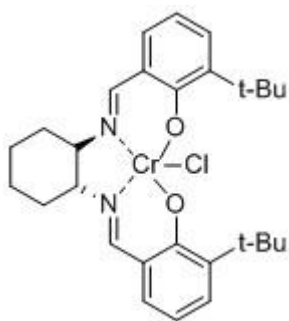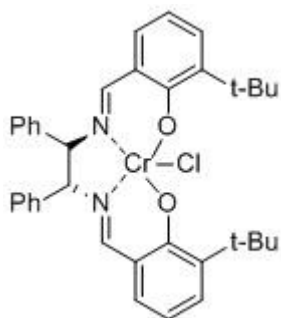

Synthesis was carried out following the procedure for (*R,R*)-*N,N′*-bis(3,5-di-*tert*-butylsalicylidene)-1,2-cyclohexanediaminochromium(III) chloride (**4a**). A dry round-bottomed flask was charged with (*R,R*)-*N,N′*-bis(3-*tert*-butyl-salicylidene-1,2-diphenyl-1,2-ethanediamine (0.23 g, 0.47 mmol) and chromium(II) chloride (63 mg, 0.51 mmol). Dry, degassed THF (15 mL) was syringed in to form a brown solution. The solution was stirred under N_2 for 3 h, and under air for 18 h. The solution was washed with saturated NH_4Cl (aq) (10 mL), dried (Na_2SO_4) and solvent removed *in vacuo* to yield a brown solid. The solid was used without further purification. Yield: 0.28 g, 97 %. M.P: > 290 °C. FT-IR (ATR): υ [cm^{-1}] 2955 (m), 1655 (s), 1595 (s), 1544(s), 1421 (s), 1322 (s), 815 (s), 717 (s). HRMS (ESI): Calculated for [$C_{36}H_{38}CrN_2O_2$] ([M-Cl]$^+$): 582.2333; Found: 582.2324. LRMS (LIFDI): Calculated for [$C_{36}H_{38}{}^{35}ClCrN_2O_2$] ([M]$^+$): 617.20; Found: 617.22. [α]$_D$ -360 (c = 0.041, EtOH)

5.6.   Preparation of *N*-(2,3-Epoxypropyl)diphenylamine
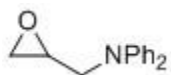
Synthesis was carried out according to a modified literature procedure.[94] A suspension of K_2CO_3 (5.18 g, 37.5 mmol) and diphenylamine (4.23 g, 25.0 mmol) in epichlorohydrin (20.2 mL, 250 mmol) was stirred for 20 minutes at r.t. Powdered KOH (35.05 g, 625 mmol) was added slowly. The suspension was stirred at r.t. for 3 days. Reaction progress was monitored by TLC using petroleum ether/chloroform (1:1). The mixture was quenched with water (250 mL), and extracted with Et_2O (250 mL). The solvent was removed *in vacuo*. The crude product was purified by distillation under vacuum (160 °C) to yield a pale yellow oil, R_f (petroleum ether/chloroform 1:1) 0.20. Yield: 4.96 g, 78 %. ^{1}H NMR (400 MHz, $CDCl_3$) δ: 7.33 – 7.20 (m, 5H), 7.08 – 6.91 (m, 5H), 3.91 (dq, J = 15.5, 3.8 Hz, 2H), 3.26 – 3.19 (m, 1H), 2.78 (t, J = 4.3 Hz, 1H), 2.56 (dd, J = 5.2 Hz, 5.1 Hz, 1H). ^{13}C NMR (101 MHz, $CDCl_3$) δ: 148.0, 129.5, 121.8, 121.1, 53.9,m 50.5, 46.1. FT-IR (ATR): υ [cm^{-1}] = 1591 (s), 1494 (s), 1364 (m), 1254 (m), 1230 (m), 749 (s), 695 (m). HRMS (ESI): Calculated for [$C_{15}H_{16}NO$] ([M+H]$^+$): 226.1226; Found: 226.1223.

5.7. General procedure for the conversion of epoxides to cyclic carbonates

Setup. Kinetic experiments were performed anhydrously in oven-dried 25 mL Schlenk vessels. The Schlenk vessels were charged with 12 mm stirrer bars, then evacuated and refilled with CO_2 before charging with catalyst and co-catalyst. 99.9 % purity liquid CO_2 was obtained from BOC Industrial Gases UK and used without purification. The vessels were evacuated and refilled thrice. Solvent was added and the setup was allowed to equilibrate thermally in a water bath for at least 15 minutes, after which epoxide was added *via* syringe. Stirring was carried out at 500 rpm. Samples were removed at regular intervals and passed through a silica plug using ispropanol as the eluent prior to chiral HPLC analysis to determine the enantiomeric excess of the cyclic carbonate.

If anhydrous conditions were not necessary the kinetic experiments were carried out in glass mixing vessels charged with 12 mm stirrer bars. These vessels were 28 mL, O.D. 28 mm borosilicate vials. The reagents were added in the following order: catalyst, co-catalyst, then solvent. The resultant mixture was allowed to equilibrate thermally in a water bath for at least 15 minutes, after which epoxide (1.66 mmol) was added. The glass vessel was sealed with a rubber septum. Carbon dioxide was obtained by evaporation of Cardice pellets without drying of the resulting gas. The rubber septum was pierced with a balloon containing the carbon dioxide, and with a separate vent needle to facilitate flushing. The vent needle was removed after 15 seconds. Stirring was carried out at 500 rpm. Samples were removed at regular intervals and passed through a silica plug using ispropanol as the eluent prior to chiral HPLC analysis to determine the enantiomeric excess of the cyclic carbonate.

Materials. Commercially available substrates and co-catalysts were purchased from *Aldrich*, *Fluka*, *Acros*, and *Alfa Aesar*. They were used as received with the following exceptions: Tetrabutylammonium chloride, which was dried *in vacuo* prior to use to remove water.

Instrumentation. The conversion of epoxides to carbonates was obtained by ^{1}H NMR (400 MHz, $CDCl_3$), with the exception of (phenoxymethyl)ethylene

carbonate and 4-*(N,N*-diphenylaminomethyl)-1,3-dioxolan-2-one which were determined by HPLC on an Agilent 1220.

5.7.1. Preparation of propylene carbonate
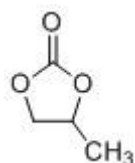
Propylene oxide was removed *in vacuo*. Propylene carbonate was isolated as a colourless oil by flash chromatography using hexane/ EtOAc (4:1) as eluent. R_f (hexane/EtOAc 4:1) 0.15. ^{1}H NMR (400 MHz, CDCl$_3$) δ: 4.82 (m, 1H), 4.52 (t, J = 8.4 Hz, 1H), 3.99 (dd, J = 8.4, 7.3, 1H), 1.45 (d, J = 6.1 Hz, 3H). ^{13}C NMR (101 MHz, CDCl$_3$) δ: 155.11, 73.65, 70.66, 19.24.

(R)-propylene carbonate: [α]$_D$ +2.435 ° (neat) (lit. +2 °)[95]

5.7.2. Preparation of butylene carbonate
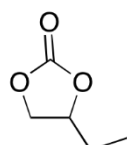
Butylene carbonate was isolated as a colourless oil by flash chromatography using hexane/EtOAc (3:1) as eluent. R_f (hexane/EtOAc 3:1) 0.24. ^{1}H NMR (400 MHz, CDCl$_3$) δ: 4.69 (m, 1H), 4.55 (t, J = 8.8 Hz, 1H), 4.11 (dd, J = 8.4, 7.4 Hz, 1H), 1.91 - 1.67 (m, 2H), 1.10 - 0.90 (m, 3H). ^{13}C NMR (101 MHz, CDCl$_3$) δ: 155.2, 69.1, 63.9, 27.0, 14.4, 8.6.

5.7.3. Preparation of hexylene carbonate
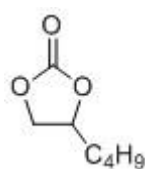
Hexylene carbonate was isolated as a colourless oil by flash chromatography using hexane/EtOAc (3:1) as eluent. R_f (hexane/EtOAc 3:1) 0.24. ^{1}H NMR (400 MHz, CDCl$_3$) δ: 4.69 (m, 1H), 4.51 (t, J = 7.9 Hz, 1H), 4.04 (dd, J = 8.4, 7.2 Hz, 1H), 2.0 - 1.6 (m, 2H), 1.6 - 1.2 (m, 4H), 1.00 (t, J = 7.1 Hz, 3H). ^{13}C NMR (101 MHz, CDCl$_3$) δ: 155.2, 69.4, 33.5, 26.4, 22.2, 13.8.

5.7.4. Preparation of styrene carbonate
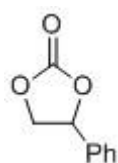
Styrene carbonate was isolated as a colourless solid by flash chromatography using hexane/EtOAc (4:1) as eluent. R_f (hexane/EtOAc 4:1) 0.21. ^{1}H NMR (400 MHz, CDCl$_3$) δ: 7.48 - 7.20 (m, 5H), 5.66 (t, J = 7.8 Hz, 1H), 4.78 (t, J = 8.6 Hz, 1H), 4.33 (dd, J = 9.0, 8.0

Hz, 1H). ^{13}C NMR (101 MHz, CDCl$_3$) δ: 154.9, 135.8, 129.8, 129.3, 125.9, 78.1, 71.2, 31.0.

The % ee of styrene carbonate was obtained by chiral HPLC on an Agilent 1220. The following HPLC column was used: Chiralcel OD (25 cm by 4.6 mm), using hexane/isopropanol (80:20 %v/v) as eluent and a flow rate of 1.00 mL/min. $t_{R[SC]}$ = 16.1 min, 18.2 min. Detection wavelength: 216 nm. % ee values were accurate for a racemic sample with concentration greater than 300 ppm.
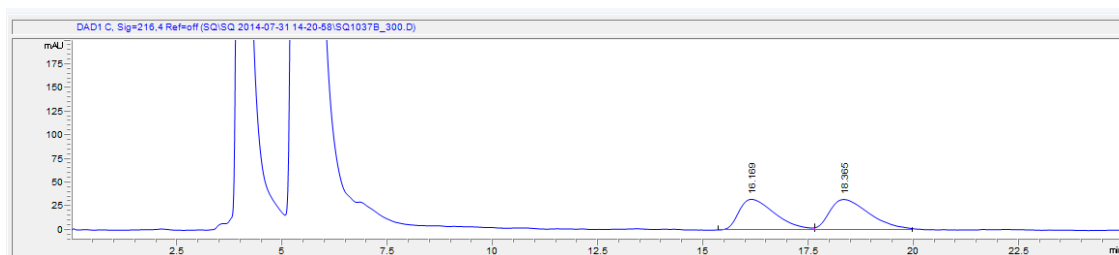
Figure 28: HPLC trace of a racemic sample of styrene carbonate.
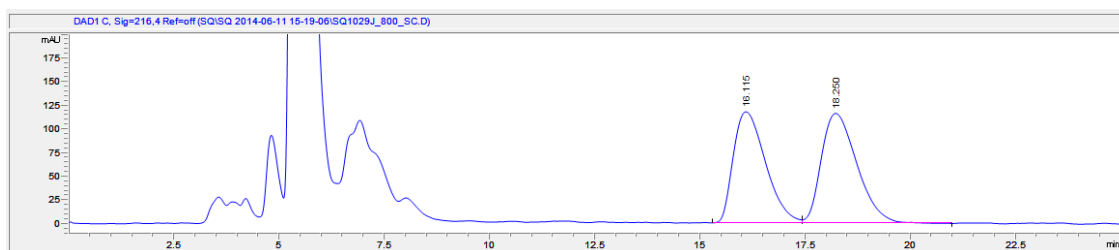
Figure 29: HPLC trace of a sample of styrene carbonate with 5 % ee in favour of the second peak.

5.7.5. Preparation of (phenoxymethyl)ethylene carbonate
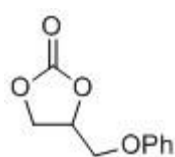
(Phenoxymethyl)ethylene carbonate was isolated as a colourless solid by flash chromatography using petroleum ether/EtOAc (3:2) as eluent. R_f (petroleum ether/EtOAc 3:2) 0.38. ^1H NMR (400 MHz, CDCl$_3$) δ: 7.35 - 7.25 (m, 2H), 6.89 (d, J = 7.6 Hz, 2H), 6.70 (t, J = 7.6 Hz, 1H), 5.00 – 5.05 (m, 1H), 4.65 - 4.50 (m, 2H), 4.25 – 4.20 (dd, J = 10.4, 4.5 Hz, 1H), 4.20 - 4.10 (dd, J = 10.4, 3.5 Hz, 1H) ^{13}C NMR (101 MHz, CDCl$_3$) δ: 157.8, 154.7, 129.8, 122.1, 114.7, 74.2, 66.9, 66.3.

The conversion of phenyl glycidyl ether to (phenoxymethyl)ethylene carbonate was monitored by HPLC on an Agilent 1220. The following HPLC column was used: Chiralcel IA (25 cm by 4.6 mm), using hexane/isopropanol (85:15 %v/v) as eluent and a flow rate of 1.000 mL/min. $t_{R[substrate]}$ = 4.87 min, Rf = 923109, $t_{R[carbonate]}$ = 11.90 min, Rf = 901514. Detection wavelength: 216 nm.
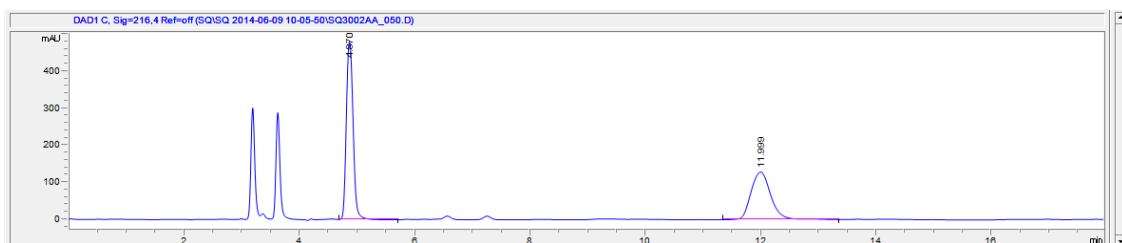
Figure 30: HPLC trace of a sample containing phenyl glycidyl ether and (phenoxymethyl)ethylene carbonate.

The % ee of phenyl glycidyl ether was obtained by chiral HPLC on an Agilent 1220. The following HPLC column was used: Chiralcel IA (25 cm by 4.6 mm), using hexane/isopropanol (99.5:0.5 %v/v) as eluent and a flow rate of 0.60 mL/min. $t_{R[PGE]}$ = 50.5 min, 56.3 min. Detection wavelength: 216 nm.
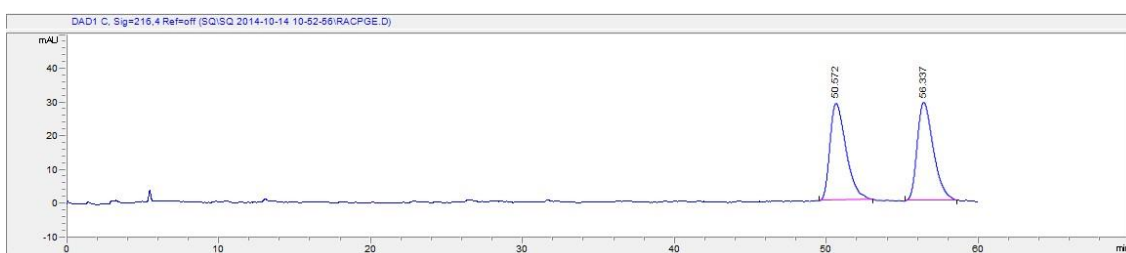
Figure 31: HPLC trace of a sample of racemic phenyl glycidyl ether.
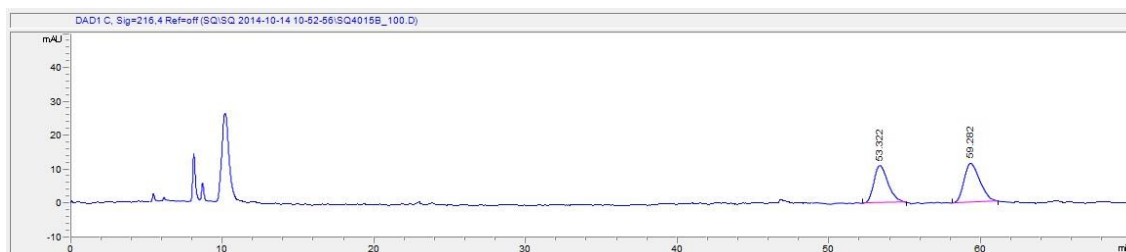
Figure 32: HPLC trace of a sample of phenyl glycidyl ether with 7 % ee in favour of the second peak.

The % ee of (phenoxymethyl)ethylene carbonate was obtained by chiral HPLC on an Agilent 1220. The following HPLC column was used: Chiralcel OD (25 cm by 4.6 mm), using hexane/isopropanol (80:20 %v/v) as eluent and a flow rate of 1.00 mL/min. $t_{R[PMEC]}$ = 30.0 min, 41.0 min. Detection wavelength: 216 nm. % ee values were accurate for a racemic sample with concentration greater than 600 ppm.
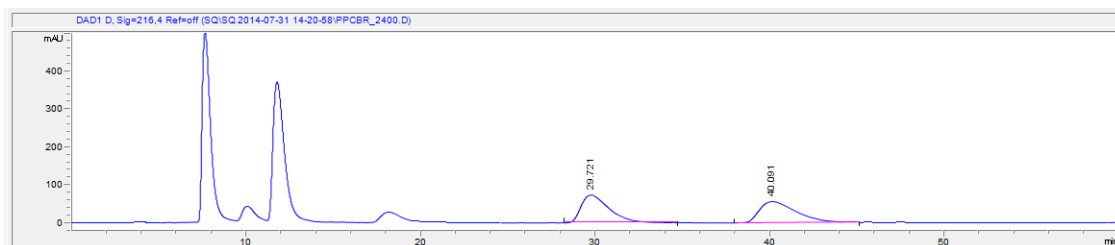
Figure 33: HPLC trace of a sample of racemic (phenoxymethyl)ethylene carbonate.
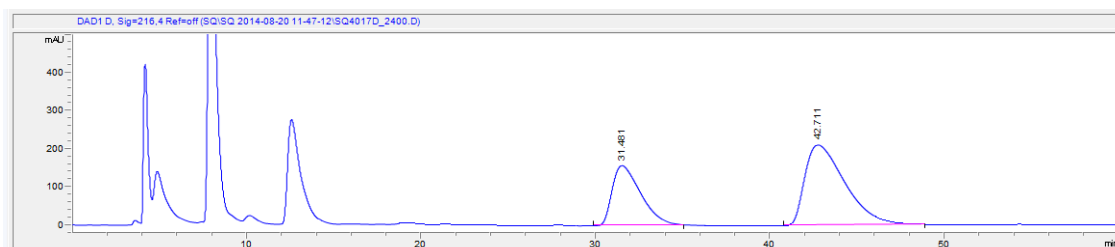
Figure 34: HPLC trace of a sample of (phenoxymethyl)ethylene carbonate with 31 % ee in favour of the second peak.

5.7.6. Preparation of 4-*(N,N*-diphenylaminomethyl)-1,3-dioxolan-2-one
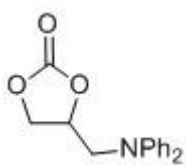
4-*(N,N*-Diphenylaminomethyl)-1,3-dioxolan-2-one was isolated as a colourless solid by flash chromatography using petroleum ether/EtOAc (2:1) as eluent. R_f (petroleum ether/EtOAc 2:1) 0.21. ^{1}H NMR (400 MHz, CDCl$_3$) δ: 7.34 - 7.25 (m, 5H), 7.00 – 6.93 (m, 5H), 5.00 – 4.90 (m, 1H), 4.45 (t, J = 8.1 Hz, 1H), 4.22 – 4.00 (m, 2H), 4.00 – 3.95 (m, 1H). ^{13}C NMR (101 MHz, CDCl$_3$) δ: 154.3, 147.4, 129.8, 122.8, 121.3, 74.5, 67.7, 54.5.

The conversion of *N*-(2,3-epoxypropyl)diphenylamine to 4-*(N,N*-diphenylaminomethyl)-1,3-dioxolan-2-one was monitored by HPLC on an Agilent 1220. The following HPLC column was used: Chiralcel IA (25 cm by 4.6 mm), using hexane/isopropanol (88:12%v/v) as eluent and a flow rate of 1.000 mL/min. $t_{R[substrate]}$ = 5.7 min, 6.9 min, Rf = 1325462, $t_{R[carbonate]}$ = 18.5 min, 21.3 min, Rf = 1086901. Detection wavelength: 286 nm.
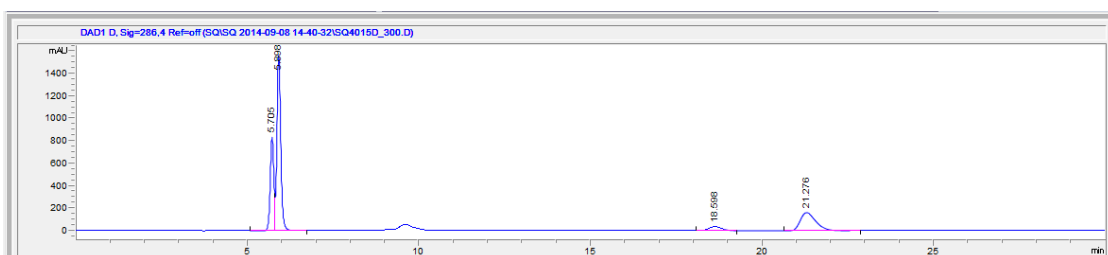
Figure 35: HPLC trace of a sample containing *N*-(2,3-epoxypropyl)diphenylamine and 4-(N,N-diphenylaminomethyl)-1,3-dioxolan-2-one.

The % ee of 4-*(N,N*-diphenylaminomethyl)-1,3-dioxolan-2-one was obtained by chiral HPLC on an Agilent 1220. The following HPLC column was used: Chiralcel IA (25 cm by 4.6 mm), using hexane/EtOAc (88:12 %v/v) as eluent and a flow rate of 1.00 mL/min. $t_{R[DPAC]}$ = 18.5 min, 21.3 min. Detection wavelength: 286 nm.
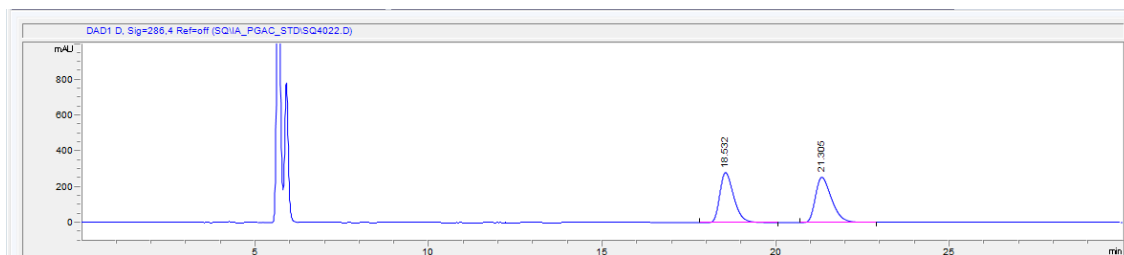
Figure 36: HPLC trace of a sample of racemic 4-*(N,N*-diphenylaminomethyl)-1,3-dioxolan-2-one.
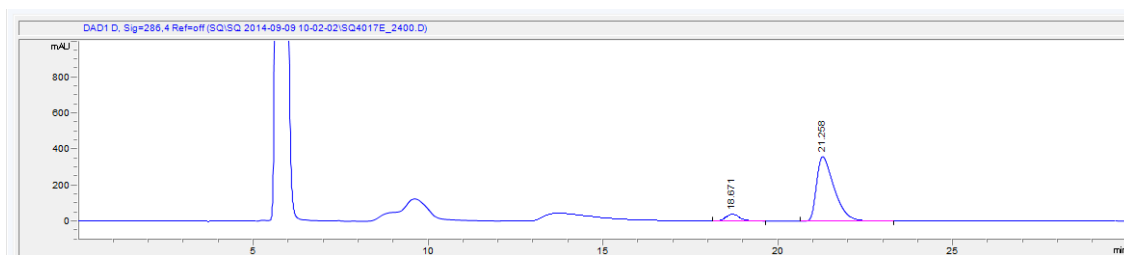
Figure 37: HPLC trace of a sample of 4-*(N,N*-diphenylaminomethyl)-1,3-dioxolan-2-one with 85 % ee in favour of the second peak.

6. Appendix A

The following pages show the parameters for each experiment, as well as the corresponding graph for determining the order of reaction w.r.t. catalyst. Each kinetic run is done in duplicate. First-order rate dependence on catalyst is demonstrated by plotting the natural logarithm of epoxide concentration against time. The small but observable changes in gradient over the duration of the experiment may be explained by gradual solvent loss.

6.1. Order with respect to aluminium(salen) complex 5b

Temperature:	75	°C
Solvent:	p-cymene	
Solvent/substrate:	20	v/v
5b:	2.5	mol %
TBAB:	2.5	mol %

Order	R^2
0	0.8972
1	0.9901
2	0.9640

k_{obs}: 0.0951 h^{-1}

y = -0.0951x - 1.0148
R² = 0.9901
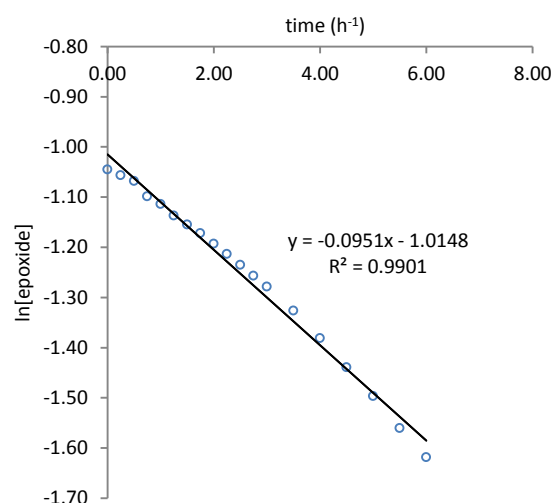
Temperature:	75	°C
Solvent:	p-cymene	
Solvent/substrate:	20	v/v
5b:	2.5	mol %
TBAB:	2.5	mol %

Order	R^2
0	0.9747
1	0.9458
2	0.8682

k_{obs}: 0.0912 h^{-1}

y = -0.0912x - 1.0182
R² = 0.9458
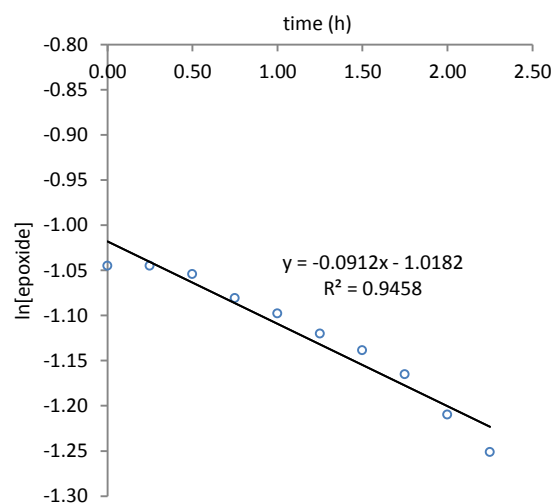
Temperature:	75	°C
Solvent:	p-cymene	
Solvent/substrate:	20	v/v
5b:	3.0	mol %
TBAB:	2.5	mol %

Order	R^2
0	0.9931
1	0.9902
2	0.8769

k_{obs}: 0.1134 h^{-1}

y = -0.1134x - 1.0345
R² = 0.9902
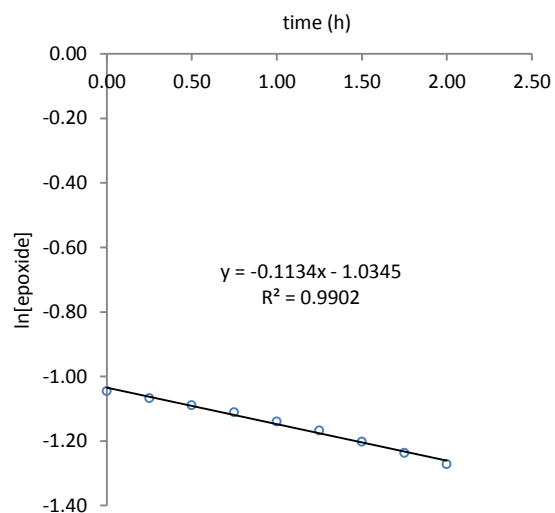
Temperature:	75	°C
Solvent:	p-cymene	
Solvent/substrate:	20	v/v
5b:	3.0	mol %
TBAB:	2.5	mol %

Order	R^2
0	0.9809
1	0.9991
2	0.9888

k_{obs}: 0.1312 h^{-1}

y = -0.1312x - 1.0451
R² = 0.9991
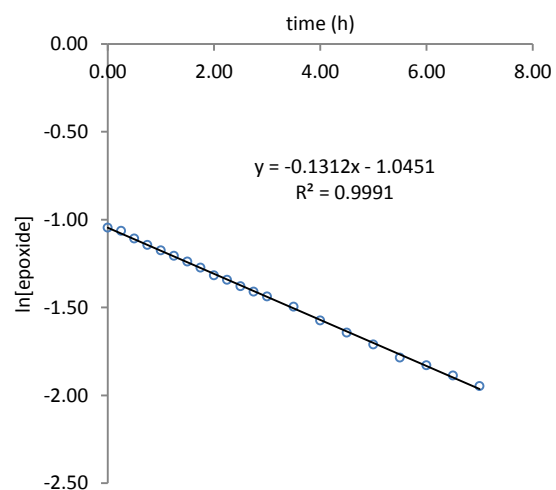
Temperature:	75	°C
Solvent:	p-cymene	
Solvent/substrate:	20	v/v
5b:	4.0	mol %
TBAB:	2.5	mol %

Order	R^2
0	0.9946
1	0.9700
2	0.9108

k_{obs}: 0.1565 h^{-1}
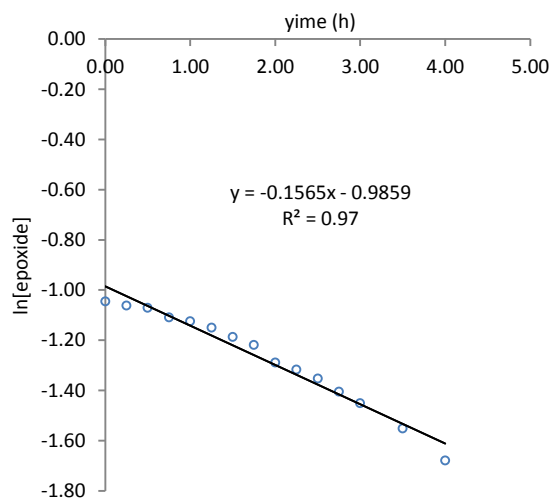
y = -0.1565x - 0.9859
R² = 0.97

Temperature: 75 °C
Solvent: p-cymene
Solvent/substrate: 20 v/v
5b: 4.0 mol %
TBAB: 2.5 mol %

Order	R^2
0	0.9986
1	0.9889
2	0.8576

k_{obs}: 0.1672 h^{-1}

y = -0.1672x - 1.0162
R² = 0.9889
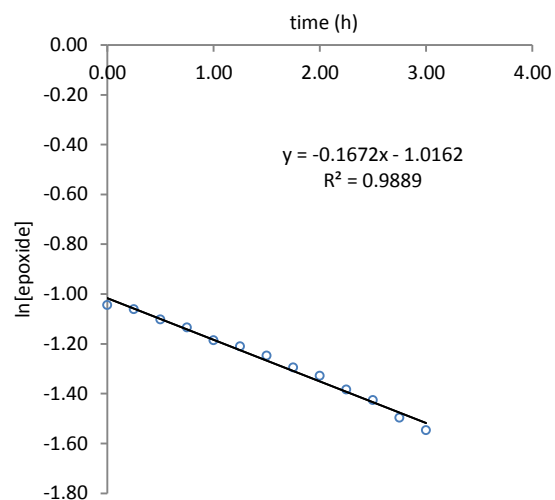
Temperature: 75 °C
Solvent: p-cymene
Solvent/substrate: 20 v/v
5b: 5.0 mol %
TBAB: 2.5 mol %

Order	R^2
0	0.9960
1	0.9815
2	0.9522

k_{obs}: 0.2184 h^{-1}
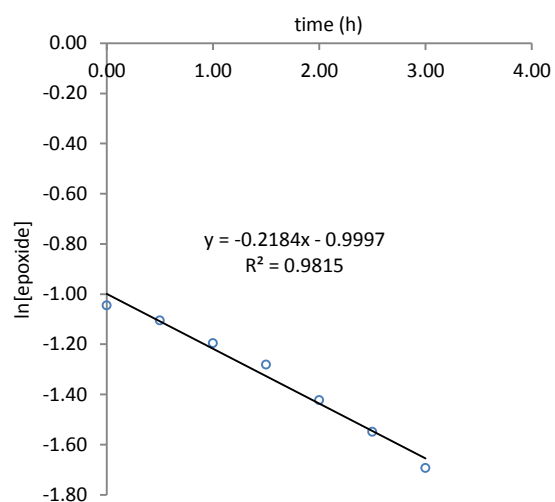
y = -0.2184x - 0.9997
R² = 0.9815

Temperature: 75 °C
Solvent: p-cymene
Solvent/substrate: 20 v/v
5b: 5.0 mol %
TBAB: 2.5 mol %

Order	R^2
0	0.9981
1	0.9710
2	0.8034

k_{obs}: 0.1779 h^{-1}

y = -0.1779x - 0.9753
R² = 0.971
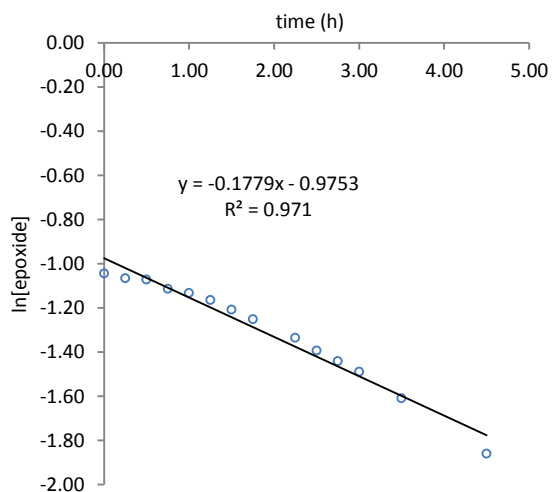
6.2.   Order with respect to cobalt(salen) complex 3c

Temperature:	25	°C
Solvent:	EtOAc	
Solvent/substrate:	20	v/v
3c:	1.0	mol %
TBAB:	10.0	mol %

Order	R^2
0	0.8808
1	0.9836
2	0.6841

k_{obs}:   0.7487 h^{-1}

Chart: time(h) vs ln[epoxide]; $y = -0.7487x - 0.8726$, $R^2 = 0.9836$
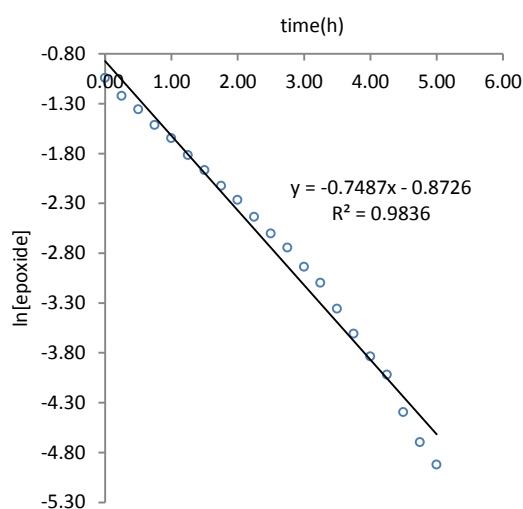
Temperature:	25	°C
Solvent:	EtOAc	
Solvent/substrate:	20	v/v
3c:	1.0	mol %
TBAB:	10.0	mol %

Order	R^2
0	0.8494
1	0.9907
2	0.7181

k_{obs}:   0.8018 h^{-1}

Chart: time(h) vs ln[epoxide]; $y = -0.8018x - 0.9384$, $R^2 = 0.9907$
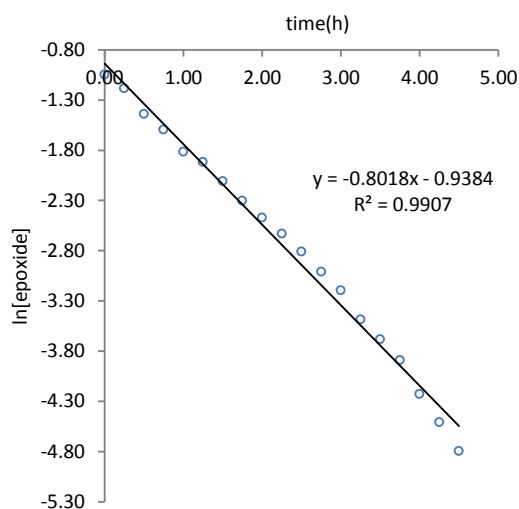
Temperature:	25	°C
Solvent:	EtOAc	
Solvent/substrate:	20	v/v
3c:	2.5	mol %
TBAB:	10.0	mol %

Order	R^2
0	0.7899
1	0.9978
2	0.7104

k_{obs}:   1.3854 h^{-1}

Chart: time(h) vs ln[epoxide]; $y = -1.3854x - 1.0223$, $R^2 = 0.9978$

83
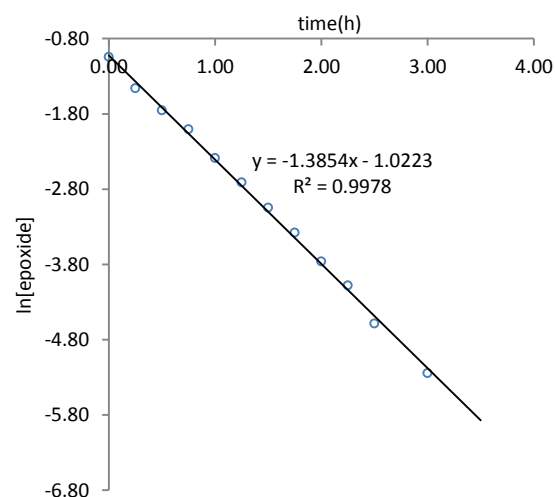
Temperature: 25 °C
Solvent: EtOAc
Solvent/substrate: 20 v/v
3c: 2.5 mol %
TBAB: 10.0 mol %

Order	R^2
0	0.7363
1	0.9978
2	0.6810

k_{obs}: 1.4216 h^{-1}

y = -1.4216x - 0.9166
R² = 0.9978
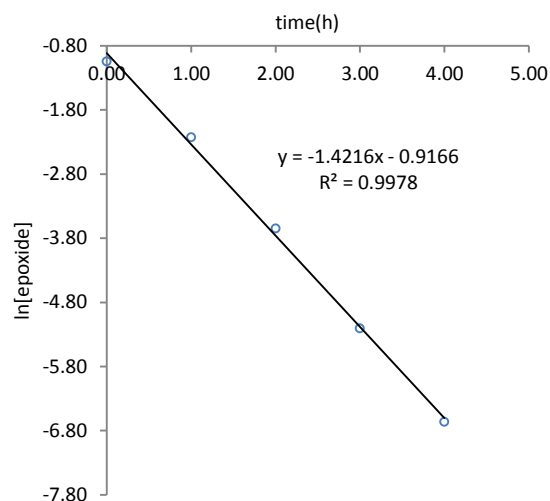
Temperature: 25 °C
Solvent: EtOAc
Solvent/substrate: 20 v/v
3c: 5.0 mol %
TBAB: 10.0 mol %

Order	R^2
0	0.7961
1	0.9981
2	0.8423

k_{obs}: 0.7564 h^{-1}

y = -0.7564x - 1.1579
R² = 0.9981
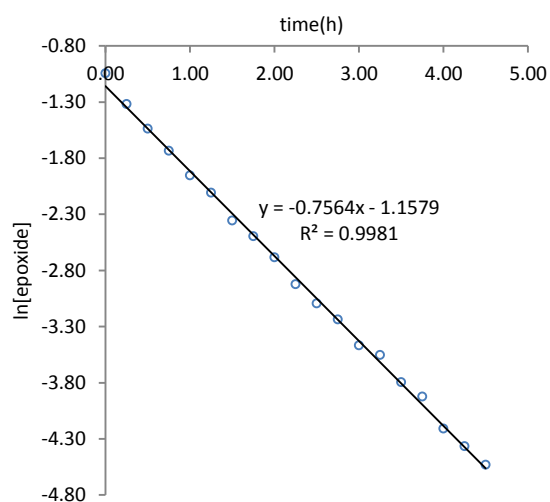
Temperature: 25 °C
Solvent: EtOAc
Solvent/substrate: 20 v/v
3c: 5.0 mol %
TBAB: 10.0 mol %

Order	R^2
0	0.7710
1	0.9966
2	0.8126

k_{obs}: 0.7824 h^{-1}

y = -0.7824x - 1.1731
R² = 0.9966
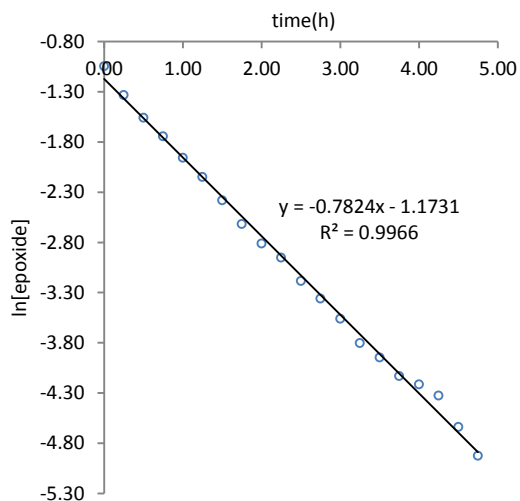
6.3. Order with respect to cobalt(salen) complex 3d in slight excess of TBAB

Temperature:	25	°C
Solvent:	EtOAc	
Solvent/substrate:	20	v/v
3d:	1.0	mol %
TBAB:	10.0	mol %

Order	R^2
0	0.9285
1	0.9987
2	0.9309

k_{obs}:	0.2784	h^{-1}

$y = -0.2784x - 1.0767$
$R^2 = 0.9987$
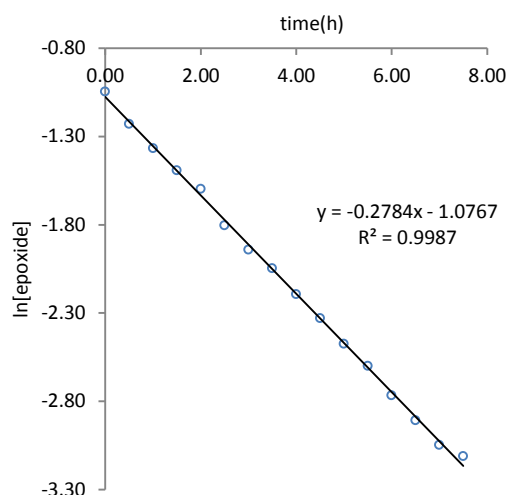
Temperature:	25	°C
Solvent:	EtOAc	
Solvent/substrate:	20	v/v
3d:	1.0	mol %
TBAB:	10.0	mol %

Order	R^2
0	0.9263
1	0.9982
2	0.9541

k_{obs}:	0.2461	h^{-1}

$y = -0.2461x - 1.1036$
$R^2 = 0.9982$

Temperature:	25	°C
Solvent:	EtOAc	
Solvent/substrate:	20	v/v
3d:	2.5	mol %
TBAB:	10.0	mol %

Order	R^2
0	0.8004
1	0.9924
2	0.3694

k_{obs}:	0.8160	h^{-1}

$y = -0.816x - 1.0869$
$R^2 = 0.9924$

Temperature:	25	°C
Solvent:	EtOAc	
Solvent/substrate:	20	v/v
3d:	2.5	mol %
TBAB:	10.0	mol %

Order	R^2
0	0.8624
1	0.9836
2	0.6730

k_{obs}: 0.8909 h^{-1}

$y = -0.8909x - 0.954$
$R^2 = 0.9836$
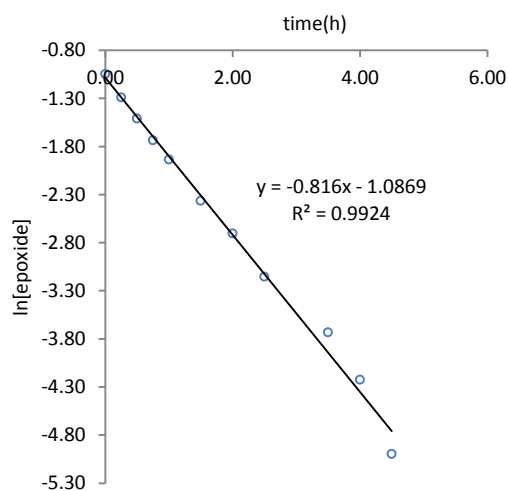
Temperature:	25	°C
Solvent:	EtOAc	
Solvent/substrate:	20	v/v
3d:	5.0	mol %
TBAB:	10.0	mol %

Order	R^2
0	0.8337
1	0.9905
2	0.7412

k_{obs}: 0.7992 h^{-1}

$y = -0.7992x - 0.8456$
$R^2 = 0.9905$
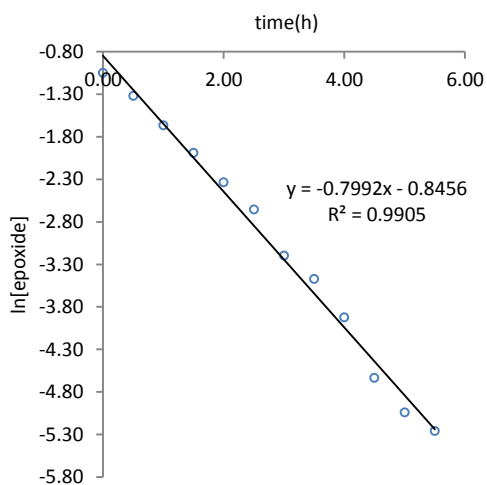
Temperature:	25	°C
Solvent:	EtOAc	
Solvent/substrate:	20	v/v
3d:	5.0	mol %
TBAB:	10.0	mol %

Order	R^2
0	0.8069
1	0.9848
2	0.6248

k_{obs}: 0.9150 h^{-1}

$y = -0.915x - 0.8581$
$R^2 = 0.9848$
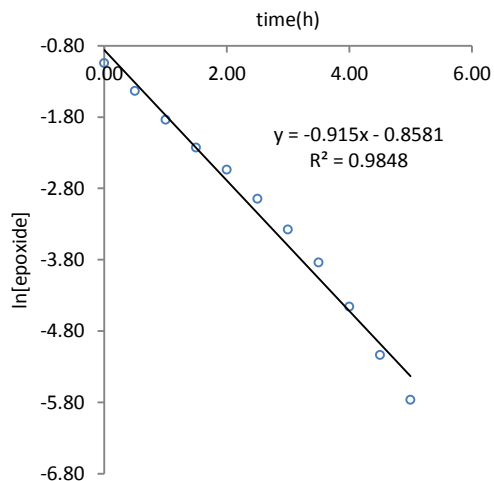
6.4.   Order with respect to TBAB

Temperature:	25 °C
Solvent:	EtOAc
Solvent/substrate:	20 v/v
3d:	2.5 mol %
TBAB:	2.5 mol %

Order	R^2
0	0.8928
1	0.9801
2	0.9923

k_{obs}:   0.2226 h^{-1}

Chart: time(h) vs ln[epoxide]; $y = -0.2226x - 1.1507$, $R^2 = 0.9801$
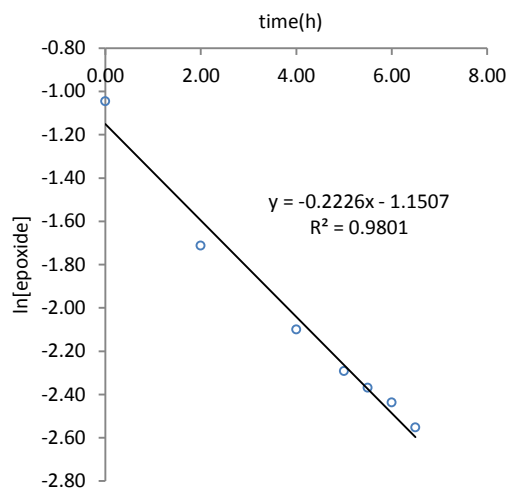
Temperature:	25 °C
Solvent:	EtOAc
Solvent/substrate:	20 v/v
3d:	2.5 mol %
TBAB:	2.5 mol %

Order	R^2
0	0.8560
1	0.9971
2	0.9658

k_{obs}:   0.2272 h^{-1}

Chart: time(h) vs ln[epoxide]; $y = -0.2272x - 1.3091$, $R^2 = 0.9971$
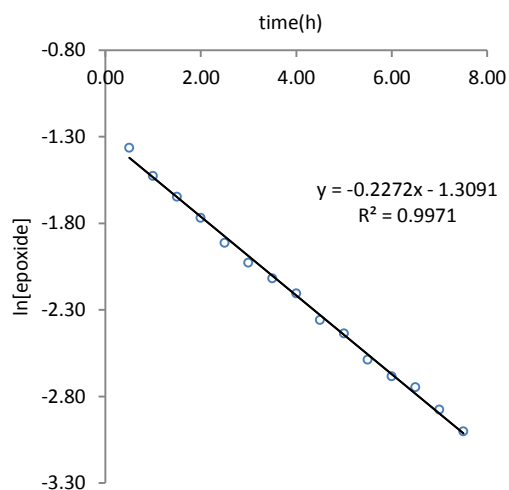
Temperature:	25 °C
Solvent:	EtOAc
Solvent/substrate:	20 v/v
3d:	2.5 mol %
TBAB:	5.0 mol %

Order	R^2
0	0.8642
1	0.9959
2	0.8491

k_{obs}:   0.4042 h^{-1}

Chart: time(h) vs ln[epoxide]; $y = -0.4042x - 1.0924$, $R^2 = 0.9959$
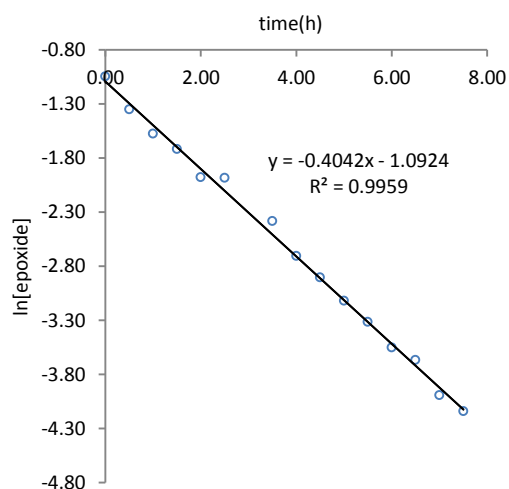
Temperature:	25	°C
Solvent:	EtOAc	
Solvent/substrate:	20	v/v
3d:	2.5	mol %
TBAB:	5.0	mol %

Order	R^2
0	0.8607
1	0.9967
2	0.8537

k_{obs}: 0.4299 h⁻¹

time(h)

y = -0.4299x - 1.103
R^2 = 0.9967

ln[epoxide]

Temperature:	25	°C
Solvent:	EtOAc	
Solvent/substrate:	20	v/v
3d:	2.5	mol %
TBAB:	10.0	mol %

Order	R^2
0	0.8624
1	0.9836
2	0.6730

k_{obs}: 0.8909 h⁻¹

time(h)

y = -0.8909x - 0.954
R^2 = 0.9836

ln[epoxide]

Temperature:	25	°C
Solvent:	EtOAc	
Solvent/substrate:	20	v/v
3d:	2.5	mol %
TBAB:	10.0	mol %

Order	R^2
0	0.8004
1	0.9924
2	0.3694

k_{obs}: 0.8160 h⁻¹

time(h)

y = -0.816x - 1.0869
R^2 = 0.9924

ln[epoxide]

88

Temperature:	25	°C
Solvent:	EtOAc	
Solvent/substrate:	20	v/v
3d:	2.5	mol %
TBAB:	15.0	mol %

Order	R^2
0	0.8604
1	0.9667
2	0.5713

k_{obs}: 1.1096 h^{-1}

$y = -1.1096x - 0.7516$
$R^2 = 0.9667$

Temperature:	25	°C
Solvent:	EtOAc	
Solvent/substrate:	20	v/v
3d:	2.5	mol %
TBAB:	15.0	mol %

Order	R^2
0	0.8350
1	0.9830
2	0.5434

k_{obs}: 1.1970 h^{-1}

$y = -1.197x - 0.7324$
$R^2 = 0.983$

6.5. Combined order with respect to cobalt(salen) complex 3d and TBAB

Temperature:	25 °C
Solvent:	EtOAc
Solvent/substrate:	20 v/v
3d:	2.5 mol %
TBAB:	15.0 mol %

Order	R^2
0	0.8604
1	0.9667
2	0.5713

k_{obs}: 1.1096 h^{-1}

$y = -1.1096x - 0.7516$
$R^2 = 0.9667$

Temperature:	25 °C
Solvent:	EtOAc
Solvent/substrate:	20 v/v
3d:	2.5 mol %
TBAB:	15.0 mol %

Order	R^2
0	0.8350
1	0.9830
2	0.5434

k_{obs}: 1.1970 h^{-1}

$y = -1.197x - 0.7324$
$R^2 = 0.983$
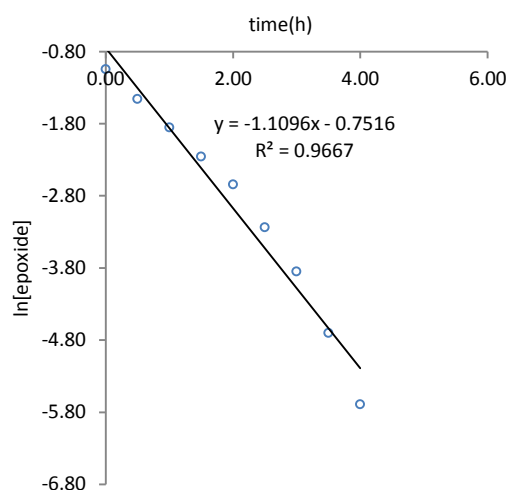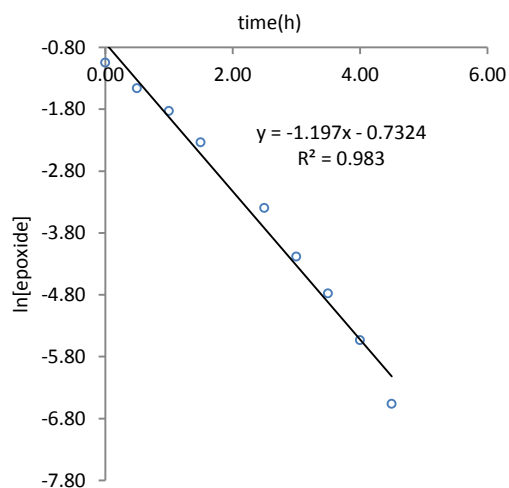
Temperature:	25 °C
Solvent:	EtOAc
Solvent/substrate:	20 v/v
3d:	3.3 mol %
TBAB:	20.0 mol %

Order	R^2
0	0.1223
1	0.9743
2	0.6449

k_{obs}: 1.7002 h^{-1}

$y = -1.7002x - 0.6565$
$R^2 = 0.9743$
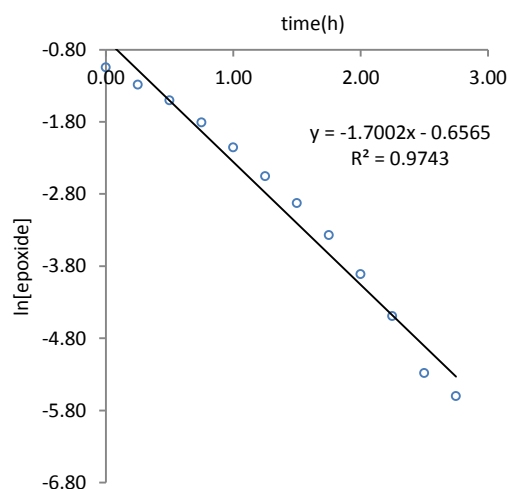
Temperature: 25   °C
Solvent: EtOAc
Solvent/substrate: 20   v/v
3d: 3.3   mol %
TBAB: 20.0   mol %

Order	R^2
0	0.8841
1	0.9550
2	0.5176

k_{obs}:   1.6863 h^{-1}
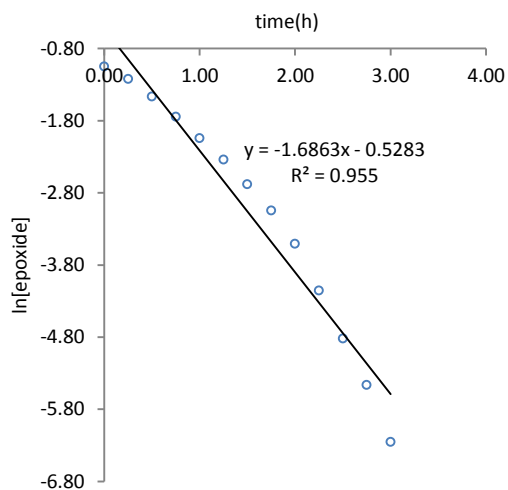
$y = -1.6863x - 0.5283$
$R^2 = 0.955$

Temperature: 25   °C
Solvent: EtOAc
Solvent/substrate: 20   v/v
3d: 5.0   mol %
TBAB: 30.0   mol %

Order	R^2
0	0.9161
1	0.9573
2	0.5801

k_{obs}:   2.7252 h^{-1}

$y = -2.7252x - 0.6834$
$R^2 = 0.9573$

Temperature: 25   °C
Solvent: EtOAc
Solvent/substrate: 20   v/v
3d: 5.0   mol %
TBAB: 30.0   mol %

Order	R^2
0	0.9215
1	0.9549
2	0.5727

k_{obs}:   2.4493 h^{-1}

$y = -2.4493x - 0.6338$
$R^2 = 0.9549$
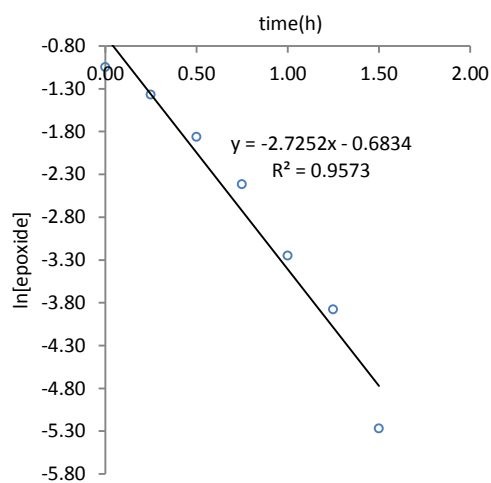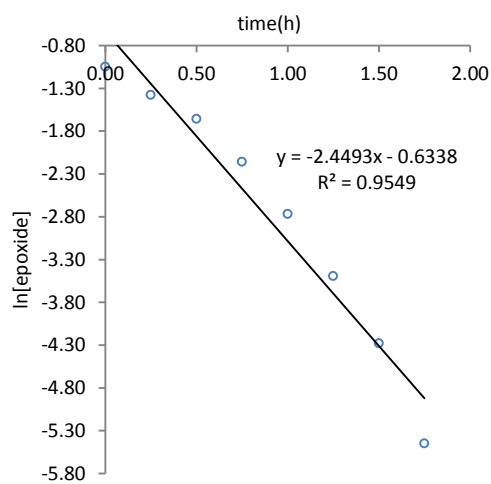
6.6. Order with respect to cobalt(salen) complex 3d in large excess of TBAB

Temperature:	25	°C
Solvent:	EtOAc	
Solvent/substrate:	20	v/v
5b:	2.0	mol %
TBAB:	30.0	mol %

Order	R^2
0	0.9337
1	0.9647
2	0.6314

k_{obs}: 1.1542 h^{-1}

y = -1.1542x - 0.7016
R^2 = 0.9647
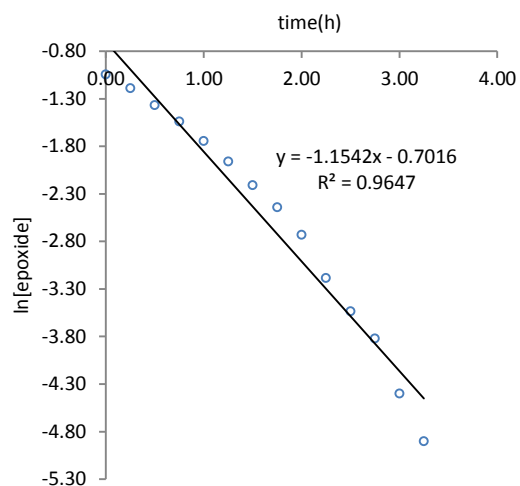
Temperature:	25	°C
Solvent:	EtOAc	
Solvent/substrate:	20	v/v
5b:	2.0	mol %
TBAB:	30.0	mol %

Order	R^2
0	0.9342
1	0.9647
2	0.6191

k_{obs}: 1.1459 h^{-1}

y = -1.1459x - 0.7067
R^2 = 0.9647
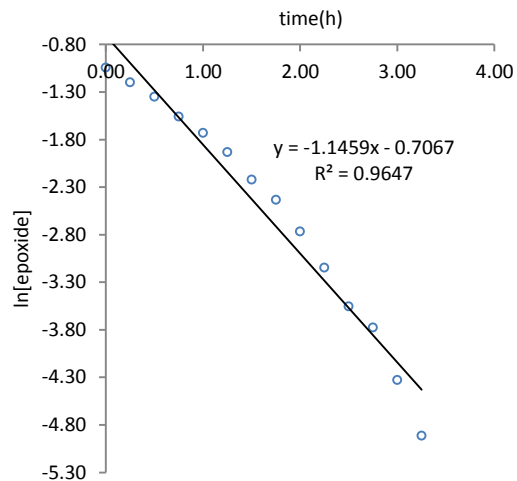
Temperature: 25   °C

Solvent: EtOAc
Solvent/substrate: 20   v/v
5b: 3.0   mol %
TBAB: 30.0   mol %

Order	R^2
0	0.8676
1	0.9755
2	0.7296

k_{obs}:   1.5079 h^{-1}

time(h)

$y = -1.5079x - 0.9656$
$R^2 = 0.9755$

ln[epoxide]
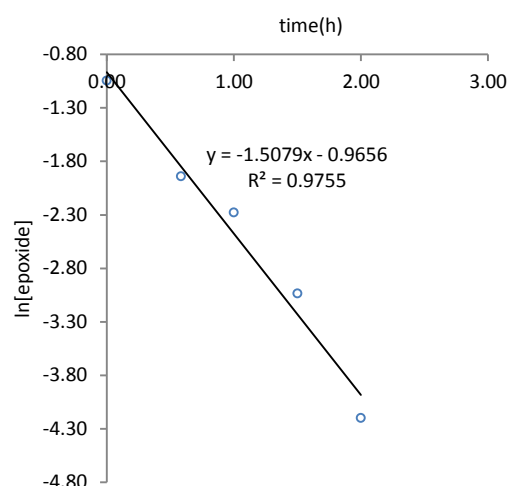
Temperature: 25   °C
Solvent: EtOAc
Solvent/substrate: 20   v/v
5b: 3.0   mol %
TBAB: 30.0   mol %

Order	R^2
0	0.9110
1	0.9530
2	0.6044

k_{obs}:   1.6616 h^{-1}

time(h)

$y = -1.6616x - 0.702$
$R^2 = 0.953$

ln[epoxide]
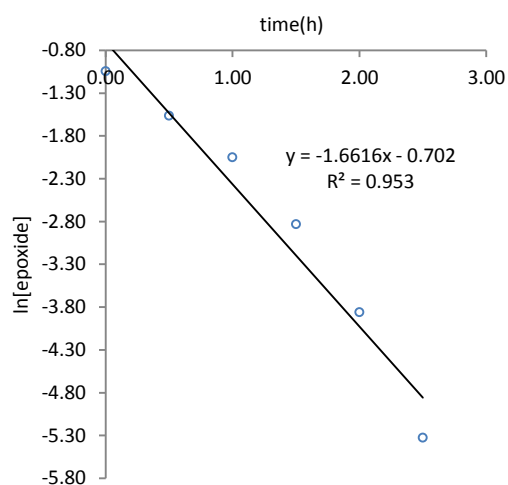
Temperature: 25   °C
Solvent: EtOAc
Solvent/substrate: 20   v/v
5b: 4.0   mol %
TBAB: 30.0   mol %

Order	R^2
0	0.9378
1	0.9566
2	0.6078

k_{obs}:   2.0653 h^{-1}

time(h)

$y = -2.0653x - 0.7298$
$R^2 = 0.9566$

ln[epoxide]

93
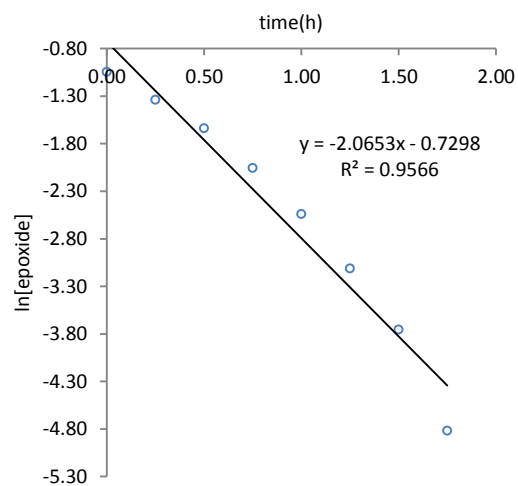
Temperature:	25	°C
Solvent:	EtOAc	
Solvent/substrate:	20	v/v
5b:	4.0	mol %
TBAB:	30.0	mol %

Order	R^2
0	0.9026
1	0.9393
2	0.4948

k_{obs}: 2.0479 h^{-1}

y = -2.0479x - 0.7556
R² = 0.9607

Temperature:	25	°C
Solvent:	EtOAc	
Solvent/substrate:	20	v/v
5b:	5.0	mol %
TBAB:	30.0	mol %

Order	R^2
0	0.9161
1	0.9573
2	0.5801

k_{obs}: 2.7252 h^{-1}

y = -2.7252x - 0.6834
R² = 0.9573

Temperature:	25	°C
Solvent:	EtOAc	
Solvent/substrate:	20	v/v
5b:	5.0	mol %
TBAB:	30.0	mol %

Order	R^2
0	0.9215
1	0.9549
2	0.5727

k_{obs}: 2.4493 h^{-1}

y = -2.4493x - 0.6338
R² = 0.9549
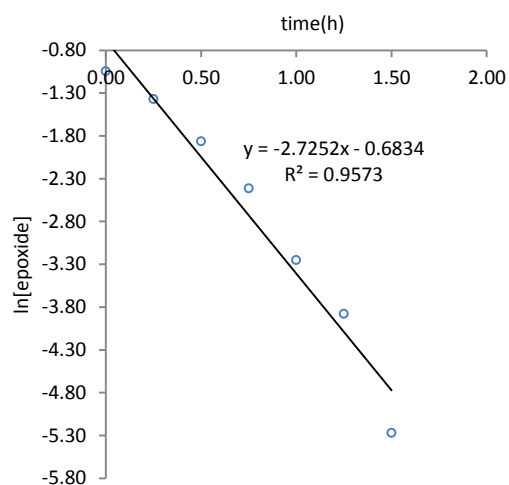
7. Appendix B

7.1. Acquisition of X-ray data

Diffraction data were collected at 110 K on an Oxford Diffraction SuperNova diffractometer with Cu-K$_\alpha$ radiation (λ = 1.54184 Å) using an EOS CCD camera. The crystal was cooled with an Oxford Instruments Cryojet. Diffractometer control, data collection, initial unit cell determination, frame integration and unit-cell refinement was carried out with CrysAlisPro.[a] Face-indexed absorption corrections were applied using spherical harmonics, implemented in SCALE3 ABSPACK scaling algorithm.[b] OLEX2[c] was used for overall structure solution, refinement and preparation of computer graphics and publication data. Within OLEX2, the direct methods algorithm was used for structure solution using SHELXS.[d] Refinement by full-matrix least-squares used the SHELXL-97 algorithm within OLEX2.[e] All non-hydrogen atoms were refined anisotropically. Hydrogen atoms were placed using a "riding model" and included in the refinement at calculated positions. One tertiary butyl group showed disorder and was modelled with the terminal carbons in two positions with refined occupancies of 0.622:0.378(18). Corresponding atoms of the major and minor component were restrained to have similar C-C distances and, due to proximity, were restrained to have the same ADP. Atoms C66, C67, C66A and C67A were also restrained to be approximately isotropic.

---

[a] CrysAlisPro, Oxford Diffraction Ltd. Version 1.171.34.40

[b] Empirical absorption correction using spherical harmonics, implemented in SCALE3 ABSPACK scaling algorithm within CrysAlisPro software, Oxford Diffraction Ltd. Version 1.171.34.40

[c] "Olex2" crystallography software, *J. Appl. Cryst.* 2009, *42*, 339–341.

[d] "SHELXS-97" - program for structure solution. G. M. Sheldrick, University of Göttingen, Göttingen, Germany, 1997.

[e] "SHELXL-97" - program for the Refinement of Crystal Structures. G. M. Sheldrick, University of Göttingen, Göttingen, Germany, 1997.
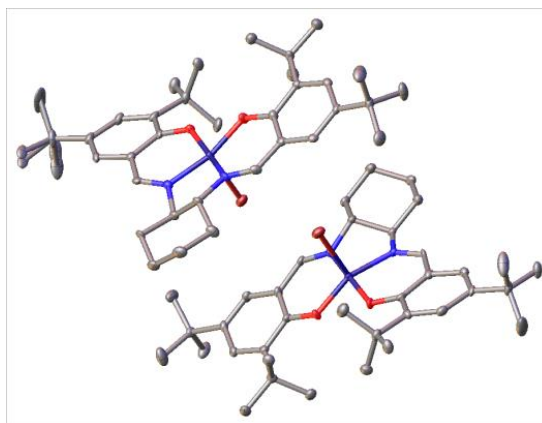
7.2. Crystal data and structure refinement for complex 3d.

Empirical formula	$C_{36}H_{52}BrCoN_2O_2$
Formula weight	683.63
Temperature/K	110.00(14)
Crystal system	triclinic
Space group	P1
a/Å	10.7950(2)
b/Å	12.6416(4)
c/Å	14.6957(4)
α/°	65.979(3)
β/°	89.9734(19)
γ/°	71.994(2)
Volume/Å³	1723.82(9)
Z	2
ρ_{calc}g/cm³	1.317
μ/mm⁻¹	5.502
F(000)	720.0
Crystal size/mm³	0.2554 × 0.1625 × 0.0289
Radiation	CuKα (λ = 1.54184)
2Θ range for data collection/°	8.01 to 142.31
Index ranges	-9 ≤ h ≤ 13, -14 ≤ k ≤ 15, -17 ≤ l ≤ 17
Reflections collected	11806
Independent reflections	7887 [R_{int} = 0.0272, R_{sigma} = 0.0400]
Data/restraints/parameters	7887/57/794
Goodness-of-fit on F²	1.025
Final R indexes [I>=2σ (I)]	R_1 = 0.0325, wR_2 = 0.0810
Final R indexes [all data]	R_1 = 0.0373, wR_2 = 0.0845
Largest diff. peak/hole / e Å⁻³	0.48/-0.47
Flack parameter	-0.017(5)

Structure solved by Natalie Pridmore

7.3. Fractional Atomic Coordinates (×10^4) and Equivalent Isotropic Displacement Parameters (Å^2×10^3) for 3d.

U$_{eq}$ is defined as 1/3 of of the trace of the orthogonalised U$_{IJ}$ tensor.

Atom	x	y	z	U(eq)
Br1	7619.5(6)	3800.4(5)	9785.1(4)	22.42(14)
C1	4439(4)	6261(4)	7480(3)	12.8(8)
C2	4273(5)	6004(5)	6584(4)	19.6(12)
C3	4362(5)	7072(5)	5631(3)	19.5(10)
C4	5644(5)	7331(5)	5706(4)	19.5(10)
C5	5793(5)	7587(5)	6619(4)	17.5(12)
C6	5734(4)	6509(4)	7556(3)	15.6(9)
C7	3824(5)	4534(5)	8587(4)	13.5(10)
C8	3732(5)	3587(5)	9508(4)	15.9(11)
C9	3006(5)	2841(5)	9449(4)	16.2(11)
C10	2866(5)	1908(5)	10302(4)	15.2(11)
C11	3517(5)	1705(5)	11237(4)	17.1(11)
C12	4226(5)	2389(5)	11348(4)	15.1(11)
C13	4275(5)	3419(5)	10453(4)	14.1(11)
C14	2137(5)	1053(5)	10282(4)	22.0(12)
C15	3181(6)	–216(5)	10505(6)	47.1(19)
C16	1374(6)	1518(6)	9242(5)	28.0(13)
C17	1167(8)	969(8)	11030(5)	54(2)
C18	4956(5)	2078(5)	12372(4)	17.7(11)
C19	4927(6)	848(5)	13192(5)	23.0(13)
C20	4304(6)	3103(5)	12713(5)	23.2(12)
C21	6406(6)	1940(6)	12298(5)	25.9(13)
C22	6260(5)	7394(5)	8636(4)	15.6(11)
C23	6404(5)	7505(5)	9550(4)	15.0(11)
C24	6913(5)	8428(5)	9527(4)	17.3(12)
C25	7050(5)	8633(5)	10358(4)	14.8(11)
C26	6651(5)	7905(5)	11234(4)	15.7(11)
C27	6125(5)	7001(5)	11319(4)	14.7(11)
C28	6023(5)	6770(5)	10450(4)	15.4(11)
C29	7539(5)	9677(5)	10315(4)	15.4(11)
C30	8104(6)	9453(5)	11353(4)	35.5(14)
C31	6366(6)	10883(5)	9887(5)	30.2(15)
C32	8604(6)	9831(5)	9636(5)	28.0(14)
C33	5752(5)	6219(5)	12311(4)	16.7(12)
C34	6682(6)	4871(5)	12697(4)	20.5(12)
C35	4310(6)	6294(6)	12168(5)	20.5(12)
C36	5862(6)	6673(6)	13128(4)	22.4(13)
Co1	5412.7(8)	5313.8(7)	9561.2(6)	12.90(18)
N1	4466(4)	5284(4)	8485(3)	12.2(9)

N2	5835(4)	6581(4)	8532(3)	12.8(9)
O1	4798(4)	4189(3)	10548(3)	15.8(8)
O2	5546(4)	5911(3)	10494(3)	16.0(8)
Br2	8323.1(5)	9044.7(5)	7051.2(4)	21.61(14)
C37	10852(5)	5994(4)	9307(3)	16.2(9)
C38	10196(6)	5344(5)	10185(4)	22.4(13)
C39	10925(5)	5166(5)	11158(4)	25.8(11)
C40	11032(5)	6349(5)	11119(3)	22.8(10)
C41	11631(5)	7020(5)	10205(4)	16.4(11)
C42	10860(5)	7194(4)	9256(3)	16.3(9)
C43	9820(5)	5465(5)	8187(4)	16.6(12)
C44	9507(5)	5427(5)	7252(4)	15.7(11)
C45	8967(5)	4523(5)	7291(4)	14.5(11)
C46	8814(5)	4306(5)	6471(4)	15.1(11)
C47	9215(5)	5022(5)	5573(4)	15.7(11)
C48	9729(5)	5937(5)	5479(4)	14.9(11)
C49	9872(5)	6157(5)	6346(4)	16.0(11)
C50	8331(6)	3274(5)	6513(5)	19.4(12)
C51	7321(6)	3728(5)	5576(4)	32.7(14)
C52	7661(6)	2818(6)	7442(5)	29.8(14)
C53	9509(6)	2202(6)	6567(6)	38.0(17)
C54	10095(6)	6718(5)	4470(4)	17.5(12)
C55	9938(6)	6280(6)	3662(5)	23.1(13)
C56	11541(6)	6644(6)	4589(5)	21.4(13)
C57	9169(6)	8056(5)	4107(5)	23.6(13)
C58	11974(5)	8533(5)	8158(4)	16.1(11)
C59	12217(5)	9351(5)	7229(4)	14.9(11)
C60	12951(5)	10096(5)	7250(5)	17.4(11)
C61	13084(5)	10999(5)	6395(5)	19.1(12)
C62	12430(5)	11193(5)	5482(5)	19.6(12)
C63	11698(5)	10508(5)	5388(4)	16.0(11)
C64	11658(5)	9496(5)	6290(4)	14.4(11)
C65	13873(5)	11826(4)	6388(3)	29.6(15)
C66	13019(10)	13191(6)	5886(9)	47(3)
C66A	12818(13)	13014(11)	6302(15)	47(3)
C67	14965(9)	11605(12)	5750(8)	43(3)
C67A	14684(15)	12159(18)	5522(10)	43(3)
C68	14517(10)	11534(11)	7432(6)	23(2)
C68A	14790(14)	11260(17)	7387(8)	23(2)
C69	10900(5)	10846(5)	4382(4)	18.2(12)
C70	9446(5)	11019(6)	4508(5)	24.7(13)
C71	11447(6)	9851(5)	4022(4)	21.0(12)
C72	10933(6)	12070(6)	3550(5)	27.1(14)
Co2	10570.2(8)	7578.9(8)	7237.0(6)	12.77(18)
N3	10335(4)	6202(4)	8299(3)	16.9(10)
N4	11272(4)	7833(4)	8272(3)	15.0(9)

Atom						
O3	10378(4)	7008(4)	6294(3)	17.8(8)		
O4	11122(4)	8716(3)	6236(3)	15.1(8)		

7.4. Anisotropic Displacement Parameters ($\text{Å}^2\times10^3$) for 3d.

The Anisotropic displacement factor exponent takes the form: -$2\pi^2[h^2a^{*2}U_{11}+2hka^*b^*U_{12}+\ldots]$.

Atom	U_{11}	U_{22}	U_{33}	U_{23}	U_{13}	U_{12}
Br1	17.7(3)	24.2(3)	21.4(3)	−6.6(2)	6.7(2)	−6.4(2)
C1	9(2)	15(2)	16(2)	−7.0(17)	4.0(16)	−4.2(16)
C2	17(3)	27(3)	19(3)	−13(2)	4(2)	−10(2)
C3	15(2)	31(3)	12(2)	−9(2)	2.0(17)	−7(2)
C4	17(2)	27(3)	16(2)	−9(2)	5.3(19)	−10(2)
C5	15(3)	21(3)	20(3)	−9(2)	8(2)	−11(2)
C6	12(2)	22(2)	18(2)	−11.9(19)	5.9(18)	−8.1(18)
C7	13(2)	16(2)	14(2)	−8.4(19)	−3.2(18)	−6.2(18)
C8	12(2)	16(2)	23(3)	−11(2)	5(2)	−5(2)
C9	14(2)	19(3)	16(3)	−9(2)	1.0(19)	−5(2)
C10	8(2)	18(2)	22(3)	−11(2)	0.9(19)	−4.8(19)
C11	16(3)	16(3)	18(3)	−5(2)	7(2)	−7(2)
C12	14(2)	17(2)	15(3)	−9(2)	0.4(19)	−3(2)
C13	12(2)	16(2)	17(3)	−8(2)	9(2)	−7(2)
C14	17(3)	25(3)	28(3)	−10(2)	1(2)	−13(2)
C15	37(4)	19(3)	74(5)	−11(3)	−23(3)	−8(3)
C16	28(3)	31(3)	27(3)	−8(3)	−3(2)	−19(3)
C17	57(5)	97(6)	32(4)	−25(4)	16(3)	−64(5)
C18	14(3)	21(3)	18(3)	−6(2)	3(2)	−10(2)
C19	27(3)	23(3)	17(3)	−4(2)	−3(2)	−11(2)
C20	26(3)	30(3)	19(3)	−13(2)	8(2)	−13(2)
C21	20(3)	31(3)	23(3)	−7(3)	1(2)	−10(2)
C22	11(2)	21(3)	16(3)	−7(2)	4(2)	−10(2)
C23	18(3)	16(2)	14(3)	−6(2)	3(2)	−11(2)
C24	18(3)	21(3)	14(3)	−5(2)	4(2)	−12(2)
C25	13(2)	14(2)	18(3)	−7(2)	0(2)	−6(2)
C26	14(2)	21(3)	14(3)	−8(2)	0(2)	−7(2)
C27	12(2)	19(3)	17(3)	−10(2)	4.3(19)	−6(2)
C28	14(3)	19(3)	17(3)	−9(2)	7(2)	−9(2)
C29	17(3)	14(2)	21(3)	−10(2)	6(2)	−9(2)
C30	52(4)	35(3)	28(3)	−10(2)	−1(3)	−30(3)
C31	18(3)	20(3)	55(4)	−18(3)	5(3)	−6(2)
C32	29(3)	29(3)	44(4)	−25(3)	18(3)	−20(2)
C33	20(3)	19(3)	13(3)	−8(2)	5(2)	−8(2)
C34	24(3)	22(3)	14(3)	−5(2)	2(2)	−9(2)
C35	20(3)	26(3)	17(3)	−7(2)	7(2)	−13(2)
C36	26(3)	35(3)	14(3)	−12(2)	8(2)	−18(2)

Co1	15.0(4)	16.2(4)	11.7(4)	−7.0(3)	4.0(3)	−9.3(3)
N1	10.1(19)	15.3(19)	11(2)	−5.2(16)	2.5(15)	−5.1(15)
N2	15(2)	13.0(19)	12(2)	−4.7(17)	3.0(16)	−6.9(16)
O1	17.1(18)	18.6(19)	18(2)	−9.0(16)	4.0(15)	−13.3(15)
O2	24(2)	19.9(19)	12.3(19)	−9.3(16)	4.9(15)	−14.2(16)
Br2	16.0(3)	25.9(3)	21.6(3)	−7.6(2)	4.9(2)	−8.8(2)
C37	18(2)	22(2)	11(2)	−10.2(18)	3.9(18)	−6.9(19)
C38	32(3)	21(3)	13(3)	−6(2)	4(2)	−11(3)
C39	27(3)	30(3)	14(2)	−6(2)	4(2)	−6(2)
C40	25(3)	34(3)	13(2)	−11(2)	5.1(19)	−11(2)
C41	19(3)	26(3)	9(2)	−11(2)	2(2)	−10(2)
C42	15(2)	25(2)	11(2)	−9.1(18)	2.2(17)	−7.7(19)
C43	22(3)	13(2)	13(3)	−4(2)	7(2)	−7(2)
C44	12(2)	19(3)	16(3)	−8(2)	3(2)	−4(2)
C45	14(3)	13(2)	16(3)	−7(2)	4(2)	−3(2)
C46	10(2)	16(2)	20(3)	−8(2)	2(2)	−6(2)
C47	14(2)	18(2)	18(3)	−11(2)	2(2)	−4(2)
C48	14(2)	18(3)	13(3)	−7(2)	3.0(19)	−6(2)
C49	17(3)	18(3)	14(3)	−7(2)	2(2)	−7(2)
C50	19(3)	19(3)	23(3)	−9(2)	−2(2)	−10(2)
C51	40(3)	39(3)	27(3)	−9(2)	−1(3)	−30(3)
C52	32(3)	28(3)	37(4)	−14(3)	8(3)	−20(2)
C53	30(3)	32(3)	66(5)	−33(3)	8(3)	−12(3)
C54	20(3)	27(3)	11(3)	−8(2)	4(2)	−15(2)
C55	27(3)	31(3)	21(3)	−15(2)	8(2)	−16(2)
C56	23(3)	26(3)	19(3)	−10(2)	7(2)	−13(2)
C57	27(3)	23(3)	16(3)	−3(2)	−1(2)	−10(2)
C58	13(2)	21(3)	17(3)	−13(2)	6.2(19)	−4.1(19)
C59	12(2)	17(2)	18(3)	−10(2)	5(2)	−5(2)
C60	10(2)	23(3)	25(3)	−17(2)	1(2)	−6(2)
C61	12(2)	22(3)	26(3)	−10(2)	5(2)	−9(2)
C62	14(3)	21(3)	25(3)	−8(2)	4(2)	−9(2)
C63	10(2)	16(2)	22(3)	−7(2)	6(2)	−5(2)
C64	8(2)	20(3)	19(3)	−12(2)	2(2)	−5(2)
C65	30(3)	29(3)	31(3)	−8(3)	−7(3)	−19(3)
C66	51(4)	19(3)	60(6)	1(4)	−19(4)	−22(3)
C66A	51(4)	19(3)	60(6)	1(4)	−19(4)	−22(3)
C67	44(4)	51(6)	38(5)	−3(4)	7(3)	−44(4)
C67A	44(4)	51(6)	38(5)	−3(4)	7(3)	−44(4)
C68	19(5)	13(6)	43(4)	−18(3)	4(3)	−6(4)
C68A	19(5)	13(6)	43(4)	−18(3)	4(3)	−6(4)
C69	18(3)	20(3)	16(3)	−4(2)	1(2)	−11(2)
C70	15(3)	33(3)	25(3)	−9(3)	−2(2)	−11(2)
C71	28(3)	22(3)	16(3)	−5(2)	4(2)	−17(2)
C72	26(3)	27(3)	26(3)	−4(3)	0(2)	−16(2)
Co2	15.0(4)	16.4(4)	11.0(4)	−7.2(3)	3.5(3)	−8.8(3)

N3	21(2)	20(2)	12(2)	−10.2(18)	2.0(17)	−5.3(18)
N4	15(2)	16(2)	13(2)	−7.2(16)	1.8(16)	−3.6(16)
O3	26(2)	18.9(19)	16(2)	−8.9(16)	8.5(16)	−15.7(16)
O4	18.7(19)	19.4(18)	12.2(19)	−8.1(15)	5.2(15)	−11.1(15)

7.5. Bond Lengths for 3d.

Atom	Atom	Length/Å	Atom	Atom	Length/Å
Br1	Co1	2.4727(9)	C37	C42	1.491(6)
C1	C2	1.503(7)	C37	N3	1.473(6)
C1	C6	1.538(6)	C38	C39	1.533(8)
C1	N1	1.483(6)	C39	C40	1.513(7)
C2	C3	1.528(7)	C40	C41	1.533(7)
C3	C4	1.531(6)	C41	C42	1.524(6)
C4	C5	1.522(7)	C42	N4	1.487(6)
C5	C6	1.511(7)	C43	C44	1.437(8)
C6	N2	1.480(6)	C43	N3	1.284(7)
C7	C8	1.424(8)	C44	C45	1.417(7)
C7	N1	1.302(7)	C44	C49	1.416(8)
C8	C9	1.426(7)	C45	C46	1.361(8)
C8	C13	1.414(8)	C46	C47	1.420(8)
C9	C10	1.377(8)	C46	C50	1.528(7)
C10	C11	1.431(8)	C47	C48	1.389(7)
C10	C14	1.529(7)	C48	C49	1.428(8)
C11	C12	1.373(8)	C48	C54	1.542(7)
C12	C13	1.441(7)	C49	O3	1.325(6)
C12	C18	1.539(8)	C50	C51	1.544(8)
C13	O1	1.318(6)	C50	C52	1.528(8)
C14	C15	1.552(8)	C50	C53	1.519(8)
C14	C16	1.526(8)	C54	C55	1.528(8)
C14	C17	1.513(8)	C54	C56	1.540(7)
C18	C19	1.541(8)	C54	C57	1.538(8)
C18	C20	1.547(8)	C58	C59	1.422(8)
C18	C21	1.530(7)	C58	N4	1.295(7)
C22	C23	1.420(8)	C59	C60	1.415(7)
C22	N2	1.307(7)	C59	C64	1.423(8)
C23	C24	1.424(7)	C60	C61	1.355(8)
C23	C28	1.420(7)	C61	C62	1.408(8)
C24	C25	1.366(8)	C61	C65	1.537(8)
C25	C26	1.404(7)	C62	C63	1.383(7)
C25	C29	1.545(7)	C63	C64	1.431(8)
C26	C27	1.388(7)	C63	C69	1.539(8)
C27	C28	1.432(8)	C64	O4	1.316(7)
C27	C33	1.529(7)	C65	C66	1.533(5)
C28	O2	1.318(6)	C65	C66A	1.535(5)

Atom	Atom	Length/Å		Atom	Atom	Length/Å
C29	C30	1.522(8)		C65	C67	1.535(5)
C29	C31	1.533(7)		C65	C67A	1.534(5)
C29	C32	1.528(7)		C65	C68	1.534(5)
C33	C34	1.545(7)		C65	C68A	1.534(5)
C33	C35	1.540(7)		C69	C70	1.538(7)
C33	C36	1.546(8)		C69	C71	1.515(8)
Co1	N1	1.903(4)		C69	C72	1.544(8)
Co1	N2	1.882(4)		Co2	N3	1.895(5)
Co1	O1	1.862(4)		Co2	N4	1.882(5)
Co1	O2	1.839(4)		Co2	O3	1.842(4)
Br2	Co2	2.4903(9)		Co2	O4	1.842(4)
C37	C38	1.529(7)				

7.6. Bond Angles for 3d.

Atom	Atom	Atom	Angle/°		Atom	Atom	Atom	Angle/°
C2	C1	C6	111.3(4)		C37	C38	C39	108.0(5)
N1	C1	C2	117.1(4)		C40	C39	C38	113.0(4)
N1	C1	C6	104.7(3)		C39	C40	C41	113.1(4)
C1	C2	C3	109.5(4)		C42	C41	C40	108.6(4)
C2	C3	C4	112.1(4)		C37	C42	C41	111.3(4)
C5	C4	C3	110.7(4)		N4	C42	C37	106.6(4)
C6	C5	C4	109.3(4)		N4	C42	C41	117.8(4)
C5	C6	C1	111.2(4)		N3	C43	C44	126.1(5)
N2	C6	C1	104.7(4)		C45	C44	C43	117.5(5)
N2	C6	C5	118.1(4)		C49	C44	C43	121.4(5)
N1	C7	C8	126.2(5)		C49	C44	C45	120.7(5)
C7	C8	C9	117.2(5)		C46	C45	C44	121.4(5)
C13	C8	C7	122.2(5)		C45	C46	C47	117.4(5)
C13	C8	C9	120.5(5)		C45	C46	C50	122.4(5)
C10	C9	C8	121.1(5)		C47	C46	C50	120.0(5)
C9	C10	C11	116.6(5)		C48	C47	C46	124.1(5)
C9	C10	C14	123.3(5)		C47	C48	C49	117.6(5)
C11	C10	C14	119.9(5)		C47	C48	C54	121.6(5)
C12	C11	C10	125.3(5)		C49	C48	C54	120.8(5)
C11	C12	C13	117.0(5)		C44	C49	C48	118.8(5)
C11	C12	C18	122.3(5)		O3	C49	C44	121.6(5)
C13	C12	C18	120.7(5)		O3	C49	C48	119.6(5)
C8	C13	C12	119.1(5)		C46	C50	C51	110.6(5)
O1	C13	C8	122.3(5)		C46	C50	C52	111.5(5)
O1	C13	C12	118.6(5)		C52	C50	C51	107.6(5)
C10	C14	C15	107.8(4)		C53	C50	C46	108.6(5)
C16	C14	C10	111.5(5)		C53	C50	C51	110.3(5)
C16	C14	C15	106.8(5)		C53	C50	C52	108.2(5)
C17	C14	C10	110.2(5)		C55	C54	C48	112.0(5)

C17	C14	C15	112.5(6)	C55	C54	C56	106.7(5)
C17	C14	C16	108.0(5)	C55	C54	C57	108.5(5)
C12	C18	C19	111.8(5)	C56	C54	C48	111.1(5)
C12	C18	C20	109.7(5)	C57	C54	C48	108.0(5)
C19	C18	C20	108.2(5)	C57	C54	C56	110.4(5)
C21	C18	C12	110.3(5)	N4	C58	C59	126.4(5)
C21	C18	C19	106.7(5)	C58	C59	C64	121.4(5)
C21	C18	C20	110.0(5)	C60	C59	C58	118.4(5)
N2	C22	C23	124.9(5)	C60	C59	C64	120.0(5)
C22	C23	C24	117.0(5)	C61	C60	C59	121.5(5)
C22	C23	C28	122.6(5)	C60	C61	C62	117.4(5)
C28	C23	C24	120.3(5)	C60	C61	C65	123.0(5)
C25	C24	C23	121.5(5)	C62	C61	C65	119.6(5)
C24	C25	C26	117.0(5)	C63	C62	C61	125.1(5)
C24	C25	C29	121.3(5)	C62	C63	C64	116.6(5)
C26	C25	C29	121.6(5)	C62	C63	C69	122.3(5)
C27	C26	C25	125.3(5)	C64	C63	C69	121.0(5)
C26	C27	C28	117.1(5)	C59	C64	C63	118.9(5)
C26	C27	C33	122.0(5)	O4	C64	C59	121.5(5)
C28	C27	C33	120.7(5)	O4	C64	C63	119.7(5)
C23	C28	C27	118.7(5)	C66	C65	C61	111.5(6)
O2	C28	C23	121.7(5)	C66	C65	C67	108.4(3)
O2	C28	C27	119.5(5)	C66	C65	C68	108.5(3)
C30	C29	C25	112.0(5)	C66A	C65	C61	104.0(8)
C30	C29	C31	108.7(5)	C67	C65	C61	105.5(6)
C30	C29	C32	107.6(5)	C67A	C65	C61	116.4(9)
C31	C29	C25	108.2(4)	C67A	C65	C66A	108.4(3)
C32	C29	C25	112.1(5)	C67A	C65	C68A	108.5(3)
C32	C29	C31	108.2(5)	C68	C65	C61	114.4(6)
C27	C33	C34	109.2(4)	C68	C65	C67	108.4(3)
C27	C33	C35	110.7(5)	C68A	C65	C61	110.8(9)
C27	C33	C36	112.0(5)	C68A	C65	C66A	108.4(3)
C34	C33	C36	108.6(5)	C63	C69	C72	111.9(5)
C35	C33	C34	110.3(5)	C70	C69	C63	110.0(5)
C35	C33	C36	106.1(5)	C70	C69	C72	106.7(5)
N1	Co1	Br1	103.27(13)	C71	C69	C63	110.4(5)
N2	Co1	Br1	92.16(13)	C71	C69	C70	109.8(5)
N2	Co1	N1	84.45(19)	C71	C69	C72	107.8(5)
O1	Co1	Br1	94.43(12)	N3	Co2	Br2	96.16(14)
O1	Co1	N1	93.42(18)	N4	Co2	Br2	94.35(13)
O1	Co1	N2	173.38(17)	N4	Co2	N3	84.9(2)
O2	Co1	Br1	104.60(13)	O3	Co2	Br2	102.56(13)
O2	Co1	N1	152.10(18)	O3	Co2	N3	92.63(19)
O2	Co1	N2	93.18(19)	O3	Co2	N4	163.08(19)
O2	Co1	O1	85.77(17)	O3	Co2	O4	85.37(17)
C1	N1	Co1	114.2(3)	O4	Co2	Br2	94.81(12)

A	B	C		Angle	A	B	C		Angle
C7	N1	C1		120.6(4)	O4	Co2	N3		169.02(18)
C7	N1	Co1		125.1(4)	O4	Co2	N4		93.84(18)
C6	N2	Co1		111.7(3)	C37	N3	Co2		113.9(3)
C22	N2	C6		121.7(4)	C43	N3	C37		120.8(5)
C22	N2	Co1		126.5(4)	C43	N3	Co2		125.2(4)
C13	O1	Co1		128.0(4)	C42	N4	Co2		112.2(3)
C28	O2	Co1		130.0(3)	C58	N4	C42		122.3(5)
C42	C37	C38		112.2(4)	C58	N4	Co2		125.4(4)
N3	C37	C38		116.8(4)	C49	O3	Co2		129.7(4)
N3	C37	C42		108.0(4)	C64	O4	Co2		129.4(4)

7.7. Torsion Angles for 3d.

A	B	C	D	Angle/°	A	B	C	D	Angle/°
Br1	Co1	N2	C6	79.9(3)	C38	C37	C42	C41	61.3(5)
Br1	Co1	N2	C22	-95.5(4)	C38	C37	C42	N4	-169.1(4)
Br1	Co1	O1	C13	-85.0(4)	C38	C37	N3	C43	-29.4(7)
Br1	Co1	O2	C28	81.7(5)	C38	C37	N3	Co2	152.8(4)
C1	C2	C3	C4	55.5(6)	C38	C39	C40	C41	-53.4(6)
C1	C6	N2	C22	-139.9(5)	C39	C40	C41	C42	53.1(6)
C1	C6	N2	Co1	44.4(4)	C40	C41	C42	C37	-56.7(5)
C2	C1	C6	C5	58.5(5)	C40	C41	C42	N4	179.8(4)
C2	C1	C6	N2	-172.9(4)	C41	C42	N4	C58	-20.0(7)
C2	C1	N1	C7	-29.7(6)	C41	C42	N4	Co2	163.6(3)
C2	C1	N1	Co1	153.7(3)	C42	C37	C38	C39	-57.3(6)
C2	C3	C4	C5	-56.6(6)	C42	C37	N3	C43	-157.0(5)
C3	C4	C5	C6	56.8(5)	C42	C37	N3	Co2	25.3(5)
C4	C5	C6	C1	-57.8(5)	C43	C44	C45	C46	-170.7(5)
C4	C5	C6	N2	-178.9(4)	C43	C44	C49	C48	170.0(5)
C5	C6	N2	C22	-15.6(7)	C43	C44	C49	O3	-8.0(8)
C5	C6	N2	Co1	168.8(3)	C44	C43	N3	C37	-167.6(5)
C6	C1	C2	C3	-55.7(5)	C44	C43	N3	Co2	9.9(8)
C6	C1	N1	C7	-153.6(4)	C44	C45	C46	C47	-0.1(8)
C6	C1	N1	Co1	29.8(4)	C44	C45	C46	C50	175.3(5)
C7	C8	C9	C10	-179.9(5)	C44	C49	O3	Co2	-7.2(8)
C7	C8	C13	C12	-175.7(5)	C45	C44	C49	C48	-2.1(8)
C7	C8	C13	O1	6.0(8)	C45	C44	C49	O3	180.0(5)
C8	C7	N1	C1	-177.7(5)	C45	C46	C47	C48	-1.2(8)
C8	C7	N1	Co1	-1.5(8)	C45	C46	C50	C51	137.4(6)
C8	C9	C10	C11	-2.0(8)	C45	C46	C50	C52	17.7(7)
C8	C9	C10	C14	-178.0(5)	C45	C46	C50	C53	-101.4(6)
C8	C13	O1	Co1	-20.0(7)	C46	C47	C48	C49	0.7(8)
C9	C8	C13	C12	7.5(7)	C46	C47	C48	C54	-177.5(5)
C9	C8	C13	O1	-170.8(5)	C47	C46	C50	C51	-47.4(7)
C9	C10	C11	C12	2.3(8)	C47	C46	C50	C52	-167.1(5)

C9 C10 C14 C15	105.8(6)	C47 C46 C50 C53	73.8(7)
C9 C10 C14 C16	-11.1(7)	C47 C48 C49 C44	0.9(8)
C9 C10 C14 C17	-131.0(6)	C47 C48 C49 O3	178.9(5)
C10 C11 C12 C13	2.3(8)	C47 C48 C54 C55	-5.0(7)
C10 C11 C12 C18	-177.0(5)	C47 C48 C54 C56	-124.3(6)
C11 C10 C14 C15	-70.1(7)	C47 C48 C54 C57	114.5(6)
C11 C10 C14 C16	173.0(5)	C48 C49 O3 Co2	174.9(4)
C11 C10 C14 C17	53.0(7)	C49 C44 C45 C46	1.7(8)
C11 C12 C13 C8	-7.1(7)	C49 C48 C54 C55	176.8(5)
C11 C12 C13 O1	171.3(5)	C49 C48 C54 C56	57.5(7)
C11 C12 C18 C19	7.0(7)	C49 C48 C54 C57	-63.7(7)
C11 C12 C18 C20	-113.1(6)	C50 C46 C47 C48	-176.7(5)
C11 C12 C18 C21	125.6(6)	C54 C48 C49 C44	179.2(5)
C12 C13 O1 Co1	161.7(4)	C54 C48 C49 O3	-2.8(8)
C13 C8 C9 C10	-2.9(8)	C58 C59 C60 C61	-171.9(5)
C13 C12 C18 C19	-172.2(5)	C58 C59 C64 C63	166.8(5)
C13 C12 C18 C20	67.7(6)	C58 C59 C64 O4	-13.9(8)
C13 C12 C18 C21	-53.7(7)	C59 C58 N4 C42	-167.8(5)
C14 C10 C11 C12	178.4(5)	C59 C58 N4 Co2	8.1(8)
C18 C12 C13 C8	172.2(5)	C59 C60 C61 C62	1.9(8)
C18 C12 C13 O1	-9.4(7)	C59 C60 C61 C65	180.0(5)
C22 C23 C24 C25	177.9(5)	C59 C64 O4 Co2	17.0(7)
C22 C23 C28 C27	-176.0(5)	C60 C59 C64 C63	-8.4(7)
C22 C23 C28 O2	2.1(9)	C60 C59 C64 O4	170.9(5)
C23 C22 N2 C6	-178.8(5)	C60 C61 C62 C63	-2.3(9)
C23 C22 N2 Co1	-3.9(8)	C60 C61 C65 C66	-122.7(7)
C23 C24 C25 C26	-0.9(8)	C60 C61 C65 C66A	-99.3(9)
C23 C24 C25 C29	-177.0(5)	C60 C61 C65 C67	119.9(7)
C23 C28 O2 Co1	7.5(8)	C60 C61 C65 C67A	141.6(9)
C24 C23 C28 C27	1.7(8)	C60 C61 C65 C68	0.9(8)
C24 C23 C28 O2	179.8(5)	C60 C61 C65 C68A	17.0(9)
C24 C25 C26 C27	-0.3(8)	C61 C62 C63 C64	-2.7(8)
C24 C25 C29 C30	-158.4(5)	C61 C62 C63 C69	174.0(5)
C24 C25 C29 C31	81.8(6)	C62 C61 C65 C66	55.4(7)
C24 C25 C29 C32	-37.4(7)	C62 C61 C65 C66A	78.8(9)
C25 C26 C27 C28	2.1(8)	C62 C61 C65 C67	-62.0(7)
C25 C26 C27 C33	178.1(5)	C62 C61 C65 C67A	-40.4(10)
C26 C25 C29 C30	25.6(7)	C62 C61 C65 C68	178.9(6)
C26 C25 C29 C31	-94.1(6)	C62 C61 C65 C68A	-164.9(8)
C26 C25 C29 C32	146.6(5)	C62 C63 C64 C59	7.8(7)
C26 C27 C28 C23	-2.7(8)	C62 C63 C64 O4	-171.5(5)
C26 C27 C28 O2	179.2(5)	C62 C63 C69 C70	-123.2(6)
C26 C27 C33 C34	-112.9(6)	C62 C63 C69 C71	115.4(6)
C26 C27 C33 C35	125.5(6)	C62 C63 C69 C72	-4.8(7)
C26 C27 C33 C36	7.4(7)	C63 C64 O4 Co2	-163.7(4)
C27 C28 O2 Co1	-174.5(4)	C64 C59 C60 C61	3.4(8)

C28	C23	C24	C25	0.1(8)	C64	C63	C69	C70	53.3(7)
C28	C27	C33	C34	63.0(7)	C64	C63	C69	C71	-68.1(6)
C28	C27	C33	C35	-58.6(7)	C64	C63	C69	C72	171.8(5)
C28	C27	C33	C36	-176.7(5)	C65	C61	C62	C63	179.5(5)
C29	C25	C26	C27	175.9(5)	C69	C63	C64	C59	-168.9(5)
C33	C27	C28	C23	-178.8(5)	C69	C63	C64	O4	11.8(8)
C33	C27	C28	O2	3.1(8)	N3	C37	C38	C39	177.2(4)
N1	C1	C2	C3	-176.2(4)	N3	C37	C42	C41	-168.6(4)
N1	C1	C6	C5	-174.0(4)	N3	C37	C42	N4	-38.9(5)
N1	C1	C6	N2	-45.4(4)	N3	C43	C44	C45	178.6(5)
N1	C7	C8	C9	-178.2(5)	N3	C43	C44	C49	6.3(9)
N1	C7	C8	C13	4.9(9)	N3	Co2	N4	C42	-19.8(3)
N1	Co1	N2	C6	-23.2(3)	N3	Co2	N4	C58	164.0(4)
N1	Co1	N2	C22	161.4(5)	N3	Co2	O3	C49	17.1(5)
N1	Co1	O1	C13	18.6(4)	N3	Co2	O4	C64	-90.6(11)
N1	Co1	O2	C28	-95.5(6)	N4	C58	C59	C60	176.5(5)
N2	C22	C23	C24	178.5(5)	N4	C58	C59	C64	1.3(8)
N2	C22	C23	C28	-3.8(9)	N4	Co2	N3	C37	-3.5(3)
N2	Co1	O2	C28	-11.3(5)	N4	Co2	N3	C43	178.9(5)
O1	Co1	O2	C28	175.2(5)	N4	Co2	O3	C49	98.4(7)
O2	Co1	N2	C6	-175.3(3)	N4	Co2	O4	C64	-7.4(4)
O2	Co1	N2	C22	9.3(5)	O3	Co2	N3	C37	159.8(3)
O2	Co1	O1	C13	170.6(4)	O3	Co2	N3	C43	-17.9(5)
Br2	Co2	N3	C37	-97.3(3)	O3	Co2	N4	C42	-102.1(6)
Br2	Co2	N3	C43	85.0(4)	O3	Co2	N4	C58	81.6(7)
Br2	Co2	N4	C42	76.1(3)	O3	Co2	O4	C64	-170.5(4)
Br2	Co2	N4	C58	-100.2(4)	O4	Co2	N3	C37	80.6(10)
Br2	Co2	O3	C49	-79.8(5)	O4	Co2	N3	C43	-97.1(10)
Br2	Co2	O4	C64	87.3(4)	O4	Co2	N4	C42	171.2(3)
C37	C38	C39	C40	53.1(6)	O4	Co2	N4	C58	-5.1(4)
C37	C42	N4	C58	-145.8(4)	O4	Co2	O3	C49	-173.7(5)
C37	C42	N4	Co2	37.8(4)					

7.8. Hydrogen Atom Coordinates (Å×10^4) and Isotropic Displacement Parameters (Å^2×10^3) for 3d.

Atom	x	y	z	U(eq)
H1	3713	7006	7389	15
H2A	3425	5904	6528	24
H2B	4954	5247	6667	24
H3A	3621	7806	5513	23
H3B	4307	6880	5060	23
H4A	6385	6627	5760	23
H4B	5644	8036	5100	23
H5A	6627	7711	6675	21

H5B	5092	8329	6543	21
H6	6455	5780	7608	19
H7	3382	4624	8002	16
H9	2622	2988	8823	19
H11	3455	1057	11816	20
H15A	3775	-116	10015	71
H15B	2750	-763	10473	71
H15C	3665	-555	11165	71
H16A	743	2323	9059	42
H16B	925	965	9255	42
H16C	1975	1557	8757	42
H17A	1637	580	11700	80
H17B	659	492	10967	80
H17C	590	1781	10897	80
H19A	4035	917	13304	35
H19B	5444	655	13806	35
H19C	5284	207	12977	35
H20A	4275	3884	12197	35
H20B	4807	2942	13322	35
H20C	3424	3121	12831	35
H21A	6802	1307	12081	39
H21B	6855	1723	12946	39
H21C	6472	2705	11821	39
H22	6483	7941	8069	19
H24	7157	8902	8931	21
H26	6746	8038	11803	19
H30A	7417	9477	11767	53
H30B	8467	10080	11288	53
H30C	8782	8661	11657	53
H31A	6041	11066	9213	45
H31B	6643	11539	9880	45
H31C	5681	10801	10300	45
H32A	9374	9107	9921	42
H32B	8823	10533	9581	42
H32C	8284	9950	8980	42
H34A	6673	4597	12178	31
H34B	6389	4360	13277	31
H34C	7560	4820	12877	31
H35A	3742	7131	11950	31
H35B	4099	5786	12795	31
H35C	4190	6011	11670	31
H36A	6755	6621	13261	34
H36B	5607	6169	13734	34
H36C	5293	7512	12895	34
H37	11775	5464	9443	19
H38A	10241	4552	10213	27

H38B	9277	5836	10097	27
H39A	10467	4830	11715	31
H39B	11803	4574	11287	31
H40A	11570	6165	11728	27
H40B	10161	6892	11100	27
H41A	11586	7813	10171	20
H41B	12548	6540	10264	20
H42	9945	7681	9230	20
H43	9631	4904	8764	20
H45	8713	4069	7889	17
H47	9129	4869	5013	19
H51A	6590	4415	5544	49
H51B	7013	3074	5622	49
H51C	7730	3976	4981	49
H52A	8287	2474	8038	45
H52B	7332	2200	7429	45
H52C	6944	3495	7442	45
H53A	9876	2439	5950	57
H53B	9233	1514	6666	57
H53C	10161	1973	7119	57
H55A	10489	5436	3889	35
H55B	10190	6778	3052	35
H55C	9035	6351	3540	35
H56A	11673	6952	5066	32
H56B	11746	7130	3950	32
H56C	12106	5803	4823	32
H57A	8272	8086	4052	35
H57B	9348	8552	3460	35
H57C	9311	8367	4580	35
H58	12356	8497	8742	19
H60	13351	9964	7866	21
H62	12495	11831	4898	24
H66A	13525	13680	5926	70
H66B	12266	13325	6226	70
H66C	12732	13423	5193	70
H66D	13230	13595	6281	70
H66E	12355	12832	6873	70
H66F	12209	13358	5696	70
H67A	14578	11781	5094	64
H67B	15533	10761	6071	64
H67C	15467	12133	5687	64
H67D	14105	12621	4893	64
H67E	15290	11419	5525	64
H67F	15164	12646	5607	64
H68A	15049	10680	7758	34
H68B	13845	11709	7829	34

H68C	15059	12031	7361	34
H68D	15414	10483	7477	34
H68E	14279	11139	7932	34
H68F	15249	11804	7375	34
H70A	9376	10261	4995	37
H70B	8951	11250	3874	37
H70C	9103	11652	4734	37
H71A	12355	9747	3945	32
H71B	10955	10085	3386	32
H71C	11379	9091	4506	32
H72A	10621	12711	3772	41
H72B	10379	12277	2950	41
H72C	11819	11983	3413	41

7.9. Atomic Occupancy for 3d.

Atom	Occupancy	Atom	Occupancy	Atom	Occupancy
C66	0.622(18)	H66A	0.622(18)	H66B	0.622(18)
H66C	0.622(18)	C66A	0.378(18)	H66D	0.378(18)
H66E	0.378(18)	H66F	0.378(18)	C67	0.622(18)
H67A	0.622(18)	H67B	0.622(18)	H67C	0.622(18)
C67A	0.378(18)	H67D	0.378(18)	H67E	0.378(18)
H67F	0.378(18)	C68	0.622(18)	H68A	0.622(18)
H68B	0.622(18)	H68C	0.622(18)	C68A	0.378(18)
H68D	0.378(18)	H68E	0.378(18)	H68F	0.378(18)

Abbreviations

HKR	hydrolytic kinetic resolution
$scCO_2$	supercritical CO_2
w.r.t.	With respect to
TBAB	tetrabutylammonium bromide
TBAC	tetrabutylammonium chloride
TBAI	tetrabutylammonium iodide
DNP	2,4-dinitrophenoxide
PPN^+	bis(triphenylphosphine)iminium
BMIOH	1-butyl-3-methylimidazolium hydroxide
DMAP	(4-dimethylamino)pyridine
NMP	N-methyl-2-pyrrolidone
PO	propylene oxide
PC	propylene carbonate
SO	styrene oxide
SC	styrene carbonate
PGE	phenyl glycidyl ether
PMEC	(phenoxymethyl)ethylene carbonate
e.r.	enantiomeric ratio
ee	enantiomeric excess
g	gram
M	molar
mL	millilitres
mmol	millimoles
IR	infrared
MP	melting point
NMR	nuclear magnetic resonance
ppm	parts per million
Hz	Hertz
s (^{1}H nuclear magnetic resonance)	singlet
d (^{1}H nuclear magnetic resonance)	doublet
t (^{1}H nuclear magnetic resonance)	triplets
m (^{1}H nuclear magnetic resonance)	multiplet
br	broad
s (infrared spectra)	strong
m (infrared spectra)	medium
w (infrared spectra)	weak
MS	mass spectrometry
ESI	electrospray ionisation
GC	gas chromatography
HPLC	high-performance liquid chromatography

References

(1)   Schaus, S. E.; Brandes, B. D.; Larrow, J. F.; Tokunaga, M.; Hansen, K. B.; Gould, A. E.; Furrow, M. E.; Jacobsen, E. N. *J. Am. Chem. Soc.* **2002**, *124*, 1307.

(2)   Lu, X.-B.; Liang, B.; Zhang, Y.-J.; Tian, Y.-Z.; Wang, Y.-M.; Bai, C.-X.; Wang, H.; Zhang, R. *J. Am. Chem. Soc.* **2004**, *126*, 3732.

(3)   Berkessel, A.; Brandenburg, M. *Org. Lett.* **2006**, *8*, 4401.

(4)   Ren, W.-M.; Wu, G.-P.; Lin, F.; Jiang, J.-Y.; Liu, C.; Luo, Y.; Lu, X.-B. *Chem. Sci.* **2012**, *3*, 2094.

(5)   Jang, D. Y.; Jang, H. G.; Kim, G. R.; Kim, G.-J. *Catal. Today.* **2012**, *185*, 306.

(6)   North, M.; Pasquale, R. *Angew. Chem., Int. Ed.* **2009**, *48*, 2946.

(7)   Tian, D.; Liu, B.; Zhang, L.; Wang, X.; Zhang, W.; Han, L.; Park, D.-W. *J. Ind. Eng. Chem.* **2012**, *18*, 1332.

(8)   Paddock, R. L.; Nguyen, S. T. *J. Am. Chem. Soc.* **2001**, *123*, 11498.

(9)   Ford, D. D.; Nielsen, L. P. C.; Zuend, S. J.; Musgrave, C. B.; Jacobsen, E. N. *J. Am. Chem. Soc.* **2013**, *135*, 15595.

(10)   Buysch, H.-J. In *Ullmann's encyclopedia of industrial chemistry*; Wiley-VCH Verlag GmbH & Co. KGaA: 2000.

(11)   Doscher, P. A., (Boeing Co.) US5098594 A, 1992

(12)   Doscher, P. A., (Boeing Co.) US5007969, 1991

(13)   Doscher-Good, P. A., (Boeing Co.) US5204026 (A), 1993

(14)   Stoye, D. In *Ullmann's encyclopedia of industrial chemistry*; Wiley-VCH Verlag GmbH & Co. KGaA: 2000.

(15)   Henderson, R. K.; Jimenez-Gonzalez, C.; Constable, D. J. C.; Alston, S. R.; Inglis, G. G. A.; Fisher, G.; Sherwood, J.; Binks, S. P.; Curzons, A. D. *Green Chem.* **2011**, *13*, 854.

(16)   Beyer, K. H. J.; Bergfels, W. F.; Benndt, W. D.; Carlton, W. H.; Hoffman, D. K.; Schroeter, A. L.; Shank, R. C. *J. Am. Coll. Toxicol.* **1987**, *6*, 23.

(17)   Clements, J. H. *Industrial & Engineering Chemistry Research* **2003**, *42*, 663.

(18)   Dyer, E.; Scott, H. *J. Am. Chem. Soc.* **1957**, *79*, 672.

(19)   Tunge, J. A.; Gately, D. A.; Norton, J. R. *J. Am. Chem. Soc.* **1999**, *121*, 4520.

(20)   Salvati, M. E.; Finlay, H.; Harikrishnan, L. S.; Jiang, J.; Johnson, J. A.; Kamau, M. G.; Lawrence, R. M.; Miller, M. M.; Qiao, J. X.; Wang, T. C.; Wang, Y.; Yang, W., (Squibb Bristol Myers Co) WO 2007/062314 A2, 2007

(21)   Archelas, A.; Furstoss; R *Annu. Rev. Microbiol.* **1997**, *51*, 491.

(22)   Shah, R. R. In *Stereochemical aspects of drug action and disposition*; Eichelbaum, M., Testa, B., Somogyi, A., Eds.; Springer Berlin Heidelberg: 2003; Vol. 153, p 401.

(23)   J. Hyttel; K. P. Bøgesø; J. Perregaard; Sánchez, C. *J. Neural Transmission* **1992**, *88*, 157.

(24)   Hutt, A. J. *Drug Metab. Drug Interact.* **2007**, *22*, 79.

(25)   Shaikh, A.-A. G.; Sivaram, S. *Chem. Rev.* **1996**, *96*, 951.

(26)   Ludwig, B. J.; Piech, E. C. *J. Am. Chem. Soc.* **1951**, *73*, 5779.

(27)   Coker, A. *Dimethyl carbonate report abstract*, Nexant, 2012.
(28)   Romano, U.; Tesel, R.; Mauri, M. M.; Rebora, P. *Ind. Eng. Chem. Prod. RD.* **1980**, *19*, 396.
(29)   He, L. N.; Yasuda, H.; Sakakura, T. *Green Chem.* **2003**, *5*, 92.
(30)   Yin, S.-F.; Shimada, S. *Chem. Commun.* **2009**, 1136.
(31)   Rustad, L. E. *Sci. Total Environ.* **2008**, *404*, 222.
(32)   Crowley, T. J. *Science* **2000**, *289*, 270.
(33)   D'Alessandro, D. M.; Smit, B.; Long, J. R. *Angew. Chem., Int. Ed.* **2010**, *49*, 6058.
(34)   Clegg, W.; Harrington, R. W.; North, M.; Pasquale, R. *Chem. Eur. J.* **2010**, *16*, 6828.
(35)   Yoon, T. P.; Jacobsen, E. N. *Science* **2003**, *299*, 1691.
(36)   Zhang, W.; Loebach, J. L.; Wilson, S. R.; Jacobsen, E. N. *J. Am. Chem. Soc.* **1990**, *112*, 2801.
(37)   Jacobsen, E. N.; Zhang, W.; Muci, A. R.; Ecker, J. R.; Deng, L. *J. Am. Chem. Soc.* **1991**, *113*, 7063.
(38)   Brandes, B. D.; Jacobsen, E. N. *J. Org. Chem.* **1994**, *59*, 4378.
(39)   Baronsky, T.; Beattie, C.; Harrington, R. W.; Irfan, R.; North, M.; Osende, J. G.; Young, C. *ACS Catalysis* **2013**, *3*, 790.
(40)   Beattie, C.; North, M. *RSC Advances* **2014**, *4*, 31345.
(41)   Pozzi, G.; Shepperson, I. *Coordin. Chem. Rev.* **2003**, *242*, 115.
(42)   Metcalfe, I. S.; North, M.; Villuendas, P. *Journal of CO2 Utilization* **2013**, *2*, 24.
(43)   Melendez, J.; North, M.; Villuendas, P.; Young, C. *Dalton Trans* **2011**, *40*, 3885.
(44)   Phan, N. T. S.; Brown, D. H.; Adams, H.; Spey, S. E.; Styring, P. *Dalton Trans* **2004**, 1348.
(45)   Melendez, J.; North, M.; Villuendas, P. *Chem. Commun.* **2009**, 2577.
(46)   North, M.; Villuendas, P.; Young, C. *Chem. Eur. J.* **2009**, *15*, 11454.
(47)   Achard, T. R. J.; Clegg, W.; Harrington, R. W.; North, M. *Tetrahedron* **2012**, *68*, 133.
(48)   Caló, V.; Nacci, A.; Monopoli, A.; Fanizzi, A. *Org. Lett.* **2002**, *4*, 2561.
(49)   Aoyagi, N.; Furusho, Y.; Endo, T. *J. Polym. Sci. A1* **2013**, *51*, 1230.
(50)   Aoyagi, N.; Furusho, Y.; Endo, T. *Tetrahedron Lett.* **2013**, *54*, 7031.
(51)   Chen, S.-W.; Kawthekar, R. B.; Kim, G.-J. *Tetrahedron Lett.* **2007**, *48*, 297.
(52)   Kruper, W. J.; Dellar, D. D. *J. Org. Chem.* **1995**, *60*, 725.
(53)   Niu, Y.; Zhang, W.; Li, H.; Chen, X.; Sun, J.; Zhuang, X.; Jing, X. *Polymer* **2009**, *50*, 441.
(54)   Zhang, X.; Jia, Y.-B.; Lu, X.-B.; Li, B.; Wang, H.; Sun, L.-C. *Tetrahedron Lett.* **2008**, *49*, 6589.
(55)   Martinez, L. E.; Leighton, J. L.; Carsten, D. H.; Jacobsen, E. N. *J. Am. Chem. Soc.* **1995**, *117*, 5897.
(56)   Larrow, J. F.; Schaus, S. E.; Jacobsen, E. N. *J. Am. Chem. Soc.* **1996**, *118*, 7420.
(57)   White, R. C.; Ma, S. *J. Heterocyclic Chem.* **1987**, *24*, 1203.

(58)   Keith, John M.; Larrow, Jay F.; Jacobsen, Eric N. *Advanced Synthesis & Catalysis* **2001**, *343*, 5.
(59)   Pasquale, R. PhD thesis, Newcastle University, 2009.
(60)   Desmos, I.; Online ed. 2012.
(61)   North, M.; Wang, B.; Young, C. *Energ. Environ. Sci.* **2011**, *4*, 4163.
(62)   Pazuki, G. R.; Pahlavanzadeh, H. *Theor Found Chem Eng* **2005**, *39*, 240.
(63)   Dejoye, T., Abert, V. M., Ginies, C., Elmaataoui, M., Chemat, F. *Molecules* **2012**, *17*, 8196.
(64)   Darensbourg, D. J.; Moncada, A. I. *Inorg. Chem.* **2008**, *47*, 10000.
(65)   Leung, W.-H.; Chan, E. Y. Y.; Chow, E. K. F.; Williams, I. D.; Peng, S.-M. *J. Chem. Soc. Dalton* **1996**, 1229.
(66)   Chisholm, M. H.; Patmore, N. J.; Zhou, Z. *Chem. Commun.* **2005**, 127.
(67)   Munoz-Hernandez, M.-A.; Keizer, T. S.; Wei, P.; Parkin, S.; Atwood, D. A. *Inorg. Chem.* **2001**, *40*, 6782.
(68)   Kochem, A.; Kanso, H.; Baptiste, B.; Arora, H.; Philouze, C.; Jarjayes, O.; Vezin, H.; Luneau, D.; Orio, M.; Thomas, F. *Inorg. Chem.* **2012**, *51*, 10557.
(69)   Chapman, J. J.; Day, C. S.; Welker, M. E. *Organometallics* **2000**, *19*, 1615.
(70)   Cohen, C. T.; Thomas, C. M.; Peretti, K. L.; Lobkovsky, E. B.; Coates, G. W. *Dalton Trans* **2006**, 237.
(71)   Zhang, Y.-L.; Ruan, W.-J.; Zhao, X.-J.; Wang, H.-G.; Zhu, Z.-A. *Polyhedron* **2003**, *22*, 1535.
(72)   Bobb, R.; Alhakimi, G.; Studnicki, L.; Lough, A.; Chin, J. *J. Am. Chem. Soc.* **2002**, *124*, 4544.
(73)   Hansen, K. B.; Leighton, J. L.; Jacobsen, E. N. *J. Am. Chem. Soc.* **1996**, *118*, 10924.
(74)   Darensbourg, D. J.; Yarbrough, J. C. *J. Am. Chem. Soc.* **2002**, *124*, 6335.
(75)   Lambert, P. In *Sustainability of construction materials*; Khatib, J. M., Ed.; Woolhead Publishing India Pte. Ltd.: New Delhi, India, 2009, p 138.
(76)   Müller, J. In *Iron catalysis in organis chemistry*; Plietker, B., Ed.; Wiley-VCH: 2008, p 29.
(77)   Allen, F. H. *Acta Cryst.* **2002**, *B58*, 380.
(78)   C. F. Macrae; P. R. Edgington; P. McCabe; E. Pidcock; G. P. Shields; R. Taylor; M. Towler; Streek, J. v. d. *J. Appl. Cryst.* **2006** *39*, 453.
(79)   Hansen, T. V.; Skattebøl, L. In *Organic syntheses*; John Wiley & Sons, Inc.: 2003.
(80)   Ferguson, M.; Giri, N.; Huang, X.; Apperley, D.; James, S. L. *Green Chem.* **2014**, *16*, 1374.
(81)   Yan, P.; Jing, H. *Advanced Synthesis & Catalysis* **2009**, *351*, 1325.
(82)   Hansen, T. V.; Skattebøl, L. *Tetrahedron Lett.* **2005**, *46*, 3829.
(83)   Fallis, I. A.; Murphy, D. M.; Willock, D. J.; Tucker, R. J.; Farley, R. D.; Jenkins, R.; Strevens, R. R. *J. Am. Chem. Soc.* **2004**, *126*, 15660.

(84)   Pospisil, P. J.; Carsten, D. H.; Jacobsen, E. N. *Chem. Eur. J.* **1996**, *2*, 974.

(85)   Yao, X.; Qiu, M.; Lü, W.; Chen, H.; Zheng, Z. *Tetrahedron: Asymmetr.* **2001**, *12*, 197.

(86)   Minutolo, F.; Pini, D.; Petri, A.; Salvadori, P. *Tetrahedron: Asymmetr.* **1996**, *7*, 2293.

(87)   North, M.; Young, C. *ChemSusChem* **2011**, *4*, 1685.

(88)   Chen, P.; Chisholm, M. H.; Gallucci, J. C.; Zhang, X.; Zhou, Z. *Inorg. Chem.* **2005**, *44*, 2588.

(89)   Tokunaga, M.; Tsuji, Y.; Obora, Y.; Hori, Y.; Aoyama, H., (Japan Science and Technology Agency) 2004

(90)   Rhodes, B.; Rowling, S.; Tidswell, P.; Woodward, S.; Brown, S. M. *Journal of Molecular Catalysis A: Chemical* **1997**, *116*, 375.

(91)   Nielsen, L. P. C.; Stevenson, C. P.; Blackmond, D. G.; Jacobsen, E. N. *J. Am. Chem. Soc.* **2004**, *126*, 1360.

(92)   Cohen, C. T.; Chu, T.; Coates, G. W. *J. Am. Chem. Soc.* **2005**, *127*, 10869.

(93)   Covell, D. J.; White, M. C. *Angewandte Chemie* **2008**, *120*, 6548.

(94)   Barvainiene, B.; Stanisauskaite, A.; Getautis, V. *Chem Heterocycl Compd* **2007**, *43*, 718.

(95)   Sigma-Aldrich; Sigma-Aldrich catalogue listing, (R)-(+)-Propylene carbonate: 2013.